

1-31-2014 12:00 AM

## Surface Functionalization and Bioconjugation of Nanoparticles for Biomedical Applications


Longyan Chen, *The University of Western Ontario*

Supervisor: Jin Zhang, *The University of Western Ontario*

A thesis submitted in partial fulfillment of the requirements for the Doctor of Philosophy degree in Chemical and Biochemical Engineering

© Longyan Chen 2014

Follow this and additional works at: <https://ir.lib.uwo.ca/etd>

 Part of the [Analytical Chemistry Commons](#), [Biochemical and Biomolecular Engineering Commons](#), [Bioimaging and Biomedical Optics Commons](#), [Biological Engineering Commons](#), [Biomaterials Commons](#), and the [Materials Chemistry Commons](#)

---

### Recommended Citation

Chen, Longyan, "Surface Functionalization and Bioconjugation of Nanoparticles for Biomedical Applications" (2014). *Electronic Thesis and Dissertation Repository*. 1903.  
<https://ir.lib.uwo.ca/etd/1903>

This Dissertation/Thesis is brought to you for free and open access by Scholarship@Western. It has been accepted for inclusion in Electronic Thesis and Dissertation Repository by an authorized administrator of Scholarship@Western. For more information, please contact [wlsadmin@uwo.ca](mailto:wlsadmin@uwo.ca).

# **SURFACE FUNCTIONALIZATION AND BIOCONJUGATION OF NANOPARTICLES FOR BIOMEDICAL APPLICATIONS**

(Thesis format: **Integrated Article**)

by

**Longyan Chen**

Graduate Program in Chemical and Biochemical Engineering

A thesis submitted in partial fulfillment  
of the requirements for the degree of  
Doctor of Philosophy

The School of Graduate and Postdoctoral Studies  
The University of Western Ontario  
London, Ontario, Canada

© Longyan Chen 2013

## Abstract

Colloidal inorganic nanoparticles (NPs) have been attracting considerable interest in biomedicine, from drug and gene delivery to imaging, sensing and diagnostics. It is essential to modify the surface of nanoparticles to have enhanced biocompatibility and functionality for the *in vitro* and *in vivo* applications, especially in delivering locally and recognizing biomolecules. Herein, the goal of this research work is to develop advanced NPs with well-tailored surface functionalities and/or bio-functionality for the applications in cell tracking and analytes detection.

In the first project, quantum dots incorporating with gelatin nanoparticles (QDs-GNPs) have been developed for bioimaging applications. Two different approaches have been developed, i.e. directly encapsulating QDs with gelatin polymer (QDs-GNP1) and layer-by-layer (LBL) adsorption of QDs approach (QDs-GNP2), respectively. The special hybrid structures of two QDs-GNPs nanosystems were investigated by transmittance electron microscopy, scanning electron microscopy, X-ray energy dispersion, Fourier Transform Infrared spectroscopy, fluorometer, and confocal fluorescent microscopy. Both nanosystems exhibit high intensive luminescence and good biocompatibility. Compared to free QDs, QDs-GNP2 shows improved quantum yield and longer lifetime, due to multiple layers of polyelectrolytes protection. Furthermore, QDs-GNP2 demonstrates the proton-resistant properties in term of PL intensity and lifetime. The bright and stable photoluminescence (PL) allows the QD-GNP2 for labeling living 3T3 cells *in vitro*, which may indicate the QDs-GNP2 are able to be a suitable candidate for bio-imaging application.

In the second project, fluorescent magnetic nanoparticles (FMNPs) were bioconjugated with gentamicin (Gm) for rapid capture, detection and decontamination of bacteria. The Gm-FMNPs consist of a fluorescent silica shell and an iron oxide magnetic core. Initially, we prepared the core-shell NPs through a one-pot reaction. The antibacterial efficiency is

found 20 % higher than that of the free antibiotic. We further improved NPs stability and capture efficiency by a two-step thermal decomposition method to produce the fluorescent magnetic core-shell nanoparticles. It is noted that one mg of gentamicin conjugated FMNPs are able to capture both gram-negative bacteria *Escherichia coli* and gram-positive bacteria *Staphylococcus aureus* as low as  $1 \times 10^4$  colony-forming unit/mL (cfu/mL) in less than one minute. It is expected that the Gm-FMNPs could be a promising multifunctional platform for disease control in clinic and wastewater treatment.

In addition, a nanosensor for detecting human thrombin has been designed and developed. A recombinant luciferase was covalently conjugated to gold nanoparticles (Au NPs) through 1-Ethyl-3-(3-dimethylaminopropyl) carbodiimide (EDC) mediated reaction. The conjugation enables Au NPs to quench the bioluminescence produced by luciferase. Recovery of bioluminescence has been studied as a function of the concentration of thrombin. The results indicate that the designed nanosensor can efficiently detect a protease thrombin in both buffer and human urine spiked buffer. A linear assay response is found between 300 ng/mL to 300  $\mu$ g/mL, with limit of detection (LOD) of 3 ng/mL in both buffer and human urine spiked samples. The assay time can be less than 15 min. The nanosensor can thus be a promising tool for clinical diagnostic of thrombin related diseases.

In summary, different strategies have been explored to engineer the surface of hybrid NPs with good water stability, biocompatibility and enhanced chemical and physical properties. The thesis addresses that engineered hybrid NPs in biomedicine and how the biofunctionalized NPs can find applications in imaging and diagnostics indistinctly.

**Keywords:** Fluorescent, magnetic, nanoparticles, gold nanoparticles, quantum dots, surface functionalization, bioconjugation, biosensing, bioimaging.

## Co-Authorship Statement

Chapters 1 and 2 entitled “Introduction” and “Background and Literature Review”, respectively, were written by Longyan Chen, with suggestions from Dr. Jin Zhang. Figure 2.1 is adapted with permission from (Kelly et. al., Journal of Physical Chemistry B, **107**(3): P. 668-677). Copyright (2002) American Chemical Society."

Chapter 3, 4 and 5 encompass research studies have been published or are in preparation for publication. Individual contributions of the author of each article are stated below.

Chapter 3: This chapter encompass two research studies have been published or submitted.

The experiment work and draft of manuscript related in preparation of QDs-GNP1 was conducted by co-operation with Adrienne Willoughby (a former undergraduate student supervised by Dr. Jin Zhang at Chemical and Biochemical Engineering Department, the University of Western Ontario). The manuscript was drafted by the author and reviewed several times by Dr. Jin Zhang. This work was supervised by Dr. Jin Zhang.

- Longyan Chen, Adrienne Willoughby and Jin Zhang (2013) Luminescent Gelatin Nanospheres by Encapsulating CdSe Quantum Dots, Luminescence, **29**, 74-79 ..

The experiment work of QDs-GNP2 was achieved by co-operation of Dr. Alex Siemiarzuck (Photon Technology International Inc, London, Canada), Dr. Hong Hai, Dr. Yi Chen, and Guobang Huang (Chemical and Biochemical Engineering Department, the University of Western Ontario). The manuscript of this part was drafted by the author and reviewed by Dr. Jin Zhang extensively. This work was supervised by Dr. Jin Zhang.

- Longyan Chen, Alex Siemiarzuck, Hong Hai, Yi Chen, Guobang Huang and Jin Zhang, Development of Biocompatible and Proton-resistant Quantum Dots Assembled on Gelatin Nanospheres, Langmuir (2014) Accepted.

Chapter 4: This chapter encompasses two research studies that have been published.

In the part of the experiment work relating to one-pot preparation of Gm-FMNP, the experiment work was achieved by the author with the co-operation with Dr. Fereidoon S. Razavi (Brock University), Abdul Mumin (Chemical and Biochemical Engineering Department, the University of Western Ontario), Xiaoxuan Guo and Dr. Tsun-Kong Sham (Chemistry Department, the University of Western Ontario). This work was supervised by Dr. Jin Zhang.

- Longyan Chen, Fereidoon S. Razavi, Abdul Mumin, Xiaoxuan Guo, Tsun-Kong Sham and Jin Zhang (2013) Multifunctional Nanoparticles for Rapid Bacterial Capture, Detection, and Decontamination, RSC Advances, **3**, 2390-2397.

In the work relating to the preparation of Gm-FMNPs through two-step method and study of their bacterial capture efficiency, the experiment work, analysis of data and manuscript were prepared by the author. It was reviewed by Dr. Jin Zhang, who also provided a series of revision steps for improvement.

- Longyan Chen and Jin Zhang (2012) Bioconjugated Magnetic Nanoparticles for Rapid Capture of Gram-positive Bacteria, Journal of Biosensor and Bioelectronics. **S11**:005.

Chapter 5: The experiment work was conducted by Longyan Chen under supervision of Dr. Jin Zhang. Both authors analyzed the data. Various drafts of the manuscript were reviewed by Dr. Jin Zhang. Mr. Yige Bao provided urine samples and advices for pretreatment of urine samples. This work was supervised by Dr. Jin Zhang.

- Longyan Chen, Yige Bao and Jin Zhang (2013) “Luciferase Conjugated Gold Nanoparticles for Thrombin Detection” In preparation.

Chapter 6 was written by Longyan Chen, with the suggestions from Dr. Jin Zhang.

To my wife, Shan  
for her love, patience and encouragement.

To my father, mother and my sisters for their patience and  
steady support

## Acknowledgements

This thesis would not have been in the current form without the help and guidance from several people. I would, therefore, like to offer my sincere thanks to all of them.

I would like to extend my heartfelt gratitude to my supervisor Dr. Jin Zhang, for her enthusiastic support and continued guidance throughout the course of my PhD research. The encouragement and support she has provided me over the past years have been and will continue to be indispensable for my professional development.

I would like to thank my examination committee: Drs. Amarjeet Bassi, Charles (Chunbao) Xu, Lyudmila Goncharova and Yuning Li for their guidance and feedback throughout this endeavour. I would like to express my thanks to my committee board Drs. Anand Prakash and Tim A. Newson for their time in reviewing my annual progress report and providing useful suggestions for my research.

My special thanks to Dr. Richard Gardiner and Ms. Nygard Karen in Biotron center for their assistants in using of the facilities. I appreciate very much for the advices from Dr David Litchfield, Dr Susan Koval, and Ms. Judy Sholdice for discussing part of the work in Chapter 3.

Special gratitude is extended to all of my current and previous colleagues at Multifunctional Nanocomposite Lab, Dr. Yi Chen, Guobang Huan, Andrew Tse, Dr. Robert Bi, Pei Yin, Abdule Md. Mumin, Dr. Hong Hai, Kazi Farida Akhter, Anu Alice Thomas, Adrienne Willoughby and Kim Hyung, for their continuous support, encouragement, and nice time that we have had together.

Finally, I would dearly like to thank my family for their support and encouragement. My wife, Shan, deserves much credit for her immeasurable love, support, and prayer for me.

This work has been supported by funding from Natural Science and Engineering Research Council of Canada (NSERC) through a Discovery Grant and Western Engineering Graduate Scholarship.



# Table of Content

Abstract .....	ii
Co-Authorship Statement.....	iv
Acknowledgements.....	vii
Table of Content .....	viii
List of Figures .....	xiii
List of Tables .....	xvi
List of Abbreviations .....	xvii
CHAPTER 1 .....	1
GENERAL INTRODUCTION AND MOTIVATION .....	1
1.1 Overview of nanoparticles in biomedical applications .....	2
1.1.1 Nanoparticles as imaging agents and biosensing transducer.....	4
1.1.2 Fluorescence resonance energy transfer as readout.....	5
1.2 Limitations of using NPs in biomedical fields .....	7
1.3 Aims and Objectives .....	8
1.4 References .....	9
CHAPTER 2 .....	13
BACKGROUND AND LITERATURE REVIEW .....	13
2.1 Colloidal Inorganic Nanoparticles for Biomedical Application .....	14
2.1.1 Noble metal NPs .....	14
2.1.2 Semiconductor quantum dots .....	16
2.1.3 Magnetic Nanoparticles .....	18
2.2 Synthesis of colloid NPs for biomedical use.....	21
2.2.1 Synthesis of NPs in water .....	22
2.2.2 Synthesis of NPs in organic phase.....	22

2.3	Surface Functionalization of NPs.....	23
2.3.1	Ligand exchange.....	24
2.3.2	Ligand modification .....	26
2.3.3	Ligand addition.....	27
2.4	Bioconjugation .....	29
2.4.1	Direct absorption .....	29
2.4.2	Covalent coupling.....	30
2.4.3	Biological approaches.....	33
2.5	Summary .....	35
2.6	References .....	36
CHAPTER 3 .....		48
DEVELOPMENT OF BIOCOMPATIBLE LUMINESCENT NANOPARTICLES FOR BIOIMAGING APPLICATIONS .....		48
3.1	Introduction .....	49
3.2	Experimental procedures.....	50
3.2.1	Materials and Reagents.....	50
3.2.2	Preparation of hydrophilic CdSe QDs.....	51
3.2.3	Preparation of gelatin NPs.....	51
3.2.4	Preparation of QDs-GNP1 by direct encapsulation of QDs in GNPs. ....	52
3.2.5	Preparation of QDs-GNP2.....	53
3.2.6	Characterization.....	54
3.2.7	Analysis of pH effect in photostability .....	54
3.2.8	Cell viability/cytotoxicity study .....	55
3.2.9	<i>In vitro</i> fluorescence imaging.....	55
3.3	Results and Discussion (I).....	56
3.3.1	Characterization.....	56

3.3.2	Cytotoxicity .....	59
3.4	Results and Discussion (II) .....	60
3.4.1	Materials characterization.....	61
3.4.2	Absorbance and PL spectra .....	62
3.4.3	The pH effects on photostability .....	63
3.4.4	Cytotoxicity analysis of QDs-GNP2 .....	65
3.4.5	<i>In vitro</i> bio-imaging application.....	66
3.5	Conclusions and Prospects .....	67
3.6	References .....	67
CHAPTER 4 .....		72
DEVELOPMENT OF BIOCONJUGATED MAGNETIC LUMINESCENT NANOMATERIALS FOR BACTERIAL CAPTURE, DETECTION AND ANTIBACTERIAL APPLICATIONS .....		72
4.1	Introduction .....	73
4.2	Experimental .....	75
4.2.1	Preparation of FMNP1 by one-pot method .....	76
4.2.2	Preparation of FMNP2 by two-step coating method.....	77
4.2.3	Bioconjugation of FMNPs with Gm.....	78
4.2.4	Characterization.....	79
4.2.5	Bacteria Capture .....	79
4.2.6	Analysis of the antibacterial effect .....	80
4.2.7	Determine the concentration of gentamicin on the FMNP1 .....	80
4.2.8	Preparation of thin section samples for TEM analysis .....	81
4.3	Results and Discussion.....	82
4.3.1	Characterization.....	82
4.3.2	Capture, detection and decontamination of <i>E. coli</i> by Gm-FMNP1 .....	86

4.3.3	Ubiquitous capture of bacteria by Gm-FMNP2 .....	93
4.4	Conclusion.....	94
4.5	References .....	95
CHAPTER 5 .....		100
DEVELOPMENT OF LUCIFERASE CONJUGATED GOLD NANOPARTICLES IN DETECTION OF THROMBIN.....		100
5.1	Introduction .....	101
5.2	Experimental section.....	104
5.2.1	Design of the pRluc-Au NPs nanosensor .....	104
5.2.2	Dihydrolipoic acid (DHLA) synthesis.....	105
5.2.3	Synthesis and functionalization of Gold Nanoparticles .....	105
5.2.4	Plasmid constructions .....	106
5.2.5	Protein Expression and Purification .....	106
5.2.6	Bioconjugation of Au NPs by pRluc protein.....	107
5.2.7	Characterization.....	107
5.2.8	Thrombin assay.....	108
5.3	Results and Discussion.....	108
5.3.1	Characterization of the pRluc-Au NP conjugate .....	108
5.3.2	Assay optimization .....	109
5.3.3	Determination of thrombin concentration in both buffer and urine samples .....	113
5.4	Conclusions and Prospects .....	114
5.5	References .....	114
CHAPTER 6 .....		118
SUMMARY AND RECOMMENDATIONS.....		118
6.1	Summary and Conclusion .....	119
6.2	Contributions of the Research to the Current State of Knowledge. ....	121

6.3	Limitations of the Research and Suggestions for Future Studies.....	125
6.4	References .....	126
	Appendices.....	129
	Appendix 1. Quantification of QD coated onto GNs.....	130
	Appendix 2. pH value effects on fluorescence decay of QDs and core-shell QDs-GNP2 .....	131
	Appendix 3. XANES spectra of FMNPs .....	136
	Appendix 4. Determine the concentration of gentamicin on Gm-FMNP1.....	137
	Appendix 5. Plasmid map of recombinant protein pRluc.....	138
	Appendix 6. TEM image of Au NPs and SDS-PAGE of pRluc .....	139
	Appendix 7. Copyright permission .....	140
	Curriculum Vitae .....	154

## List of Figures

Figure 1.1	Schematic illustration of FRET process	6
Figure 1.2	Strategy for bridging the unique feature of nanoparticles to biomedical applications	8
Figure 2.1	Schematic illustration of the SPR effect.	15
Figure 2.2	Size dependent photophysical properties of semiconductor quantum dots	17
Figure 2.3	The responses of materials to magnetic field.	18
Figure 2.4	Schematic illustration of common surface functionalization strategies	24
Figure 2.5	Common ligands for stabilizing NPs in water	25
Figure 2.6	Representative bioconjugation protocols	31
Figure 2.7	Reaction scheme for (a) EDC-NHS crosslinking and (b) SMCC mediated conjugation	33
Figure 2.8	Mechanism of intein mediated bioconjugation	34
Figure 3.1	Schematic illustration of preparation of QD-GNP1	52
Figure 3.2	Schematic illustration of preparation of QDs-GNP2 by LBL technique.	53
Figure 3.3	TEM micrograph of (a) MUA-CdSe QDs and (b) QD-GNP1.	56
Figure 3.4	FTIR spectra of MUA-QDs, GNPs and QD-GNP1	57
Figure 3.5	Fluorescent spectra of CdSe QDs, GNPs and QD-GNP1	58
Figure 3.6	Confocal fluorescent of microscopy images of QD-GNP1	59
Figure 3.7	Cytotoxicity analysis of GNPs, MUA-QDs and QD-GNP1	60
Figure 3.8	Characterization of QDs-GNP1 by electron microscopy	61
Figure 3.9	FTIR spectra of bare (i) GNPs, (ii) PE coating GNPs, (iii) single layer QDs coating GNPs, (iv) multilayer QDs coating GNPs, and (v) free MUA-QDs.	62
Figure 3.10	(a) Absorbance and (b) PL spectra for MUA-QDs and corresponding QDs-GNP2	63
Figure 3.11	The pH effect on (a) PL intensity and (b) average lifetimes .	64

Figure 3.12	Cytotoxicity profile of MUA-QDs and corresponding QDs-GNP2 after 24 h incubation with 3T3 cells.	65
Figure 3.13	Confocal microscopy images of (a) GNPs (0.3 mg/mL), (b) MUA-QDs (0.1 mg/mL), and (c) QDs-GNP2 (0.4 mg/mL) after co-incubation with NIH/3T3 mouse fibroblast cells.	66
Figure 4.1	Schematic illustration of the synthesis of FMNPs used for <i>E. coli</i> capture and magnetic separation in solution	76
Figure 4.2	TEM micrograph of the core-shell structures of (a) FMNP1 and (b) FMNP2 .	83
Figure 4.3	XRD profiles of the core-shell structured (a) FMNP1 and (b) FMNP.	84
Figure 4.4	Characterization of magnetic property. VSM measurement of hysteresis loops of (a) FMNP1 and (b)FMNP2; SQUID analysis of zero-field-cooled (ZFC) magnetization curve of (c) FMNP1 and (d) FMNP2 at 50 Oe	85
Figure 4.5	FTIR absorption spectra of FMNP1, glutaraldehyde (Glu) modified FMNP1 (Glu-FMNP1), and Gm-FMNP	86
Figure 4.6	Magnetic capture of bacterium <i>E. coli</i> under external magnetic field	86
Figure 4.7	Fluorescent spectra of free FITC, FMNP1, and the Gm-FMNP1 before/after detecting <i>E. coli</i> cells	88
Figure 4.8	Analysis of the interaction between NPs and bacterium <i>E. coli</i> .	90
Figure 4.9	Antimicrobial efficiency of Gm-FMNP1 (0.1 mg/mL) with <i>E. coli</i>	92
Figure 4.10	TEM micrographs of capture of bacteria <i>E. coli</i> and <i>S. aureus</i> by Gm-FMNP2.	93
Figure 5.1	Schematic diagram of detection of thrombin via pRluc conjugated gold nanoparticles	104
Figure 5.2	(a) UV-visible spectra and (b) FTIR spectra of bare Au NPs, alkanoethiol acid functionalized Au NPs and pRluc conjugated Au NPs	110

Figure 5.3	Bioluminescent spectra of pRluc-Au NPs conjugates	111
Figure 5.4	The effect of (a) ligand length, (b) the molar ratio of Au NPs and pRluc, (c) the molar ratio of Au NPs and EDC, and (d) digestion time to the relative BL ratio	112
Figure 5.5	Detection of thrombin by using pRluc-Au NPs nanosensor in (a) TBS buffer and (b) TBS buffer spiked with human urine.	113
Figure A1	Fluorescence decay of QDs-GNP2 (a-d) and CdSe QDs (e-h) when the pH value of aqueous media is 1, 4, 7, and 9, respectively;	130
Figure A2	Standard curve of the emission intensity of the QDs as a function of their concentration.	131-135
Figure A3	Fe K-edge XANES spectra of FMNPs (black line) and model compound, Fe <sub>3</sub> O <sub>4</sub> (red line)	136
Figure A4	UV-vis spectra of the <i>o</i> -phthalalehyde derived gentamicin products from standard gentamicin solutions	137
Figure A5	Map of plasmid containing recombinat protein pRluc	138
Figure A6	(a) TEM image of Au NPs and (b) SDS-PAGE of pRluc	139



## List of Tables

Table 1.1	Typical inorganic nanoparticles and their general applications in biomedicine	3
Table A1	Absorption values at 292 nm of <i>o</i> -phthalaldehyde -derived Gm- FMNPs	136

## List of Abbreviations

NPs	–	Nanoparticles
GNPs	–	Gelatin Nanoparticles
QDs	–	Quantum dots
MNPs	–	Magnetic Nanoparticles
FMNPs	–	Fluorescent magnetic nanoparticles
Au NPs	–	Gold nanoparticles
LBL	–	Layer-by-layer
FRET	–	Förster (or Fluorescent) resonance energy transfer
BRET	–	Bioluminescence resonance energy transfer
Gm	–	Gentamicin
<i>E. coli</i>	–	<i>Escherichia coli</i>
<i>S. aureus</i>	–	<i>Staphylococcus aureus</i>
FITC	–	Fluorecein isothiocyanate
BSA	–	Bovine serum albumin
CFU	–	Colony forming unit
MUA	–	11-Mercaptoundecanoic acid
DHLA	–	Dihydrolipoic acid
Rluc	–	Renilla luciferase
pRluc	–	Recombinant protein containing Rluc
PBS	–	Phosphate buffered saline
TBS	–	Tris buffered saline
TEOS	–	Tetraethyl orthosilicate
CTAB	–	Hexadecyltrimethylammonium bromide
TOP	–	Trioctylphosphine
TOPO	–	Trioctylphosphine oxide

**CHAPTER 1**  
**GENERAL INTRODUCTION AND MOTIVATION**

## 1.1 Overview of nanoparticles in biomedical applications

The term “nanotechnology” is defined as the creation and utilization of materials, devices and systems through the control of matter at the length scale of 1 to 100 nanometer (nm), i.e. at atomic, molecular or supermacromolecular level.<sup>1</sup> Yet, materials or structures with at least one dimension below 100 nm also enter into this definition. Materials built at this size scale (i.e. nanomaterials) often exhibit distinctive physical and chemical properties due to quantum mechanical effects and/or large surface-to-volume ratio.

Since last decades, a variety of nanomaterials has been developed for both research and industrial applications. For example, zinc oxide nanocrystals have been fabricated and incorporated to sunscreens for blocking ultraviolet light; and silver nanoparticles have been coated or embedded in bandages to kill microbes and prevent post-surgery infection. Possibilities of application of nanomaterials are numerous, from producing energy saving battery for vehicle, to manufacturing materials with anti-corrosion and scathing surface; from fabricating chemical and biological sensors for health care, to environmental safety solar-energy panels.

In recent, nanomaterials, in particular nanoparticles (NPs), offer immense potential for various biomedical applications from drug and gene delivery to imaging, sensing and diagnostics (Table 1.1), depending upon the nature of the materials and their chemical and physical properties. Of all biomedical applications, the development of nanoparticles based imaging agents for cancer therapy and biosensor for diagnostics stand out as the most prioritised areas of research.

Table 1.1 Typical inorganic nanoparticles and their general applications in biomedicine

Category	Examples	Intrinsic properties	Biomedical applications
Metallic NPs	Gold or Silver NPs	Surface plasmon resonance (SPR), Surface reactivity, catalysis.	Chemical/biochemical sensing, disease diagnostics; Optical imaging, Raman probe; photothermal cancer therapy; drug delivery; antimicrobial agents.
Semiconduct NPs, or/ Quantum dots	CdSe, CdS, CdTe	Fluorescence, Luminescence	High-resolution and sensitive cellular imaging; long-term cell trafficking; diagnostics and sensing based on energy transfer techniques.
Magnetic NPs	Fe <sub>3</sub> O <sub>4</sub> , Co, FePt NPs	Superparamagnetic, Large magnetic moments in a magnetic field	Magnetic separation for diagnosis and monitoring; target delivery of drugs & genes; MRI contrast agents; Thermotherapy.

### 1.1.1 Nanoparticles as imaging agents and biosensing transducer

Molecular imaging and image-guided therapy is now emerging as a most promising basic tool for monitoring disease. A variety of imaging modalities such as optical imaging, magnetic resonance imaging (MRI), X-ray and ultrasound has been established for diagnose disease and cancer therapy. Yet, these techniques are generally not sensitive enough to detect tissue changes at molecular level that are usually the first signs of evolution of healthy body to diseased ones. Further improvement of imaging involves the design of novel contrast agents. The discovery and understanding of nanomaterials with unique size dependent physical and chemical features has drawn the attention of research in using nanoparticles as new contrast agents.

The current types of NPs widely used as imaging agents are luminescent nanoprobes for optical imaging and magnetic nanoparticles for MRI. For example, the plasmon absorption and scattering properties make the use of gold nanoparticles in targeting and imaging of cells and cancer makers.<sup>2</sup> Quantum dots (QDs) have been demonstrated to be excellent agents for optical imaging, because of their bright and stable photoluminescence. In particular, the tunable emission spectrum allows QDs emission at near-infrared light (700 nm -900 nm) which could effectively penetrate in deep tissue. Superparamagnetic properties of magnetic NPs provides contrast enhancement by facilitating MRI signal strengths for non-invasive imaging.<sup>3, 4</sup>

Likewise, research in development of NPs based biosensors has showed highly fascinating and promising results in the early and accurate diagnosis of clinical conditions. For example, high surface to volume ratio of the nanomaterials enables the detection of biomolecules under extremely low concentration by using optical,<sup>5</sup> electrical or electrochemical signal.<sup>6</sup> Size-dependent physical and chemical properties make the use of NPs for high throughput labelling and detection of bioanalytes.<sup>7, 8</sup> Furthermore, superparamagnetic NPs based systems that can be automated and miniaturized, which provide enormous advantages over others for their potentials use in field situations.<sup>9, 10</sup> Due to these great advantages, a number of nanosensors have now been developed in detection of proteins, nucleic acid, bioactive molecules, bacterial and viral agents.<sup>11, 12</sup>

A sensor generally consists of two components: a recognition element for target recognizing and a transducer to convert the biological events into measurable signal (typically optical signal). Bio-labelled NPs usually have been demonstrated to be excellent transducers. In this case, NPs with unique optical property can be directly labelled with a biological recognition element such as nucleic acid probe, antibody, enzyme, aptamer or small bioactive ligands for detection.<sup>13</sup> The concentrations of the analytes are thus linked directly to the changes of optical signal.

### 1.1.2 Fluorescence resonance energy transfer as readout

Apart from providing signals for directly labelling in sensing and imaging applications, NPs can also provide fluorescent signals in the form of Förster/fluorescence resonance energy transfer (FRET), which is a process that nonradiative energy transfer occurs from an excited fluorophore (donor) to a proximal ground state fluorophore (acceptor). This process results in reduction of donor fluorescence intensity and increasing of acceptor emission intensity (Figure 1.1).<sup>14, 15</sup> The efficiency of energy transfer is strongly dependent on the distance between the donor and acceptor. By measuring the efficiency of energy transfer (e.g. through the changes of fluorescent signal from either donor and/or acceptor), one can determine the distance between two fluorophore-partners. Based on this, FRET has shown as a powerful tool for probing biological interactions, sensing analytes and imaging applications.

The pair of donor and acceptor in conventional FRET system can be organic dyes pair (Cy3-Cy5), fluorescent proteins pair (e.g. cyan fluorescent protein and red fluorescent protein pair), or dye-fluorescent proteins pair. Fluorescent NPs, such as QDs can also be used in FRET system. For example, by taking the advantage of broad absorption spectra and tunable emission profile, QD is particularly suitable as a donor in the FRET system.<sup>16-18</sup> Numerous investigators have utilized the QD-based FRET system for various applications, such as detection of pathogenic DNA and DNA point mutation,<sup>19, 20</sup> immunoassay,<sup>21, 22</sup> tracking and quantifying enzyme activity,<sup>23-26</sup> protein conformation changes,<sup>27, 28</sup> sensing pH<sup>29</sup> and ion changes,<sup>30</sup> and interaction between of biomolecules.<sup>28</sup> In some cases, the system was also used for multiplex detection of analytes.<sup>31</sup>

QDs can also be energy acceptor, particularly while incorporated into bioluminescence resonance energy transfer (BRET)<sup>32</sup> and chemiluminescence resonance energy transfer (CRET),<sup>33</sup> whereby non-radiative energy transferring from substrate catalyzed by enzyme and chemiluminescent donor to QDs, respectively. The major advantages for those systems are low background noise and high excitation efficiency, as there is no need for an extra excitation source, typically high-energy laser. In this way, in particular, QD based BRET system has showed great potential in deep tissue imaging with low harmful effect on bodies.<sup>32</sup>

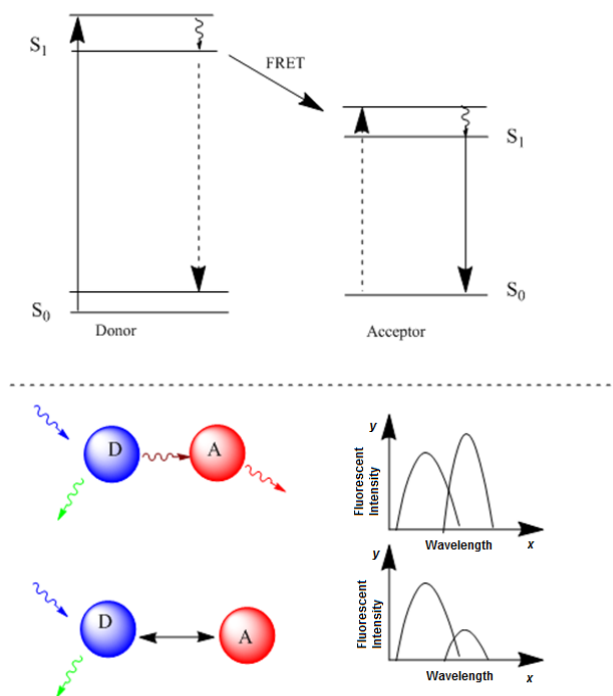


Figure 1.1 Schematic illustration of FRET process

Nanomaterials with special surface chemical properties can be used as a quenching energy acceptor incorporating in the FRET system. Au NP was used as a quencher for QD based FRET probe in a multiplexed assay in detection of the activity of enzymes and their inhibitors.<sup>25</sup>



## 1.2 Limitations of using NPs in biomedical fields

Despite that colloidal inorganic NPs offer immense promise for biomedical applications, several concerns remain to be addressed.

The primary concern probably is the stability of NPs in water, as most biochemical process occurs in aqueous environment. However, generally used methods usually provide nanoparticles with hydrophobic ligands, meaning they are unstable in aqueous solution. Another important concerning is the potential health and safety issues while exploring nanomaterials to human body and environment. The determinants of particle toxicity are known to be the large surface area and chemical reactivity in relation to small size (and thus the ability to generate reactive oxygen species) and the capability to penetrate tissues and cells.<sup>34</sup> Thus, particles in nano-scale are likely to be more hazardous than their bulk compartments, and free particles more toxic than fixed ones.<sup>35</sup> One of the examples to be considered is the potential cytotoxicity of QDs, because the heavy metals core is toxicity, and particularly at high concentrations they could cause harmful effects on embryo development and cell viability and function.<sup>36</sup> Lastly, a nanoparticle must be conjugated to a well-defined biological molecule, such as antibody, receptor, enzyme or nucleic acid, for targeting application. Hence, there exists a gap between the nature of NPs and their uses in biomedicine.

One method to bridge such a gap is the surface functionalization of nanoparticles (Figure 1.2). A proper surface coating can stabilize particles and avoid agglomeration, which hence may increase the sensitivity of NPs based sensor. In addition, a proper surface coating enables the nanoparticles in response specifically to biological species and avoids non-specific interactions with components in the complex matrix. Coating is also an effective manner of preventing the dissolution and release of core materials that may cause toxicity to biological system.<sup>37</sup> Furthermore, the steric hindrance of coating can affect the fate of NPs in biological system, such as cellular uptake and accumulation, circulation and clearance from body.<sup>38-40</sup> In addition, the surface can affect the maintenance of the intrinsic nanocrystal properties such as fluorescence and magnetic

behaviour. Moreover, appropriate surface functionality is the prerequisite for conjugating biomolecules to NPs for biomedical applications.



Figure 1.2 Strategy for bridging the unique feature of nanoparticles to biomedical applications.

## 1.3 Aims and Objectives

In view of the above overview, the overall objective of current research projects is to design and develop advanced NPs with suitable surface for cellular imaging and biosensing applications. Several goals are set up to fulfill the objective as showed below.

- (1) To develop hybrid fluorescent nanoparticles with unique proton resistant property for cellular imaging application.
- (2) To synthesize and prepare bioconjugated magnetic fluorescent nanoparticles for simultaneous capture, detection and deactivation of bacteria for infectious disease control.
- (3) To develop sensitive and fast responsive luminescent nanosensors for disease early diagnostics

To achieve these goals, the following specific objectives are sought in various chapters of the thesis:

- Chapter 1: Introduction  
This chapter provides an overview of biomedical application of NPs, the outline of objectives and the layout of the thesis.
- Chapter 2: Background and Literature Review  
This chapter presents a general review of strategies for surface functionalization and bioconjugation of colloidal inorganic nanoparticles.

- Chapter 3: Development of biocompatible luminescent nanoparticles for bioimaging applications.  
This chapter presents preparation of biocompatible polymer-quantum dots hybrid nanocomposites and their potential application in bioimaging. Two approaches were developed to produce the nanocomposites. In particular, multiple layer coating NPs prepared by the second approach shows its advantages in stabilizing QDs luminescence in term of intensity and lifetime among different pH range.
- Chapter 4: Development of bioconjugated magnetic luminescent nanoparticles for bacterial capture, detection and antibacterial applications.  
This chapter describes preparation of antibiotic gentamicin functionalized fluorescent magnetic nanoparticles. The nanoparticles have a fluorescent silica/iron oxide core/shell structure. The gentamicin conjugated fluorescent magnetic nanoparticles shows an all-in-one method for capture, detection and deactivation of both Gram-negative and positive bacteria.
- Chapter 5: Luciferase conjugated nanoparticles for biosensing applications.  
Following the success of my developed advance nanoparticles, in this chapter, I extended the application of bioconjugated fluorescent nanoparticles into nanosensors. The detection manner is based on energy transfer from bioluminescence from enzyme catalytic reaction to gold nanoparticles. We found the nanosensor could detect thrombin at nano-gram range in 15 min from both buffer and human urine samples.
- Chapter 6: General discussion and recommendation.  
This chapter provides a general conclusion of the above studies and recommendations for future work on the surface modification and conjugation of the nanoparticles.

## 1.4 References

1. National Science and Technology Council, National Nanotechnology Initiative Strategic Plan In 2011.
2. Boisselier, E.; Diallo, A. K.; Salmon, L.; Ruiz, J.; Astruc, D., Gold nanoparticles synthesis and stabilization via new "clicked" polyethyleneglycol dendrimers. *Chemical Communications* **2008**, (39), 4819-4821.

3. Shen, T.; Weissleder, R.; Papisov, M.; Bogdanov, A.; Brady, T. J., Monocrystalline iron oxide nanocompounds (MION): Physicochemical properties. *Magnetic Resonance in Medicine* **1993**, 29, (5), 599-604.
4. Weissleder, R.; Bogdanov, A.; Neuwelt, E. A.; Papisov, M., Long-circulating iron oxides for MR imaging. *Advanced Drug Delivery Reviews* **1995**, 16, (2-3), 321-334.
5. Nam, J.-M.; Thaxton, C. S.; Mirkin, C. A., Nanoparticle-Based Bio-Bar Codes for the Ultrasensitive Detection of Proteins. *Science* **2003**, 301, (5641), 1884-1886.
6. Luo, X.; Morrin, A.; Killard, A. J.; Smyth, M. R., Application of Nanoparticles in Electrochemical Sensors and Biosensors. *Electroanalysis* **2006**, 18, (4), 319-326.
7. Stroh, M.; Zimmer, J. P.; Duda, D. G.; Levchenko, T. S.; Cohen, K. S.; Brown, E. B.; Scadden, D. T.; Torchilin, V. P.; Bawendi, M. G.; Fukumura, D.; Jain, R. K., Quantum dots spectrally distinguish multiple species within the tumor milieu in vivo. *Nature Medicine* **2005**, 11, (6), 678-682.
8. Resch-Genger, U.; Grabolle, M.; Cavaliere-Jaricot, S.; Nitschke, R.; Nann, T., Quantum dots versus organic dyes as fluorescent labels. *Nature Methods* **2008**, 5, (9), 763-775.
9. Gijs, M. M., Magnetic bead handling on-chip: new opportunities for analytical applications. *Microfluidics and Nanofluidics* **2004**, 1, (1), 22-40.
10. Sung Kim, K.; Park, J.-K., Magnetic force-based multiplexed immunoassay using superparamagnetic nanoparticles in microfluidic channel. *Lab on a Chip* **2005**, 5, (6), 657-664.
11. Doria, G.; Conde, J.; Veigas, B.; Giestas, L.; Almeida, C.; Assunção, M.; Rosa, J.; Baptista, P. V., Noble metal nanoparticles for biosensing applications. *Sensors* **2012**, 12, (2), 1657-1687.
12. El-Ansary, A.; Faddah, L. M., Nanoparticles as biochemical sensors. *Nanotechnology, science and applications* **2010**, 3, 65-76.
13. Syed, M. A., Advances in nanodiagnostic techniques for microbial agents. *Biosensors and Bioelectronics* **2014**, 51, (0), 391-400.
14. Tran, P. T.; Anderson, G. P.; Mauro, J. M.; Mattoussi, H., Use of Luminescent CdSe-ZnS Nanocrystal Bioconjugates in Quantum Dot-Based Nanosensors. *Physica Status Solidi B* **2002**, 229, (1), 427-432.
15. Willard, D. M.; Van Orden, A., Quantum dots: Resonant energy-transfer sensor. *Nature Materials* **2003**, 2, (9), 575-576.
16. Medintz, I. L.; Uyeda, H. T.; Goldman, E. R.; Mattoussi, H., Quantum dot bioconjugates for imaging, labelling and sensing. *Nature Materials* **2005**, 4, (6), 435-446.
17. Goldman, E. R.; Clapp, A. R.; Anderson, G. P.; Uyeda, H. T.; Mauro, J. M.; Medintz, I. L.; Mattoussi, H., Multiplexed Toxin Analysis Using Four Colors of Quantum Dot Fluororeagents. *Analytical Chemistry* **2003**, 76, (3), 684-688.
18. Dennis, A. M.; Bao, G., Quantum Dots-Fluorescent Protein Pairs as Novel Fluorescence Resonance Energy Transfer Probes. *Nano Letters* **2008**, 8, (5), 1439-1445.
19. Zhang, C.-Y.; Yeh, H.-C.; Kuroki, M. T.; Wang, T.-H., Single-quantum-dot-based DNA nanosensor. *Nature Materials* **2005**, 4, (11), 826-831.

20. Freeman, R.; Girsh, J.; Willner, I., Nucleic Acid/Quantum Dots (QDs) Hybrid Systems for Optical and Photoelectrochemical Sensing. *ACS Applied Materials & Interfaces* **5**, (8), 2815-2834.
21. Goldman, E. R.; Medintz, I. L.; Whitley, J. L.; Hayhurst, A.; Clapp, A. R.; Uyeda, H. T.; Deschamps, J. R.; Lassman, M. E.; Mattoussi, H., A Hybrid Quantum Dots-Antibody Fragment Fluorescence Resonance Energy Transfer-Based TNT Sensor. *Journal of the American Chemical Society* **2005**, *127*, (18), 6744-6751.
22. Nikiforov, T. T.; Beechem, J. M., Development of homogeneous binding assays based on fluorescence resonance energy transfer between quantum dots and Alexa Fluor fluorophores. *Analytical Biochemistry* **2006**, *357*, (1), 68-76.
23. Kim, G. B. K., Y-P., Analysis of Protease Activity Using Quantum Dots and Resonance Energy Transfer. *Theranostics* **2012**, *2*, (2), 11.
24. Choi, Y.; Lee, J.; Kim, K.; Kim, H.; Sommer, P.; Song, R., Fluorogenic assay and live cell imaging of HIV-1 protease activity using acid-stable quantum dot-peptide complex. *Chemical Communications* **2010**, *46*, (48), 9146-9148.
25. Kim, Y.-P.; Oh, Y.-H.; Oh, E.; Ko, S.; Han, M.-K.; Kim, H.-S., Energy Transfer-Based Multiplexed Assay of Proteases by Using Gold Nanoparticle and Quantum Dot Conjugates on a Surface. *Analytical Chemistry* **2008**, *80*, (12), 4634-4641.
26. Kimura, R. H.; Steenblock, E. R.; Camarero, J. A., Development of a cell-based fluorescence resonance energy transfer reporter for Bacillus anthracis lethal factor protease. *Analytical Biochemistry* **2007**, *369*, (1), 60-70.
27. Krusinski, T.; Ozyhar, A.; Dobryszewski, P., Dual FRET assay for detecting receptor protein interaction with DNA. *Nucleic Acids Research* **2010**, *38*, (9), e108.
28. Zhang, C.-y.; Johnson, L. W., Quantifying RNA-Peptide Interaction by Single-quantum Dot-Based Nanosensor: An Approach for Drug Screening. *Analytical Chemistry* **2007**, *79*, (20), 7775-7781.
29. Dennis, A. M.; Rhee, W. J.; Sotto, D.; Dublin, S. N.; Bao, G., Quantum Dots-Fluorescent Protein FRET Probes for Sensing Intracellular pH. *ACS Nano* **6**, (4), 2917-2924.
30. Liu, B.; Zeng, F.; Wu, G.; Wu, S., Nanoparticles as scaffolds for FRET-based ratiometric detection of mercury ions in water with QDs as donors. *Analyst* **137**, (16), 3717-3724.
31. Suzuki, M.; Husimi, Y.; Komatsu, H.; Suzuki, K.; Douglas, K. T., Quantum Dot FRET Biosensors that Respond to pH, to Proteolytic or Nucleolytic Cleavage, to DNA Synthesis, or to a Multiplexing Combination. *Journal of the American Chemical Society* **2008**, *130*, (17), 5720-5725.
32. So, M.-K.; Xu, C.; Loening, A. M.; Gambhir, S. S.; Rao, J., Self-illuminating quantum dot conjugates for in vivo imaging. *Nat Biotech* **2006**, *24*, (3), 339-343.
33. Huang, X.; Li, L.; Qian, H.; Dong, C.; Ren, J., A Resonance Energy Transfer between Chemiluminescent Donors and Luminescent Quantum-Dots as Acceptors (CRET). *Angewandte Chemie International Edition* **2006**, *45*, (31), 5140-5143.
34. Nel, A.; Xia, T.; MÅrdler, L.; Li, N., Toxic Potential of Materials at the Nanolevel. *Science* **2006**, *311*, (5761), 622-627.

35. Cavaliere-Jaricot, S.; Darbandi, M.; KuÅşur, E.; Nann, T., Silica coated quantum dots: a new tool for electrochemical and optical glucose detection. *Microchimica Acta* **2008**, 160, (3), 375-383.
36. Michalet, X.; Pinaud, F. F.; Bentolila, L. A.; Tsay, J. M.; Doose, S.; Li, J. J.; Sundaresan, G.; Wu, A. M.; Gambhir, S. S.; Weiss, S., Quantum Dots for Live Cells, in Vivo Imaging, and Diagnostics. *Science* **2005**, 307, (5709), 538-544.
37. Kirchner, C.; Liedl, T.; Kudera, S.; Pellegrino, T.; Muñoz Javier, A.; Gaub, H. E.; Stölzle, S.; Fertig, N.; Parak, W. J., Cytotoxicity of Colloidal CdSe and CdSe/ZnS Nanoparticles. *Nano Letters* **2004**, 5, (2), 331-338.
38. Otsuka, H.; Nagasaki, Y.; Kataoka, K., PEGylated nanoparticles for biological and pharmaceutical applications. *Advanced Drug Delivery Reviews* **2003**, 55, (3), 403-419.
39. Moon, H. S.; Guo, D. D.; Song, H. H.; Kim, I. Y.; Jin, H. L.; Kim, Y. K.; Chung, C. S.; Choi, Y. J.; Lee, H. K.; Cho, C. S., Regulation of adipocyte differentiation by PEGylated all-trans retinoic acid: reduced cytotoxicity and attenuated lipid accumulation. *The Journal of Nutritional Biochemistry* **2007**, 18, (5), 322-331.
40. Kato, T.; Yashiro, T.; Murata, Y.; Herbert, D.; Oshikawa, K.; Bando, M.; Ohno, S.; Sugiyama, Y., Evidence that exogenous substances can be phagocytized by alveolar epithelial cells and transported into blood capillaries. *Cell and Tissue Research* **2003**, 311, (1), 47-51.

## **CHAPTER 2**

### **BACKGROUND AND LITERATURE REVIEW**

## 2.1 Colloidal Inorganic Nanoparticles for Biomedical Application

Colloidal inorganic nanoparticles (NPs) are small objects sized between 1 and 100 nanometers (nm) that can be dispersed in a solvent. During the last two decades, colloidal NPs have been attracting considerable interest from a wide range of disciplines, including materials science, chemistry, physics, biology and engineering, because of their unique physical and chemical properties. The change in those properties at this length scale from their bulk counterparts can be attributed to a combination of scaling factors and nature material of the NPs. These NPs can be composed of various materials including noble metal, semiconductor, magnetic compounds and a hybrid of them.

The biomedical utility of colloidal NPs can arise from a variety of attributes, including their physical properties such as optical (absorption or emission of light) and magnetic properties.<sup>1</sup> In addition, as biological processes generally occur at molecule level, the similar scale of NPs makes it a suitable platform for investigating those processes. For example, biomacromolecules surface recognition by NPs offer a potential tool for studying transcription regulation, enzymatic inhibition, delivery, sensing etc.

The aim of this chapter is to give a brief introduction of NPs of biomedical use and current strategies of surface functionalization and bioconjugation of colloidal inorganic NPs with a special focus the NPs with optical (semiconductor NPs, such as QDs) and magnetic properties.

### 2.1.1 Noble metal NPs

Noble metal NPs such as gold NPs and silver NPs are an important class of nanomaterials used in biomedicine due to their unique surface plasmon resonance (SPR) absorption. The SPR is caused by the interaction between incident light and oscillation of electron charge on the surface of NPs (Figure 2.1).



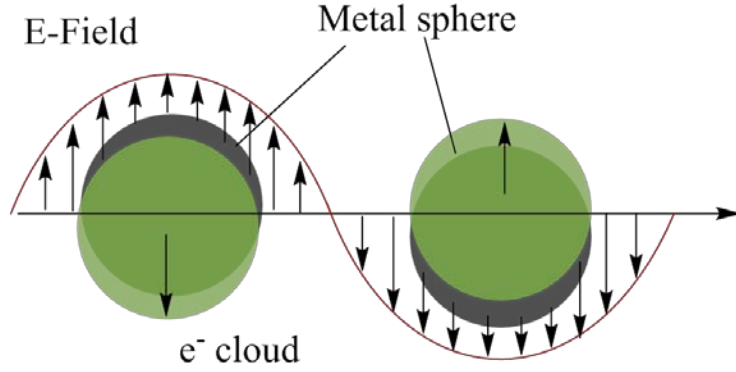


Figure 2.1 Schematic illustration of the SPR effect. The electromagnetic field of the light induces a coherent dipole oscillation of the metal conduction electrons across the nanoparticle (Adapted from Ref <sup>2</sup>).

The response of noble NPs to oscillating electric field can be described by Mie theory, if the diameter of a spherical NPs is much smaller than the wavelength of the incident light ( $\lambda$ ).<sup>3,4</sup> As shown in equation 2.1, the extinction cross section ( $C_{\text{ext}}$ ) of a particle (radius of  $R$ ), which defines the energy loss in the direction of incident light due to both absorption and scattering, is described in term of dielectric function of the metal ( $\epsilon = \epsilon' + i\epsilon''$ ) and dielectric constant of the medium  $\epsilon_m$ .<sup>3</sup> For small size of Au NPs (<60 nm), the absorption cross section dominates in the  $C_{\text{ext}}$ .<sup>5</sup>

$$C_{\text{ext}} = \frac{24\pi^2 R^3 \epsilon_m^{3/2}}{\lambda} \frac{\epsilon''}{(\epsilon' + 2\epsilon_m)^2 + \epsilon''^2} \quad \text{Equation (2.1)}$$

where  $\epsilon = \epsilon' + i\epsilon''$  is the wavelength-dependent, complex dielectric function of the NPs material and  $\epsilon_m$  is the dielectric constant of the surrounding/embedding medium.

The frequency of SPR is thus dependent on the size and composition of NPs, as well as the dielectric constant of medium. The change in SPR frequency yields the change of NPs color that can even be observed through bare eye. The SPR frequency is strongly sensitive to the dielectric constant ( $\epsilon$ ) of the surrounding media, such as surface ligand changes and inter-particle aggregation. This great sensitivity makes Au NPs and Ag NPs well suited for bioassay applications. For example, analytes such as DNA, metal ions and antibodies can be detected by observing the visible color changes due to Au NPs

aggregation.<sup>6-8</sup> Other examples are reviewed elsewhere including utilizing surface-enhanced Raman scattering (SERS) for sensing.<sup>9, 10</sup> In addition, the maximum wavelength of SPR absorption for Au NPs fall into the visible range (520 nm to 600 nm), which makes Au NPs as an excellent quencher to some common fluorophores for bioimaging and biosensing application via resonance energy transfer process.<sup>11</sup>

Au NPs also find their applications in assisting drug delivery and therapy, due to the high absorption cross-section. For instant, Halas *et. al.*, reported near-infrared light triggered gold nanoshells loaded hydrogels for delivering a soluble drug.<sup>12</sup> The mechanism is that heat generated from the absorption of light by Au NPs triggered the hydrogels to collapse and subsequently caused the release of the drug. Based on the similar concept, recently, functionalized Au NPs or Au-hybrid NPs have been shown as a versatile tool for photothermal cancer therapy<sup>13, 14</sup> and thermal ablation of pathogens.<sup>15</sup> It is a great advantage for such applications operating at NIR region, a transparent window for blood and other types of biological samples.

### 2.1.2 Semiconductor quantum dots

Quantum dots (QDs) are semiconductive and fluorescent crystalline particles that typically have diameters ranging from 2 nm and 10 nm. Semiconductors have a valence band filled with electrons and an empty conduction band separated by a band gap (Figure 2.2). An electron in the valence band can be excited into the highest level of the conduction band by absorbing a photon with energy higher than the band gap energy, leaving a hole of opposite charge in the valence band. An electron and its hole are attracted towards each other by Coulomb force, and together form an exciton. The distance between the excited electron and its hole is called the Bohr radius. QDs fluorescence occurs when the excited electron reverts to its hole in the lowest level of the valence band and emits a photon with equivalent to the band gap energy (lower than the absorbed).

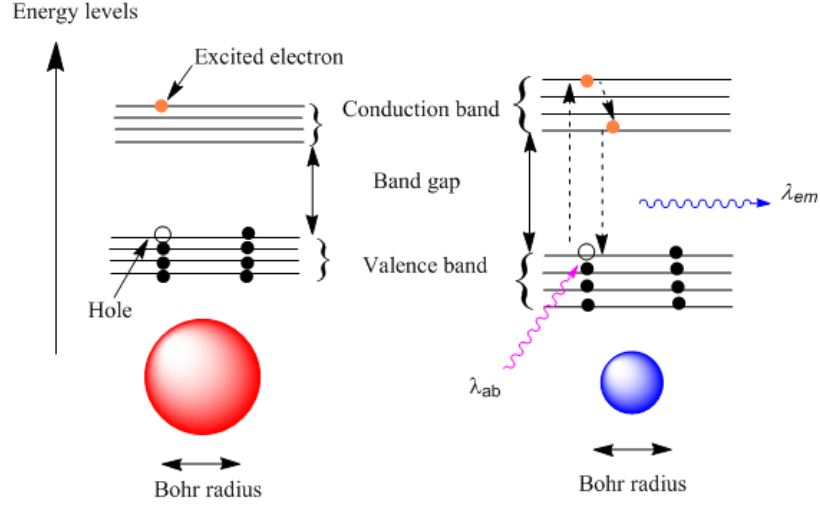


Figure 2.2 Size dependent photophysical properties of semiconductor quantum dots.

As the diameter of QDs is in the same order as its exciton Bohr radius, the excitons are squeezed, leading to quantum confinement effect. The energy required to excite the electron can be estimated in equation 2.2,<sup>16, 17</sup>

$$\Delta E = \frac{\hbar^2 \pi^2}{2R^2} \left[ \frac{1}{m_e} + \frac{1}{m_h} \right] - \frac{1.786e^2}{\epsilon R} - 0.248E_{Ry}^* \quad (\text{Equation 2.2})$$

where  $m_e$  is the free electron mass,  $m_h$  is the hole mass, and  $\epsilon$  is the size-dependent dielectric constant,  $R$  is the particle radius,  $\hbar$  is the reduced plank constant and  $E_{Ry}^*$  is the effective Rydberg energy that is usually small. The first term is band gap energy obtained by “particle in a box” model. The second and third term indicate Coulomb force and spatial correlation effect, respectively. The implications of the equation are clear that the energy of the QDs are dependent on their size due to the quantum confinement effects. Typically, smaller particles exhibit higher band gap energy and blue-shift emission.

The size-dependent fluorescent properties of QDs are superior to that of organic dyes in biomedical applications. Firstly, QDs possess broad absorption spectra while maintaining the same emission spectra. In addition, the emission profile is narrow and tunable, allowing for multiplexing labeling. Furthermore, the bright fluorescence and significant resistant to photobleaching, ensure a high ratio of signal to noise while applying them in imaging.

The pioneer work for utilizing QDs in biomedicine were reported by two groups in 1998, demonstrating water-soluble bioconjugated QDs as an excellent labeling agent for cell imaging.<sup>18, 19</sup> Since then QDs have been tested in various biological applications due to its bright fluorescence, including DNA array technology, immunofluorescence assays, labeling in cell and animal biology.<sup>20</sup> One benefit of using QDs as labeling agents is the ability to excite and detect several species simultaneously using one single light source.<sup>21, 22</sup> Besides severing as staining agents for bioimaging, QDs with bright fluorescence can be also used to study the dynamic process inside living cells at molecule level .<sup>23</sup> Apart from directly labelling, the narrow emission profile makes QDs as excellent donors for FRET based sensing and imaging (see also in Chapter 1). In addition to imaging, QDs were also used as photosensitizing agents for photodynamic therapy (PDT).<sup>24</sup>

### 2.1.3 Magnetic Nanoparticles

Magnetic nanoparticles (MNPs) are a class of NPs, which commonly consist of magnetic elements such iron, nickel and cobalt or their chemical compounds. The magnetic properties in matter are generally the consequence of the response of electrons magnetic moments (due to their rotation around nucleus and spinning up and down) to an external magnetic field. As shown in Figure 2.3, the materials can be classified into three categories including diamagnetic (zero net moment, repelled by external field), paramagnetic (zero net moment, attracted by external field), or ferromagnetic (exist net moment, attracted by external field), depending on their response to an external magnetic field.<sup>25</sup>

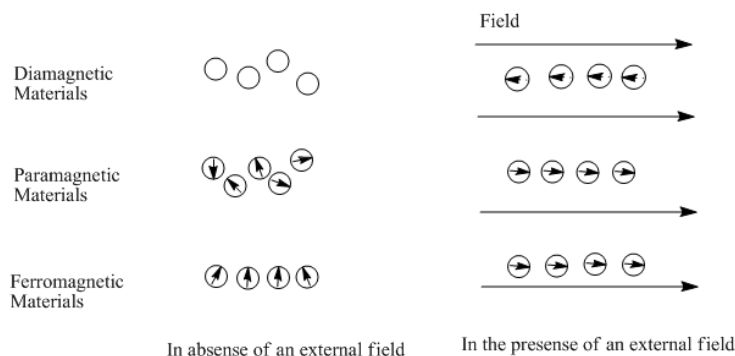


Figure 2.3 The responses of materials to magnetic field.

MNPs exploited in biomedical fields are commonly made of ferromagnetic materials. In such materials, the unpaired electron spins of an atom are interacting, leading to a parallel oriented magnetic moment and maintain a low energy state. The regions where the parallel orientation occurs are called magnetic domains. For energetic reasons, the size of the magnetic domain is usually smaller than the grain size. If the size of the magnetic materials is reduced when only one domain is reached (ranging from ~20 nm to several hundred nm), as in case of magnetic NPs, the magnetic behaviors are different from their bulk materials.

In single domain particles, the electron spins rotate in unison, flipping the entire magnetic moment of particles coherently and leaving a net magnetization and preferred aligned direction. As the size of particle ( diameter  $d$  for spherical particles) is reduced, the coercivity ( $H_c$ ), which is the intensity of the applied field to overcome this magnetization, drops to zero at the superparamagnetic limit  $d_{sp}$  (typically less than 40 nm). In such a case, particles that were originally aligned will have random directions at the measurement time without external field, due to thermal fluctuations of energy  $k_B T$  ( $k_B$  is Boltzman constant,  $T$  is measure temperature). For the same particles, their magnetic behavior can be affected by temperature. If the superparamagnetic particles are cooled, at certain temperature, the measurement time will be insufficient for complete magnetic relaxation, i.e. the particles will exhibit hysteresis ( $H_c > 0$ ). This temperature is known as the blocking temperature ( $T_b$ ). For example,  $T_B$  of 26 nm  $Fe_3O_4$  NPs is about 300 K (room temperature). Therefore, particles large than ~26 nm are predicated to exhibit ferromagnetism, while smaller ones should have superparamagnetism.<sup>26</sup>

Blocking temperature can be affected by particle size. The relationship between them can be obtained from Equation 2.3,<sup>27</sup>

$$T_B = \frac{E_a}{k_B \ln ft} \quad (\text{Equation 2.3})$$

Where  $t$  is the experimental measuring time,  $E_a$  is the anisotropy energy barrier that the magnetization flip has to overcome by thermal energy. The term in the denominator can

be treated as constant.  $E_a = KV$ , where  $K$  is the anisotropy energy density constant and  $V$  is the volume of particles. Thus, blocking temperature is size dependent.

Superparamagnetic NPs, in particular iron oxide MNPs, are widely designed for pre-concentration, separation, and identification of molecules and specific biological units and are particularly suitable for integration in micro fluidic devices.<sup>28, 29</sup> Additionally, the advantages of a very large surface area and good biocompatibility make these NPs suitable for integration with biological system.

The most important utilization of MNPs is separation and targeting of analytes. Numerous reports took the advantage of immuno-separation by antibody functionalized MNPs in detection of bacteria. In one example, Mujika and co-workers reported a magneto-resistive immunosensor for the analysis of *Escherichia coli* O157:H7 in food and clinical samples. This biosensor enabled to detect and quantify small magnetic field variations caused by the presence of superparamagnetic particles bound to the antigens previously immobilized on the sensor surface via an antibody–antigen reaction.<sup>30</sup> However, different methods for detection of MNPs become more and more important while incorporation with immuno-separation. Other common reported detection methods are impedimetric measurements<sup>31</sup> and electrochemical magneto-genosensing.<sup>32</sup> In the latter case, Liebana and colleagues reported the integration of immunomagnetic separation/double-tagging PCR/electrochemical magneto-genosensing to detect *Salmonella* in skimmed-milk samples with a limit of detection (LOD) of 1 colony forming-unit (cfu)/mL. By combining the magnetic separation and miniature technology, individual cells can now be separated through a microfluidic device system and visualized in a low power microscopy.<sup>33</sup> Another important aspect for taking the advantage of magnetic attraction property is the transport of drugs and gens by magnetic NPs. MNP medicated drug delivery can be performed via passive, active or direct ways.<sup>34</sup> Research work about the functionalization of MNP with emphasis on the active in vitro or in vivo drug delivery and related recent clinic results are reviewed by Pankhurst *et al.*<sup>35</sup>

In addition to separation and identification of target from matrix, MNPs have recently been used as labels in biosensing and bioimaging. For example, Koets and co-workers reported using streptavidin-coated superparamagnetic particles as detection labels for *E. coli* and *Salmonella* via a Giant Magneto Resistance (GMR) sensor.<sup>36</sup> An important use of MNPs now is for magnetic resonance imaging (MRI) application where the NPs are introduced as contrast-providing agents which have been summarized elsewhere.<sup>37-40</sup>

Despite of few examples, MNPs can also be used as antiseptic agents. There are main two methods to modify magnetic NPs to obtain the antimicrobial NPs. The first one is to functionalize NPs with biomolecules of antimicrobial activity. For example, in the study conducted by Kaittanis, C. *et. al.*, Con A-conjugated polysaccharide magnetic NPs have been shown with significant and fast inhibition of the growth of *E. coli* and *S. marcescens* in blood culture.<sup>41</sup> In another work, Chen *et. al.* reported that the immobilization of antimicrobial peptide LL-37 on the surface of polyacrylic acid coated NPs can effectively kill *E. coli*.<sup>42</sup> The second method to enable magnetic particles with antimicrobial properties is to coat them with inorganic/organic antibacterial layers. For instance, silver NPs and TiO<sub>2</sub> layer have been deposited onto the surface of magnetic particles to produce antibacterial agents.<sup>43, 44</sup>

## 2.2 Synthesis of colloid NPs for biomedical use

Colloidal inorganic NPs can be synthesized by various physical and chemical methods, with the particles differing in their elemental composition, shape, size and chemical or physical properties.<sup>45</sup> The physical methods in general involve vapor deposition approaches which dependent on sub-dividing of bulk materials to smaller NPs. Typical chemical ways involve the reduction of ions into atoms in the presence of stabilizing agents, followed by controlled growth of atoms into NPs (so called “bottom-up” process).<sup>46</sup> In the case of biomedical applications, solution based chemical synthesis methods have been proved preferable ways, as they are more effective to control the size distribution and ready for further modification or conjugation with biological species. In this way, as-synthesized NPs are dispersed in a solvent either water- based or an organic solvent for hydrophilic or hydrophobic particles, respectively; meanwhile amphophilic NPs can be dispersed in both kinds of solvents.

### 2.2.1 Synthesis of NPs in water

A variety of NPs including Au,<sup>47, 48</sup> Ag,<sup>49</sup> Co,<sup>50</sup> Fe<sub>3</sub>O<sub>4</sub>,<sup>35</sup> Fe<sub>2</sub>O<sub>3</sub>,<sup>51</sup> SiO<sub>2</sub><sup>52</sup> and CdTe<sup>53, 54</sup> have been synthesized in aqueous solution. These methods produce water-dispersible NPs, a necessity for the application in biological systems. One typical example is the synthesis of noble metal NPs such as Au NPs by reduction of Au(III) salts using reducing agents such as sodium citrate, citric acid, ascorbic acid or amines.<sup>55</sup> In addition, biomolecules (e.g. starch) are also used as reducing agents providing a green protocol. In another way, aqueous co-precipitation process, which involves nucleation growth, coarsening and /or agglomeration, has been widely used in preparation of metallic and metal (hydr) oxides NPs. The composition and morphology of the NPs are controlled by precisely adjusting the reaction parameters.<sup>56</sup> Stöber method, an aqueous sol-gel process, is established to synthesize SiO<sub>2</sub> NPs.<sup>52</sup> Success has also been achieved in synthesis of water-soluble semiconductor CdSe and CdTe quantum dots.<sup>54</sup> However, limits in controlling a narrow size distribution and low ordered crystalline structure remain as main challenges, which subsequently affect their physical properties and stabilities.

### 2.2.2 Synthesis of NPs in organic phase

NPs composed of noble metals, transition metals, oxides and semiconducting materials have been synthesized in organic phase via a thermal decomposition process. The process general involves high temperature thermolysis of metal-organic precursor in the presence of a hydrophobic capping agent, as well as in a non-polar organic solvent. The resultant NPs usually gain high quality of nanocrystals.<sup>57</sup> The growth of NPs, the crystal structure and the cessation of growth depend on the environment and are fundamentally regulated by the hydrophobic ligand. These ligands are either surfactant species such as fatty acid or alkane thiols. The obtained NPs are thus inevitably hydrophobic. The ligands in some cases also serve as solvent. One example is using tri-*n*-octyl phosphine oxide (TOPO) for capping the semiconductor quantum dots.<sup>58</sup>

Hydrophilic NPs can also be produced in one-pot synthesis in organic phase by using dedicatedly selected stabilisation ligands. For instant, amphiphilic ligands such as peptides<sup>50</sup> and thermo-responsive polymers<sup>59</sup> have been used in preparation of Co NPs.



However, only few examples have been reported due to the limit of amphiphilic materials.

## 2.3 Surface Functionalization of NPs

A large portion of NPs used in biomedicine is produced in organic phase through high temperature process. High-temperature synthesis in organic phase offers a number of advantages over aqueous synthesis. Firstly, high temperature allows the impurities of NPs be annealed out to obtain good crystallite structure. Furthermore, long chain of organic ligands enables steric stabilization of NPs and allows higher concentration of NPs to be produced. Moreover, temperature can be used to manipulate the morphology and size of the NPs through controlling the growth kinetics of crystals. However, the resultant NPs with apolar ligand are only soluble in organic solvents, e.g., hexane, toluene or chloroform. They usually cannot be used directly for most applications in biomedicine, as most biological process occurs at aqueous environment. Therefore, it is necessary to bring them with water solubility, prior to the use them in biomedicine. One method to circumvent this problem is development of strategies for surface functionalization of NPs. Such strategies should satisfy certain criteria: i) they can enable NPs with good water solubility, ii) they should offer a reduction of toxicity of NPs in some instances, iii) they can provide additional functionalities for further conjugation of biomolecules for targeting applications, and iv) they can stabilize the physical properties of NPs. Here a variety of strategies for surface functionalization of NPs are evaluated and compared to their effect on parameters relevant to stability, nonspecific binding, and biocompatibility of NPs. The discussion falls in three categories: ligand exchange, ligand modification and ligand addition (encapsulation), as shown in Figure 2.4.

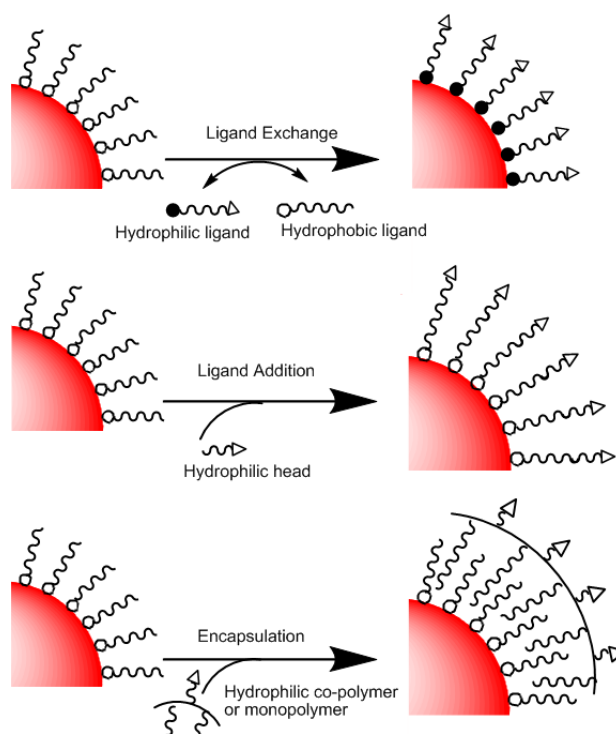


Figure 2.4 Schematic illustrations of common surface functionalization strategies.

### 2.3.1 Ligand exchange

For biomedical applications, ligand exchange of NPs usually involve a process that the initial hydrophobic ligands are replaced by other more strongly bonding hydrophilic ligands that allow the transferring of NPs from organic phase to aqueous solution. A number of hydrophilic ligands have been reported to exchange the nature ligand on the surface of NPs and bring them to aqueous solution, including small molecules with functional headgroups (e.g. thiol, carboxyl, amine, phosphine group, etc.), PEG derivatives and biological molecules (Figure 2.5).

*Small molecules.* Small molecules with high affinity head functional group are primary candidates for generating water-soluble particles, as they produce NPs with a smaller hydrodynamic radius, which promotes *in vivo* trans membrane permeation and excretion of NPs.<sup>60</sup> Common examples of small molecules are alkylthiol terminated molecules that can strongly bind to the inorganic surface of NPs, e.g. Au and Ag<sup>61</sup> or CdSe QDs,<sup>18, 62-65</sup> by replacing weaker ligands. However, the colloid stability of the resultant NPs in buffer solution is often poor which is partially attributed to the desorption of ligands from

NPs.<sup>64</sup> To overcome this problem, bidentate ligands such as dihydropolipoic acid (DHPLA) and dithiocarbamate ligands are used to stabilize the NPs by increasing the number of anchor points to particle surface.<sup>66-68</sup> In addition to alkyl thiol terminated ligand molecules, many molecules with other functional headgroups have also been developed to transfer NPs from organic phase to aqueous solution. Excellent examples include tetraalkylammonium salts such as tetraoctylammonium bromide (TOAB) for transfer of AuNPs, and hexadecyltrimethylammonium bromide (CTAB) for iron oxide NPs;<sup>69, 70</sup> oligomeric phosphine (oxide) ligands for transfer TOP/TOPO capped QDs;<sup>71</sup> amphiphilic species such as 2, 3-dimercaptosuccinic acid (DMSA)<sup>72</sup> and cyclodextrin<sup>73</sup> for transferring of oleic acid capped NPs, respectively. However, one drawback is that the small ligands rely on electrostatic interaction to stabilize NPs. Therefore, when the solution condition such as pH and salt concentration changed, the NPs may be “salting out” and forming aggregation.

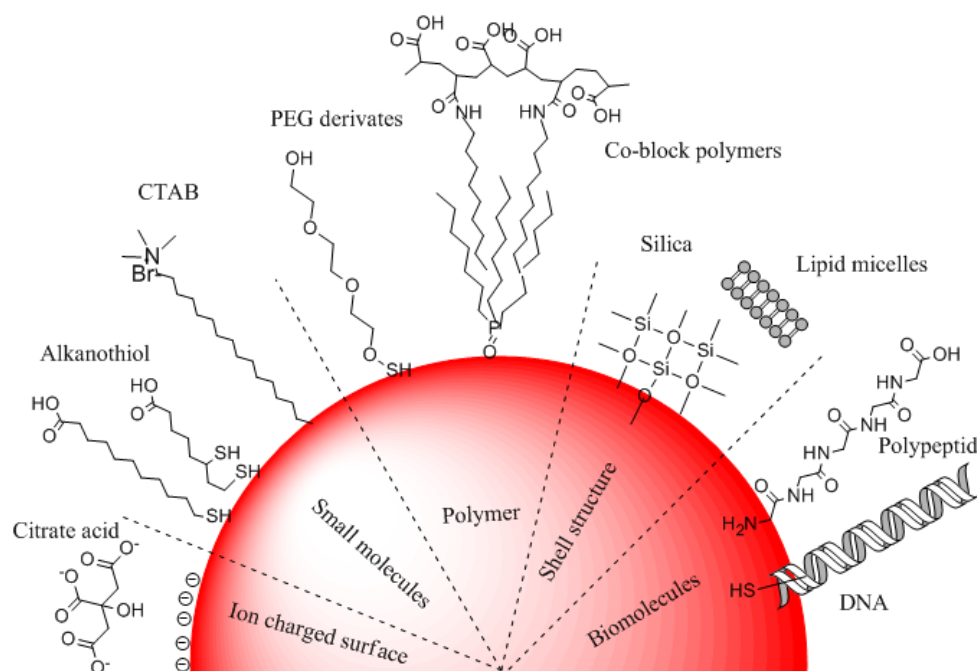


Figure 2.5 Common ligands for stabilizing NPs in water.

*PEG derivatives ligands.* An alternative is using polymeric ligands as ligand exchange agents to overcome the poor colloidal stability of NPs that capped by small molecules. A number of polymers have been reported to offer NPs with good stability and water solubility. Among them, poly (ethylene glycol) (PEG) is the most common reported ligands for stabilizing NPs especially in biomedical applications. The ether group in the backbone of PEG chains utilizes hydrogen bonding and steric stabilization for water solubility, instead of electrostatic interactions. It is thus expected that PEG based NPs would confer well stability over a wide pH range and even at high salt concentration. Taking advantage of this, Mattoussi's group developed a set of DHLA-PEG derivatives for capping QDs through ligand exchange.<sup>74, 75</sup> As a result, by combining the benefit of strong bonding through dithiol moiety to particle surface, the PEG based QDs confer water solubility over a wide pH range and high salt concentration. In addition to good particle stability, PEG based NPs also were also found with low degree of nonspecific binding to biological components, less cytotoxicity and longer circulation time in vivo.<sup>76, 77</sup> Due to those advantages, it has been now increasing common to use PEG segments for capping NPs to improve the biocompatibility.<sup>78</sup> However, it should note that PEG itself is simply a polyether, in general it should be modified with reactive terminal functional group to serve as an anchor to the NPs.

*Biomolecules.* Other exchange ligands involved are biomolecules such as sugars, peptide, nucleic acid and their derivatives. In one example, glucose and sucrose have been used in reduction and post-synthesis stabilization of Ag and Au NPs in aqueous salts.<sup>79</sup> Small peptides are also used as QDs surface ligands. Pinaud and co-workers developed phytochelatin-like peptides replacing TOPO for coating CdSe/ZnS QDs.<sup>80</sup> The advantage to use peptides as surface ligands is they offer an all-in-one solution for particles solubilisation and biofunctionalization. Several other examples will be discussed in the biofunctionalization part.

### 2.3.2 Ligand modification

A different strategy from ligand exchange is in situ modification of ligand for phase transfer, which can prevent NPs aggregations due to irreversible desorption of replaced ligands. This strategy can be achieved by either modifying a compound that can change

the polarity (e.g. oxidation of oleic acid to form carboxyl group or vicinal diol <sup>81</sup>), or addition of hydrophilic agent which can interact with the hydrophobic ligand (e. g. formation of a complex of cyclodextrin with oleic acid,<sup>73</sup> or covalent conjugation with amphiphilic agents (e. g. conjugation with V-shaped ligand <sup>82</sup>). Despite of high efficient phase transfer, this concept is merely limited to certain systems.

### 2.3.3 Ligand addition

Ligand addition involves an addition of the external surface of the NPs shell without removal of any initial ligands. The strategies include addition of a layer of inorganic materials and encapsulation of a layer by intercalating hydrophobic polymers into the initial hydrocarbon shell of NPs.

*Inorganic core-shell structures.* One of the major challenges for functionalizing NPs is find a common agent/ligand for ubiquitously capping the NPs. However, as for organic molecules capping, it is necessary to select specific head groups of ligands that have high affinity the NP core. This will limit its applications. Alternatively, coating NPs with an inorganic layer/shell for which the ligand has a high affinity is of great interesting. Materials, such as noble metal (Au and Ag), semiconductor (e.g. ZnS) and silica, have been used as NP shell to protect the core, add functionality or introduce chemical group for further functionalization.

Probably, one of the most widely used methods for surface coating of NPs is silica coating. The advantages silica coating includes enhanced water soluble, good colloidal stability, low non-specific interaction and biocompatibility.<sup>83</sup> A typical process to grow a silica shell around NPs involves firstly exchanging of hydrophobic ligands with primer molecules, such as 3-(trimethoxysilyl) propyl methacrylate (MPS) and 3-aminopropyl-triethoxysilane (APTS) by selection of the precursors specific for each NP material. Then the growth of a amorphous silica shell can be processed via hydrolysis of sodium silicate (Iler process) or tetraethoxyxillane in alcohol (Stöber method).<sup>84, 85</sup> A modified method involving the base-catalysed hydrolysis of tetraethyl orthosilicate (TEOS) has now been widely used. One advantage of this method is the capability of controlling of silica shell thickness by simple adjusting the ratio of component in the reaction mixture

(ethanol:water).<sup>86</sup> The pH is very important for hydrolysis of TEOS. Mildly alkaline pH (7.5) is found as the optimum point for formation of core-shell structure.

Using the same chemistry, secondary silanes with ionizable hydrophilic groups can be introduced on the initial silica shell to render NPs hydrophilic or add chemical functionality. For example, incorporation of PEG chains can improve the stability and biocompatibility of the silica coated NPs. Functionalization with APS and MPS can facilitate the covalent binding with biomolecules through amine and thiol group, respectively. Mesoporous silica can also grow on the surface of NPs, just after the formation of a thin layer of amorphous silica as describe above. Cationic surfactants such as CTAB have been used as templating materials to synthesize mesoporous silica shell on NPs surface.<sup>69, 87-89</sup> The mesopores allow loading of drugs such as doxorubicin and ibuprofen to serve as devilry cargo.<sup>89, 90</sup>

So far, the silica shell have been successfully deposited on a variety of colloidal particles of metals,<sup>84, 91-93</sup> metal oxides,<sup>94, 95</sup> and semiconductors.<sup>19</sup> However, the growth of silica shell in general results in increasing of the hydrodiameter of the NPs, which consequently may affect the physical properties of NPs, e.g. deterioration of saturation magnetisation whiling coating magnetic particles.<sup>96</sup> In addition, polymeric silica present in the NPs surface can cause NPs aggregation by slow hydrolysis process without further surface modification.<sup>97</sup>

*Polymer encapsulation via hydrophobic interactions.* Polymer encapsulation involves over-coating hydrophobic ligand capped NPs with amphiphilic polymers. The encapsulation is achieved by intercalating the hydrophobic portion of polymer with the initial ligand on the NPs surface and rendering hydrophilic portion towards the solution. Head groups, such as carboxyl or amine groups, and/or PEG segment within the hydrophilic portion of the polymer, bring NPs water solubility. The functional group can further allow for bio-conjugation or bio-modification of NPs. Initially, phospholipids, which can form micelles with 5 nm hydrophobic interior, were used to over-coat TOPO capped NPs and render them water-dispersibility.<sup>98-101</sup> However, the resultant NPs suffered from poor stability because of desorption of the relative weak anchoring

phospholipids from the NPs. To improve the stability, low water-soluble fatty acids were used to generate lipid bilayers coated NPs.<sup>102</sup> An alternative is using amphiphilic co-block polymers, of which a single polymer contains multiple hydrophobic side chains to enforce the hydrophobic interaction. Wu *et. al.*, developed a co-block polymer for coating TOP/TOPO capped QDs.<sup>103</sup> The strategy involves appending a poly(acrylic acid) (PAA) back-bone by hydrophobic octylamine chains through EDC mediated conjugation, following by coating to QDs. In their report, 40% of the carboxylic group of on the PAA back-bone were converted by hydrophobic alkyl chain. The octylamine chains then intercalated into hydrophobic TOP/TOPO ligands on the QD surface, and the remaining negative carboxylic groups could then promote the particle water-soluble. Some other amphiphilic co-polymers such as poly(maleic anhydride alt-1-tetradecene)<sup>104</sup> and PEGylated polymer<sup>105, 106</sup> were also reported to generate hydrophilic QDs. The significant advantage of using polymer coating is that, theoretically, a wide range of different NPs can be transferred into water with one optimal amphiphilic polymer. The over-coated NPs in general can also benefit from excellent colloidal stability over a wide pH rang and at high salt concentrations.

## 2.4 Bioconjugation

Surface functionalization can render NPs water-solubility, functionality and stability in physiological environment. After that, NPs are required to conjugate with biomolecules of interest (e.g. small bioactive molecules, peptide, proteins, nucleic acid, etc.) for further biomedical applications. Many conjugation strategies have been developed. Here some common used methods are discussed below (Figure 2.6).

### 2.4.1 Direct absorption

Biological species can interact directly with different kinds of NPs. Non-specific staining of certain cellular structure may be achieved by injecting hydrophilic NPs into cytoplasm.<sup>107</sup> The NPs even without additional functionalization have been shown to attach to certain place inside cell.<sup>108</sup> However, the interaction is usually weak and non-specific, and has limited uses. Instead, the signal generated from non-specific interaction may interfere with the real measurement. Thereby, the direct absorption of biomolecules

by NPs mentioned here refers to the specific attachment of certain biological molecules to NPs with relative strong non-covalent interaction.

Biomolecules with special functional groups can be directly linked to NPs. For examples, thiol groups from cysteine amino residue can be used to coordinated peptides or proteins to noble metal NPs<sup>109</sup> and QDs.<sup>110</sup> Similarly, DNAs oligos terminated with thiol group have also been labelled to those NPs.<sup>63, 111, 112</sup> Furthermore, metal-affinity driven self-assembly is also utilized for the conjugation of biomolecules to NPs. One example is polyhistidine (six histidine residues) tags (His tag) can allow strong and reversible conjugation of proteins or peptides on the Ni-nitrilotriacetic acid (Ni-NTA) modified NPs.<sup>113-115</sup> More interesting, His tag appended protein were also found to directly coordinate with the metal zinc ions of the ZnS coated QDs.<sup>116</sup>

A different approach is the absorption of biomolecules to NPs surface via electrostatic interactions. For instant, negatively charged nucleic acid can be attached to the positive charged surface of NPs.<sup>117, 118</sup> Proteins, which have a natural positive (or negative) charge under physiochemical environment, can also adhere to NPs with negative (or positive) charges. Others neutral charged proteins could be engineered with charged domain to enhance the adsorption to NPs surface. Mattoussi *et. al.*, have engineered maltose binding protein (MBP)<sup>66</sup> and protein G with a positively leucine zipper domain.<sup>119</sup> The engineered proteins can then adhere to the surface of DHLA capped QDs. As the attachment is mediated by electrostatic interaction, the conjugation is simple dependent on the surface charge of NPs, regardless of the material of NPs. There are, however, some drawbacks with this approach, including sensitive to pH and salt concentration, high degree of non-specific binding, and required engineering of proteins in some cases.

#### 2.4.2 Covalent coupling

Covalent coupling provide specific and stable conjugation of biomolecules with NPs. Typically, functional groups on the NPs surface including carboxylic group, amide group and thiol group can cross-link with biomolecules through various coupling strategies (Figure 2.6). Some common strategies are discussed below based on the functional groups involved.



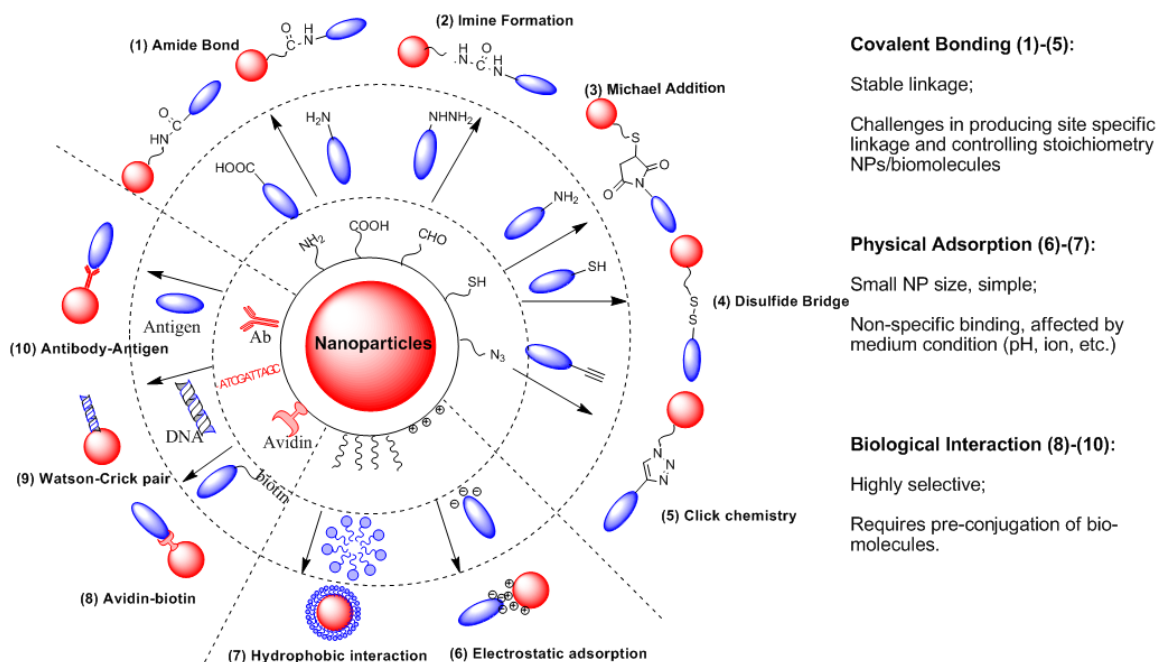


Figure 2.6 Representative bioconjugation protocols.

*Amine group involved coupling.* Probably the most commonly coupling methods for bioconjugation of NPs involve amine functional group. Primary amine can react with carboxylic group to form a “zero length” amide bonds. The linkage is usually mediated by carbodiimide agents, such as most commonly used 1-ethyl-3-(dimethylaminopropyl) carbodiimide (EDC) (Figure 2.7a). The conjugation strategy has been applied to coupling of various proteins (e. g. enzyme and antibodies) <sup>18, 120-125</sup> amine-terminated nucleic acid, <sup>124, 126</sup> small molecules with amine groups, <sup>127, 128</sup> etc., to carboxylic group functionalized NPs. Few cases are also found between amine functionalized NPs and carboxylic groups on biomolecules. More specifically, the coupling efficiency can be enhanced by addition of stabilising agents such as *n*-hydroxysuccinimide (NHS) or sulfo-NHS by formation of a succinimide ester intermediate.<sup>129</sup> A variation of this strategy is using bis-NHS to cross-link two amines group.<sup>130</sup>

In addition to carboxylic group, the active nucleophilicity allows amine group to react some other functional groups, such as aldehydes, thiol group, epoxides and isocyanates.

For example, glutaraldehyde was used to conjugate enzymes to NPs surface by bridging two amines from each species.<sup>131</sup> The space of the linkage is approximately 0.7 nm.<sup>132</sup>

*Thiol group involved coupling.* The thiol group can selectively conjugate with primary amine groups. The reaction starts rapidly under the mediation of reagents such as maleimides and iodoacetamides.<sup>133, 134</sup> Most commonly, the coupling reagent is sulfosuccinimidyl-4-(maleimidomethyl) cyclohexane-1-carboxylate (sulfo-SMCC) (Figure 2.7b). To take advantage of this reaction, amine-functionized NPs can be conjugated with various thiolated biomolecules, including thiol modified peptide,<sup>135</sup> residue thiol-terminated DNA,<sup>107</sup> or peptides and proteins with free or reduced cysteine,<sup>136</sup> or verse vice.<sup>137, 138</sup> Disulfide bridges can be also used for reversible coupling of NPs. By utilizing of glutathione (GSH) disulfide and dithiothreitol, Tian *et al.*, showed reversible oxidation and reduction of disulfide bridges between silica NPs and Fe<sub>3</sub>O<sub>4</sub> NPs,<sup>139</sup> respectively. The same approach was adapted for delivering and releasing of drug via hybrid nanostructures, under the regulation of GSH.<sup>140</sup>

*Click chemistry.* Another common approach for bioconjugation is the so called “click chemistry”. The reaction basically involves coupling of alkyne to an azide giving a 1,2,3-triazole ring under catalyst of Cu (I). The process has been demonstrated to be highly versatile and great potentials for bioconjugation of NPs.<sup>141</sup> The one-step click process has also been shown to give the possibility of introducing multiple functionalities onto NPs.<sup>142</sup> The limitation probably is that it requires special preparation of the azide or alkyne-functional bioactive species, which is often involved a labor work and has low yielding.<sup>143</sup> Fortunately, now many commercial kits have been developed to simplify the process and improve the products yield.<sup>144</sup>

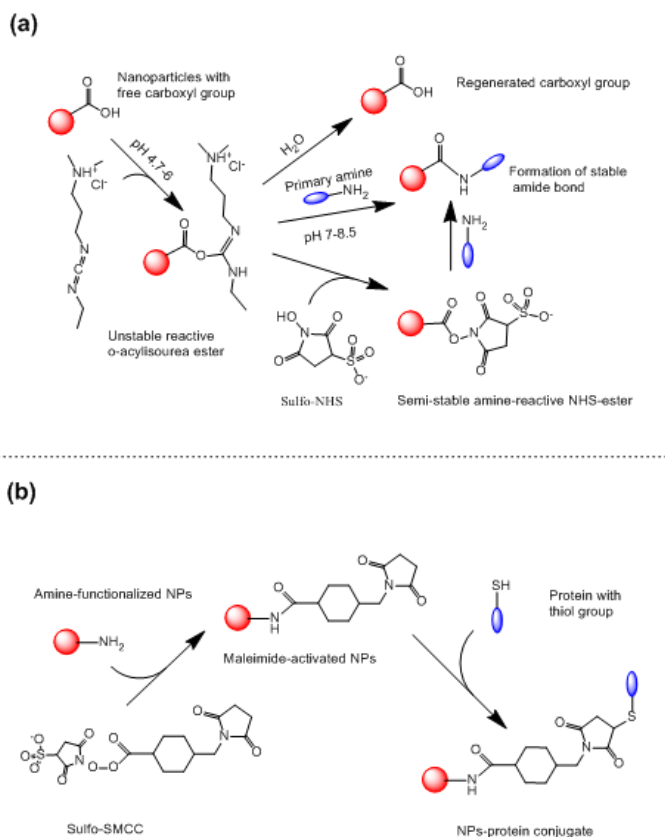


Figure 2.7 Reaction scheme for EDC-NHS crosslinking (a) and (b) SMCC mediated conjugation.

### 2.4.3 Biological approaches

Biological processes are often completed by highly specific interactions of biomolecules, such as antibody-antigen interaction, receptor and target interaction, enzyme and substrate interaction, and complementary base pair of nucleic acid. It is thus possible to take the advantages of those high specific interactions for bioconjugation of NPs. For example, single oligo DNA functionalized NPs were used to specific recognize target genetic materials.<sup>145, 146</sup> Furthermore, DNA aptamers functionalized Au NPs were reported to bind and response to different of analytes.<sup>147</sup> Moreover, protein G functionalized NPs have been used to immobilize IgG via interactions with Fc region of the antibody, leaving the free Fab region for capturing staphylococcus bacteria.<sup>148</sup> One of the most common used biological interaction is the (strept)avidin-bintin interaction which has a very high affinity ( $K_{diss} > 1.3 \times 10^{15}$  M). NPs can firstly functionalized with

(strept)avidin via either electrostatic absorption or covalent coupling methods. After that, the NPs can then be used to label biotinylated peptides, proteins, antibodies and DNA.<sup>121, 149-</sup>

<sup>152</sup> Antibodies and receptor/ligand biomolecules require a binding domain to be exposed and accessible in order to be biologically active. However, even taking advantages of high specific interaction and high efficiency covalent coupling strategies, it is still a problem to control the orientation of biomolecules attached to NPs.

To overcome the problem, recently expressed protein ligation (EPL) attracts some interest as it allows for site-specific conjugation of targeting molecules to NPs. EPL refers to a native auto-processing chemical ligation mediated by a protein called intein in a biological system. The process involves a recombinant protein with a C-terminal thioester and a second agent with an N-terminal cysteine. This C-terminal thioester is usually introduced by intein which can be cloned downstream of the target protein (Figure 2.8).<sup>153</sup> A transthioesterification reaction occurs between thioester and amine of the cysteine, followed by a rapid S → N acyl transfer to form an amide. Several studies have shown the versatility of EPL for site-specific bioconjugation of hydrazine nucleophiles modified NPs with engineered proteins.<sup>154, 155</sup> However, as the efficiency of the conjugation depends on high concentration of both functional groups, it is relatively low while applied in NPs conjugation due to low concentration of NPs used. To overcome this problem, a two-step strategy was developed, which involves ligation of azide (alkyne) modified small nucleophilic molecule with engineered protein by EPL, and followed by conjugating of the azide (alkyne) linked protein with alkyne (azide) modified NPs via click chemistry.<sup>156, 157</sup> It is expected that this EPL can offer great opportunities for conjugation of NPs with various enzymes or other proteins, particularly for biosensing applications. The limitation is that it is still required to genetically modify proteins by recombinant DNA technology.

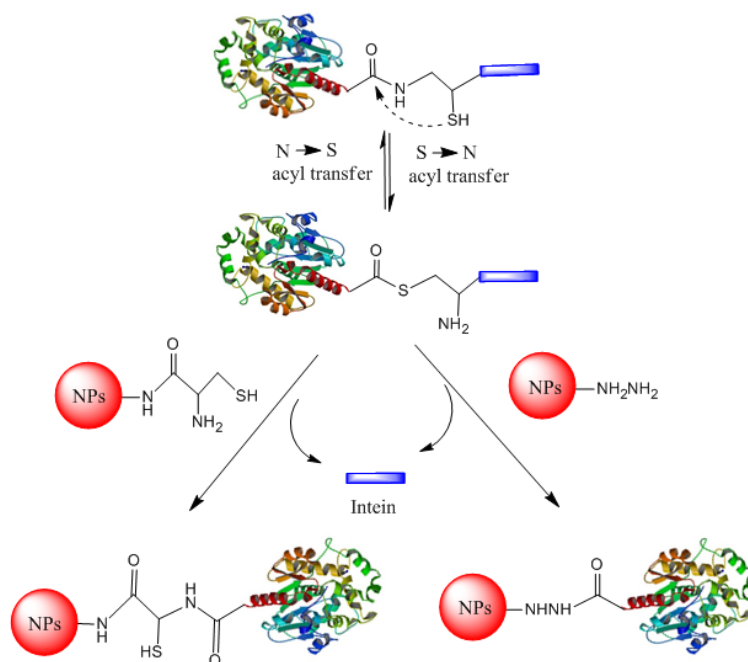


Figure 2.8 Mechanism of intein mediated bioconjugation.

## 2.5 Summary

Surface functionalization of NPs is considered as a prerequisite for their biomedical applications. In general, an ideal surface should satisfy criteria such as providing good water stability and chemical functionality for further functionalization, maintaining NPs physical and chemical properties, and biocompatibility. Through the approaches discussed above, ligand exchange involves a simple process, even without affecting the particles size. However, it often compromises the stability of NPs, as the ligands tend to dissociate from the surface leading to the particles aggregation. In the case of QDs, the dissociation of ligand can result in decreasing of fluorescence efficiency. Polymer encapsulation is of great advantage, as it results in better stability and preservation of NPs physical properties (e.g. magnetization and photoluminescence). However, additional steps are required for formation of polymer and hydrodiameter of polymer coated NPs is usually large. In addition, the universal amphiphilic polymer to coat a wide range of NPs, though possible, is still under research. Incorporation of PEG backbone can increase the

biocompatibility. The drawback, however, is that encapsulation increases the particle size significantly. Therefore, it remains a challenge to satisfy all the criteria.

On the other hand, directly coating peptide and protein on NPs are not often used, which could achieve relative small hydrodynamic diameter of NPs. For example, absorption relying on type of NPs and biomolecules with certain groups; meanwhile, electrostatic assembly requires strict physiological conditions, to avoid dissociation and nonspecific binding. Covalent bioconjugation approach probably is the most widely used bioconjugation method as it forms stable linkages. However, the stoichiometry of NPs/biomolecule is hard to control and it may cause self-assembly and biomolecules and aggregation of NPs. In addition, the controlling of the orientation of biomolecules immobilized to the surface of NPs is still a challenge. While biological affinity based methods, such as antibody/antigen conjugation, offer highly specific interaction, the drawback is it often leads to a large structure. Small protein mediated conjugation is attractive, as the reaction is highly selective, similar to enzyme catalysis. The efficiency may need to improve. It is anticipated that these biomacromolecules (such as enzyme or bio-molecules likewise) will be promising agents for biofunctionalization of NPs in future, just like they work inside of biological systems.

Therefore, the challenges remain in development of proper strategies in surface functionalization and bioconjugation of NPs with enhanced chemical and physical properties for desired applications in biomedicine.

## 2.6 References

1. Ferrari, M., Cancer nanotechnology: opportunities and challenges. *Nature Reviews Cancer* **2005**, 5, (3), 161-171.
2. Kelly, K. L.; Coronado, E.; Zhao, L. L.; Schatz, G. C., The Optical Properties of Metal Nanoparticles: The Influence of Size, Shape, and Dielectric Environment. *The Journal of Physical Chemistry B* **2002**, 107, (3), 668-677.
3. Mulvaney, P., Surface Plasmon Spectroscopy of Nanosized Metal Particles. *Langmuir* **1996**, 12, (3), 788-800.
4. Link, S.; El-Sayed, M. A., Optical properties and ultrafast dynamics of metallic nanocrystals. *Annual Review of Physical Chemistry* **2003**, 54, (1), 331-366.
5. Hodak, J. H.; Henglein, A.; Hartland, G. V., Photophysics of Nanometer Sized Metal Particles: Electron-phonon Coupling and Coherent Excitation of Breathing

- Vibrational Modes. *The Journal of Physical Chemistry B* **2000**, 104, (43), 9954-9965.
6. Liu, J.; Lu, Y., Colorimetric Biosensors Based on DNAzyme-Assembled Gold Nanoparticles. *Journal of Fluorescence* **2004**, 14, (4), 343-354.
  7. Oldenburg, S. J.; Genick, C. C.; Clark, K. A.; Schultz, D. A., Base pair mismatch recognition using plasmon resonant particle labels. *Analytical Biochemistry* **2002**, 309, (1), 109-116.
  8. Reynolds, R. A.; Mirkin, C. A.; Letsinger, R. L., Homogeneous, Nanoparticle-Based Quantitative Colorimetric Detection of Oligonucleotides. *Journal of the American Chemical Society* **2000**, 122, (15), 3795-3796.
  9. Tian, Z.-Q.; Ren, B.; Wu, D.-Y., Surface-Enhanced Raman Scattering: From Noble to Transition Metals and from Rough Surfaces to Ordered Nanostructures. *The Journal of Physical Chemistry B* **2002**, 106, (37), 9463-9483.
  10. Storhoff, J. J.; Elghanian, R.; Mucic, R. C.; Mirkin, C. A.; Letsinger, R. L., One-Pot Colorimetric Differentiation of Polynucleotides with Single Base Imperfections Using Gold Nanoparticle Probes. *Journal of the American Chemical Society* **1998**, 120, (9), 1959-1964.
  11. Sen, T.; Patra, A., Recent Advances in Energy Transfer Processes in Gold-Nanoparticle-Based Assemblies. *The Journal of Physical Chemistry C* **2012**, 116, (33), 17307-17317.
  12. Serksen, S. R.; Westcott, S. L.; Halas, N. J.; West, J. L., Temperature-sensitive polymer-nanoshell composites for photothermally modulated drug delivery. *Journal of Biomedical Materials Research* **2000**, 51, (3), 293-298.
  13. Nam, J.; Won, N.; Jin, H.; Chung, H.; Kim, S., pH-Induced Aggregation of Gold Nanoparticles for Photothermal Cancer Therapy. *Journal of the American Chemical Society* **2009**, 131, (38), 13639-13645.
  14. Xu, C.; Wang, B.; Sun, S., Dumbbell-like Au-Fe<sub>3</sub>O<sub>4</sub> Nanoparticles for Target-Specific Platin Delivery. *Journal of the American Chemical Society* **2009**, 131, (12), 4216-4217.
  15. Wang, C.; Irudayaraj, J., Multifunctional Magnetic-Optical Nanoparticle Probes for Simultaneous Detection, Separation, and Thermal Ablation of Multiple Pathogens. *Small* **2010**, 6, (2), 283-289.
  16. Kayanuma, Y., Quantum-size effects of interacting electrons and holes in semiconductor microcrystals with spherical shape. *Physical Review B* **1988**, 38, (14), 9797-9805.
  17. Wang, Y.; Herron, N., Nanometer-sized semiconductor clusters: materials synthesis, quantum size effects, and photophysical properties. *The Journal of Physical Chemistry* **1991**, 95, (2), 525-532.
  18. Chan, W. C. W.; Nie, S., Quantum Dot Bioconjugates for Ultrasensitive Nonisotopic Detection. *Science* **1998**, 281, (5385), 2016-2018.
  19. Bruchez, M.; Moronne, M.; Gin, P.; Weiss, S.; Alivisatos, A. P., Semiconductor Nanocrystals as Fluorescent Biological Labels. *Science* **1998**, 281, (5385), 2013-2016.
  20. Strosio, M.; Dutta, M.; Singhal, A.; Fischer, H.; Wong, J.; Chan, W. W., Biomedical Applications of Semiconductor Quantum Dots. In *Biological*

- Nanostructures and Applications of Nanostructures in Biology*, Springer US: 2004; pp 37-50.
21. Goldman, E. R.; Clapp, A. R.; Anderson, G. P.; Uyeda, H. T.; Mauro, J. M.; Medintz, I. L.; Mattoussi, H., Multiplexed Toxin Analysis Using Four Colors of Quantum Dot Fluororeagents. *Analytical Chemistry* **2003**, 76, (3), 684-688.
  22. Han, M.; Gao, X.; Su, J. Z.; Nie, S., Quantum-dot-tagged microbeads for multiplexed optical coding of biomolecules. *Nat Biotech* **2001**, 19, (7), 631-635.
  23. Bulte, J. M.; Modo, M. J.; Dahan, M., Investigating the Dynamics of Cellular Processes at the Single Molecule Level with Semiconductor Quantum Dots. In *Nanoparticles in Biomedical Imaging*, Springer New York: 2008; Vol. 102, pp 427-441.
  24. Yaghini, E.; Seifalian, A. M.; MacRobert, A. J., Quantum dots and their potential biomedical applications in photosensitization for photodynamic therapy. *Nanomedicine* **2009**, 4, (3), 353-363.
  25. Callister, W. D.; Rethwisch, D. G., *Fundamentals of Materials Science and Engineering: An Integrated Approach*. Wiley: 2012.
  26. Bishop, K. J. M.; Wilmer, C. E.; Soh, S.; Grzybowski, B. A., Nanoscale Forces and Their Uses in Self-Assembly. *Small* **2009**, 5, (14), 1600-1630.
  27. Malkinski, L. M.; Wang, J.-Q.; Dai, J.; Tang, J.; O'Connor, C. J., Thickness dependence of magnetic properties of granular thin films with interacting particles. *Applied Physics Letters* **1999**, 75, (6), 844-846.
  28. Lin, X.-M.; Samia, A. C. S., Synthesis, assembly and physical properties of magnetic nanoparticles. *Journal of Magnetism and Magnetic Materials* **2006**, 305, (1), 100-109.
  29. Yuan, Q.; Williams, R. A., Large scale manufacture of magnetic polymer particles using membranes and microfluidic devices. *China Particuology* **2007**, 5, 26-42.
  30. Mujika, M.; Arana, S.; Castaño, E.; Tijero, M.; Vilares, R.; Ruano-López, J. M.; Cruz, A.; Sainz, L.; Berganza, J., Magnetoresistive immunosensor for the detection of *Escherichia coli* O157:H7 including a microfluidic network. *Biosensors & bioelectronics* **2009**, 24, (5), 1253-1258.
  31. Maalouf, R.; Hassen, W.; Fournier-Wirth, C.; Coste, J.; Jaffrezic-Renault, N., Comparison of two innovative approaches for bacterial detection: paramagnetic nanoparticles and self-assembled multilayer processes. *Microchimica Acta* **2008**, 163, (3-4), 157-161.
  32. Liébana, S.; Lermo, A.; Campoy, S.; Barbel, J.; Alegret, S.; Pividori, M. a. I., Magneto Immunoseparation of Pathogenic Bacteria and Electrochemical Magneto Genosensing of the Double-Tagged Amplicon. *Analytical Chemistry* **2009**, 81, (14), 5812-5820.
  33. Inglis, D. W.; Riehn, R.; Austin, R. H.; Sturm, J. C., Continuous microfluidic immunomagnetic cell separation. *Applied Physics Letters* **2004**, 85, (21), 5093-5095.
  34. Sun, C.; Lee, J. S. H.; Zhang, M., Magnetic nanoparticles in MR imaging and drug delivery. *Advanced Drug Delivery Reviews* **2008**, 60, (11), 1252-1265.
  35. Q. A. Pankhurst, N. T. K. T., S. K. Jones and J Dobson, Progress in applications of magnetic nanoparticles in biomedicine. *Journal of Physics D: Applied Physics* **2009**, 42, (22), 224001.



36. Koets, M.; van der Wijk, T.; van Eemeren, J. T. W. M.; van Amerongen, A.; Prins, M. W. J., Rapid DNA multi-analyte immunoassay on a magneto-resistance biosensor. *Biosensors and Bioelectronics* **2009**, 24, (7), 1893-1898.
37. Cheng, W.; Ping, Y.; Zhang, Y.; Chuang, K.-H.; Liu, Y., Magnetic Resonance Imaging (MRI) Contrast Agents for Tumor Diagnosis. *Journal of Healthcare Engineering* 4, (1), 23-46.
38. Lee, J.-H.; Kim, J.-w.; Cheon, J., Magnetic nanoparticles for multi-imaging and drug delivery. *Molecules and Cells* 35, (4), 274-284.
39. Zhu, D.; Liu, F.; Ma, L.; Liu, D.; Wang, Z., Nanoparticle-Based Systems for T1-Weighted Magnetic Resonance Imaging Contrast Agents. In Vol. 14, pp 10591-10607.
40. Thomas, R.; Park, I.-K.; Jeong, Y., Magnetic Iron Oxide Nanoparticles for Multimodal Imaging and Therapy of Cancer. In Vol. 14, pp 15910-15930.
41. Kaittanis, C.; Nath, S.; Perez, J. M., Rapid Nanoparticle-Mediated Monitoring of Bacterial Metabolic Activity and Assessment of Antimicrobial Susceptibility in Blood with Magnetic Relaxation. *PLoS ONE* **2008**, 3, (9), e3253.
42. Guangliang Chen and Mingyan Zhou and Shihua Chen and Guohua Lv and Juming, Y., Nanolayer biofilm coated on magnetic nanoparticles by using a dielectric barrier discharge glow plasma fluidized bed for immobilizing an antimicrobial peptide. *Nanotechnology* **2009**, 20, (46), 465706.
43. Lee, D.; Cohen, R. E.; Rubner, M. F., Antibacterial Properties of Ag Nanoparticle Loaded Multilayers and Formation of Magnetically Directed Antibacterial Microparticles. *Langmuir* **2005**, 21, (21), 9651-9659.
44. Chen, W.-J.; Tsai, P.-J.; Chen, Y.-C., Functional Fe<sub>3</sub>O<sub>4</sub>/TiO<sub>2</sub> Core/Shell Magnetic Nanoparticles as Photokilling Agents for Pathogenic Bacteria. *Small* **2008**, 4, (4), 485-491.
45. Masala, O.; Seshadri, R., Synthesis routes for large volumes of nanoparticles. *Annual Review of Materials Research* **2004**, 34, (1), 41-81.
46. Chen, H. M.; Liu, R.-S., Architecture of Metallic Nanostructures: Synthesis Strategy and Specific Applications. *The Journal of Physical Chemistry C* **2011**, 115, (9), 3513-3527.
47. Turkevich, J.; Stevenson, P. C.; Hillier, J., A study of the nucleation and growth processes in the synthesis of colloidal gold. *Discussions of the Faraday Society* **1951**, 11, (0), 55-75.
48. Wang, S.; Sato, S.; Kimura, K., Preparation of Hexagonal-Close-Packed Colloidal Crystals of Hydrophilic Monodisperse Gold Nanoparticles in Bulk Aqueous Solution. *Chemistry of Materials* **2003**, 15, (12), 2445-2448.
49. Sun, Y.; Xia, Y., Shape-Controlled Synthesis of Gold and Silver Nanoparticles. *Science* **2002**, 298, (5601), 2176-2179.
50. Lu, L. T.; Tung, L. D.; Robinson, I.; Ung, D.; Tan, B.; Long, J.; Cooper, A. I.; Fernig, D. G.; Thanh, N. T. K., Size and shape control for water-soluble magnetic cobalt nanoparticles using polymer ligands. *Journal of Materials Chemistry* **2008**, 18, (21), 2453-2458.
51. Gnanaprakash, G.; Mahadevan, S.; Jayakumar, T.; Kalyanasundaram, P.; Philip, J.; Raj, B., Effect of initial pH and temperature of iron salt solutions on formation

- of magnetite nanoparticles. *Materials Chemistry and Physics* **2007**, 103, (1), 168-175.
52. Stober, W.; Fink, A.; Bohn, E., Controlled growth of monodisperse silica spheres in the micron size range. *Journal of Colloid and Interface Science* **1968**, 26, (1), 62-69.
  53. Bao, H.; Wang, E.; Dong, S., One-Pot Synthesis of CdTe Nanocrystals and Shape Control of Luminescent CdTe–Cystine Nanocomposites. *Small* **2006**, 2, (4), 476-480.
  54. Rogach, A. L., Nanocrystalline CdTe and CdTe(S) particles: wet chemical preparation, size-dependent optical properties and perspectives of optoelectronic applications. *Materials Science and Engineering: B* **2000**, 69, (0), 435-440.
  55. Daniel, M.-C.; Astruc, D., Gold Nanoparticles: Assembly, Supramolecular Chemistry, Quantum-Size-Related Properties, and Applications toward Biology, Catalysis, and Nanotechnology. *Chemical Reviews* **2003**, 104, (1), 293-346.
  56. Tan, L., Synthesis of nanoparticles and their self-assembly: bottom-up approach. In *Fundamentals and applications of nanomaterials*, Guo, Z.; Tan, L., Eds. Artech House: Boston, 2009.
  57. Peng, E.; Choo, E. S. G.; Sheng, Y.; Xue, J. M., Monodisperse transfer of superparamagnetic nanoparticles from non-polar solvent to aqueous phase. *New Journal of Chemistry* **2013**, 37, (7), 2051-2060.
  58. Murray, C. B.; Norris, D. J.; Bawendi, M. G., Synthesis and characterization of nearly monodisperse CdE (E = sulfur, selenium, tellurium) semiconductor nanocrystallites. *Journal of the American Chemical Society* **1993**, 115, (19), 8706-8715.
  59. Robinson, I.; Alexander, C.; Lu, L. T.; Tung, L. D.; Fernig, D. G.; Thanh, N. T. K., One-step synthesis of monodisperse water-soluble 'dual-responsive' magnetic nanoparticles. *Chemical Communications* **2007**, (44), 4602-4604.
  60. Longmire, M.; Choyke, P. L.; Kobayashi, H., Clearance properties of nano-sized particles and molecules as imaging agents: considerations and caveats. *Nanomedicine* **2008**, 3, (5), 703-717.
  61. Gittins, D. I.; Caruso, F., Biological and Physical Applications of Water-Based Metal Nanoparticles Synthesised in Organic Solution. *ChemPhysChem* **2002**, 3, (1), 110-113.
  62. Willard, D. M.; Carillo, L. L.; Jung, J.; Van Orden, A., CdS/ZnS Quantum Dots as Resonance Energy Transfer Donors in a Model Protein-Protein Binding Assay. *Nano Letters* **2001**, 1, (9), 469-474.
  63. Mitchell, G. P.; Mirkin, C. A.; Letsinger, R. L., Programmed Assembly of DNA Functionalized Quantum Dots. *Journal of the American Chemical Society* **1999**, 121, (35), 8122-8123.
  64. Aldana, J.; Wang, Y. A.; Peng, X., Photochemical Instability of CdSe Nanocrystals Coated by Hydrophilic Thiols. *Journal of the American Chemical Society* **2001**, 123, (36), 8844-8850.
  65. Hoshino, A.; Fujioka, K.; Oku, T.; Nakamura, S.; Suga, M.; Yamaguchi, Y.; Suzuki, K.; Yasuhara, M.; Yamamoto, K., Quantum dots targeted to the assigned organelle in living cells. *Microbiology and immunology* **2004**, 48, (12), 985-994.

66. Mattoussi, H.; Mauro, J. M.; Goldman, E. R.; Anderson, G. P.; Sundar, V. C.; Mikulec, F. V.; Bawendi, M. G., Self-Assembly of CdS-ZnS Quantum Dot Bioconjugates Using an Engineered Recombinant Protein. *Journal of the American Chemical Society* **2000**, 122, (49), 12142-12150.
67. Goldman, E. R.; Balighian, E. D.; Mattoussi, H.; Kuno, M. K.; Mauro, J. M.; Tran, P. T.; Anderson, G. P., Avidin: A Natural Bridge for Quantum Dot-Antibody Conjugates. *Journal of the American Chemical Society* **2002**, 124, (22), 6378-6382.
68. Dubois, F.; Mahler, B. t.; Dubertret, B. t.; Doris, E.; Mioskowski, C., A Versatile Strategy for Quantum Dot Ligand Exchange. *Journal of the American Chemical Society* **2006**, 129, (3), 482-483.
69. Kim, J.; Kim, H. S.; Lee, N.; Kim, T.; Kim, H.; Yu, T.; Song, I. C.; Moon, W. K.; Hyeon, T., Multifunctional Uniform Nanoparticles Composed of a Magnetite Nanocrystal Core and a Mesoporous Silica Shell for Magnetic Resonance and Fluorescence Imaging and for Drug Delivery. *Angewandte Chemie International Edition* **2008**, 47, (44), 8438-8441.
70. Pazos-Pérez, N.; Gao, Y.; Hilgendorff, M.; Irsen, S.; Pérez-Juste, J.; Spasova, M.; Farle, M.; Liz-Marzán, L. M.; Giersig, M., Magnetic-Noble Metal Nanocomposites with Morphology-Dependent Optical Response. *Chemistry of Materials* **2007**, 19, (18), 4415-4422.
71. Kim, S.; Bawendi, M. G., Oligomeric Ligands for Luminescent and Stable Nanocrystal Quantum Dots. *Journal of the American Chemical Society* **2003**, 125, (48), 14652-14653.
72. Huh, Y.-M.; Jun, Y.-w.; Song, H.-T.; Kim, S.; Choi, J.-s.; Lee, J.-H.; Yoon, S.; Kim, K.-S.; Shin, J.-S.; Suh, J.-S.; Cheon, J., In Vivo Magnetic Resonance Detection of Cancer by Using Multifunctional Magnetic Nanocrystals. *Journal of the American Chemical Society* **2005**, 127, (35), 12387-12391.
73. Wang, Y.; Wong, J. F.; Teng, X.; Lin, X. Z.; Yang, H., "Pulling" Nanoparticles into Water: Phase Transfer of Oleic Acid Stabilized Monodisperse Nanoparticles into Aqueous Solutions of  $\alpha$ -Cyclodextrin. *Nano Letters* **2003**, 3, (11), 1555-1559.
74. Susumu, K.; Uyeda, H. T.; Medintz, I. L.; Pons, T.; Delehanty, J. B.; Mattoussi, H., Enhancing the Stability and Biological Functionalities of Quantum Dots via Compact Multifunctional Ligands. *Journal of the American Chemical Society* **2007**, 129, (45), 13987-13996.
75. Uyeda, H. T.; Medintz, I. L.; Jaiswal, J. K.; Simon, S. M.; Mattoussi, H., Synthesis of Compact Multidentate Ligands to Prepare Stable Hydrophilic Quantum Dot Fluorophores. *Journal of the American Chemical Society* **2005**, 127, (11), 3870-3878.
76. Ballou, B.; Lagerholm, B. C.; Ernst, L. A.; Bruchez, M. P.; Waggoner, A. S., Noninvasive Imaging of Quantum Dots in Mice. *Bioconjugate Chemistry* **2003**, 15, (1), 79-86.
77. Lipka, J.; Semmler-Behnke, M.; Sperling, R. A.; Wenk, A.; Takenaka, S.; Schleh, C.; Kissel, T.; Parak, W. J.; Kreyling, W. G., Biodistribution of PEG-modified gold nanoparticles following intratracheal instillation and intravenous injection. *Biomaterials* **2010**, 31, (25), 6574-6581.

78. Nikolic, M. S.; Krack, M.; Aleksandrovic, V.; Kornowski, A.; Förster, S.; Weller, H., Tailor-Made Ligands for Biocompatible Nanoparticles. *Angewandte Chemie International Edition* **2006**, 45, (39), 6577-6580.
79. Schofield, C. L.; Haines, A. H.; Field, R. A.; Russell, D. A., Silver and Gold Glyconanoparticles for Colorimetric Bioassays. *Langmuir* **2006**, 22, (15), 6707-6711.
80. Pinaud, F.; King, D.; Moore, H.-P.; Weiss, S., Bioactivation and Cell Targeting of Semiconductor CdSe/ZnS Nanocrystals with Phytochelatin-Related Peptides. *Journal of the American Chemical Society* **2004**, 126, (19), 6115-6123.
81. Wang, M.; Peng, M.-L.; Cheng, W.; Cui, Y.-L.; Chen, C., A Novel Approach for Transferring Oleic Acid Capped Iron Oxide Nanoparticles to Water Phase. *Journal of Nanoscience and Nanotechnology* **2011**, 11, (4), 3688-3691.
82. Zubarev, E. R.; Xu, J.; Sayyad, A.; Gibson, J. D., Amphiphilic Gold Nanoparticles with V-Shaped Arms. *Journal of the American Chemical Society* **2006**, 128, (15), 4958-4959.
83. Giaume, D.; Poggi, M. I.; Casanova, D.; Mialon, G. V.; Lahlil, K.; Alexandrou, A.; Gacoin, T.; Boilot, J.-P., Organic Functionalization of Luminescent Oxide Nanoparticles toward Their Application As Biological Probes. *Langmuir* **2008**, 24, (19), 11018-11026.
84. Liz-Marzán, L. M.; Giersig, M.; Mulvaney, P., Synthesis of Nanosized Gold-Silica Core-Shell Particles. *Langmuir* **1996**, 12, (18), 4329-4335.
85. Liz-Marzán, L. M.; Mulvaney, P., The Assembly of Coated Nanocrystals. *The Journal of Physical Chemistry B* **2003**, 107, (30), 7312-7326.
86. Fujita, H. S. P. a. G. D. a. L. F. C. a. T., Synthesis of silica-coated ferromagnetic fine powder by heterocoagulation. *Journal of Physics: Condensed Matter* **2008**, 20, (20), 204105.
87. Kresge, C. T.; Leonowicz, M. E.; Roth, W. J.; Vartuli, J. C.; Beck, J. S., Ordered mesoporous molecular sieves synthesized by a liquid-crystal template mechanism. *Nature* **1992**, 359, (6397), 710-712.
88. Gorelikov, I.; Matsuura, N., Single-Step Coating of Mesoporous Silica on Cetyltrimethyl Ammonium Bromide-Capped Nanoparticles. *Nano Letters* **2007**, 8, (1), 369-373.
89. Kim, J.; Lee, J. E.; Lee, J.; Yu, J. H.; Kim, B. C.; An, K.; Hwang, Y.; Shin, C.-H.; Park, J.-G.; Kim, J.; Hyeon, T., Magnetic Fluorescent Delivery Vehicle Using Uniform Mesoporous Silica Spheres Embedded with Monodisperse Magnetic and Semiconductor Nanocrystals. *Journal of the American Chemical Society* **2005**, 128, (3), 688-689.
90. Sakura, T.; Takahashi, T.; Kataoka, K.; Nagasaki, Y., One-pot preparation of mono-dispersed and physiologically stabilized gold colloid. *Colloid and Polymer Science* **2005**, 284, (1), 97-101.
91. Hardikar, V. V.; Matijević, E., Coating of Nanosize Silver Particles with Silica. *Journal of Colloid and Interface Science* **2000**, 221, (1), 133-136.
92. Pastoriza-Santos, I.; Pérez-Juste, J.; Liz-Marzán, L. M., Silica-Coating and Hydrophobation of CTAB-Stabilized Gold Nanorods. *Chemistry of Materials* **2006**, 18, (10), 2465-2467.

93. Kobayashi, Y.; Katakami, H.; Mine, E.; Nagao, D.; Konno, M.; Liz-Marzán, L. M., Silica coating of silver nanoparticles using a modified Stöber method. *Journal of Colloid and Interface Science* **2005**, 283, (2), 392-396.
94. Lu, Y.; Yin, Y.; Mayers, B. T.; Xia, Y., Modifying the Surface Properties of Superparamagnetic Iron Oxide Nanoparticles through A Sol-Gel Approach. *Nano Letters* **2002**, 2, (3), 183-186.
95. Yu, Y.; Du, F.-P.; Yu, J. C.; Zhuang, Y.-Y.; Wong, P.-K., One-dimensional shape-controlled preparation of porous Cu<sub>2</sub>O nano-whiskers by using CTAB as a template. *Journal of Solid State Chemistry* **2004**, 177, (12), 4640-4647.
96. Salgueiriño-Maceira, V.; Correa-Duarte, M. A.; Spasova, M.; Liz-Marzán, L. M.; Farle, M., Composite Silica Spheres with Magnetic and Luminescent Functionalities. *Advanced Functional Materials* **2006**, 16, (4), 509-514.
97. Bagwe, R. P.; Hilliard, L. R.; Tan, W., Surface Modification of Silica Nanoparticles to Reduce Aggregation and Nonspecific Binding. *Langmuir* **2006**, 22, (9), 4357-4362.
98. Geissbuehler, I.; Hovius, R.; Martinez, K. L.; Adrian, M.; Thampi, K. R.; Vogel, H., Lipid-Coated Nanocrystals as Multifunctionalized Luminescent Scaffolds for Supramolecular Biological Assemblies. *Angewandte Chemie International Edition* **2005**, 44, (9), 1388-1392.
99. Liu, W.; He, Z.; Liang, J.; Zhu, Y.; Xu, H.; Yang, X., Preparation and characterization of novel fluorescent nanocomposite particles: CdSe/ZnS core-shell quantum dots loaded solid lipid nanoparticles. *Journal of Biomedical Materials Research Part A* **2008**, 84A, (4), 1018-1025.
100. Dubertret, B.; Skourides, P.; Norris, D. J.; Noireaux, V.; Brivanlou, A. H.; Libchaber, A., In Vivo Imaging of Quantum Dots Encapsulated in Phospholipid Micelles. *Science* **2002**, 298, (5599), 1759-1762.
101. Fan, H.; Leve, E. W.; Scullin, C.; Gabaldon, J.; Tallant, D.; Bunge, S.; Boyle, T.; Wilson, M. C.; Brinker, C. J., Surfactant-Assisted Synthesis of Water-Soluble and Biocompatible Semiconductor Quantum Dot Micelles. *Nano Letters* **2005**, 5, (4), 645-648.
102. Prakash, A.; Zhu, H.; Jones, C. J.; Benoit, D. N.; Ellsworth, A. Z.; Bryant, E. L.; Colvin, V. L., Bilayers as Phase Transfer Agents for Nanocrystals Prepared in Nonpolar Solvents. *ACS Nano* **2009**, 3, (8), 2139-2146.
103. Wu, X.; Liu, H.; Liu, J.; Haley, K. N.; Treadway, J. A.; Larson, J. P.; Ge, N.; Peale, F.; Bruchez, M. P., Immunofluorescent labeling of cancer marker Her2 and other cellular targets with semiconductor quantum dots. *Nature Biotechnology* **2003**, 21, (1), 41-46.
104. Pellegrino, T.; Manna, L.; Kudera, S.; Liedl, T.; Koktysh, D.; Rogach, A. L.; Keller, S.; Rädler, J.; Natile, G.; Parak, W. J., Hydrophobic Nanocrystals Coated with an Amphiphilic Polymer Shell: A General Route to Water Soluble Nanocrystals. *Nano Letters* **2004**, 4, (4), 703-707.
105. Yu, W. W.; Chang, E.; Falkner, J. C.; Zhang, J.; Al-Somali, A. M.; Sayes, C. M.; Johns, J.; Drezek, R.; Colvin, V. L., Forming Biocompatible and Nonaggregated Nanocrystals in Water Using Amphiphilic Polymers. *Journal of the American Chemical Society* **2007**, 129, (10), 2871-2879.

106. Sperling, R. A.; Pellegrino, T.; Li, J. K.; Chang, W. H.; Parak, W. J., Electrophoretic Separation of Nanoparticles with a Discrete Number of Functional Groups. *Advanced Functional Materials* **2006**, 16, (7), 943-948.
107. Dubertret, B.; Skourides, P.; Norris, D. J.; Noireaux, V.; Brivanlou, A. H.; Libchaber, A., In Vivo Imaging of Quantum Dots Encapsulated in Phospholipid Micelles. In 2002; Vol. 298, pp 1759-1762.
108. Bruchez, M.; Moronne, M.; Gin, P.; Weiss, S.; Alivisatos, A. P., Semiconductor Nanocrystals as Fluorescent Biological Labels. In 1998; Vol. 281, pp 2013-2016.
109. Hermanson, G. T., Chapter 24 - Preparation of Colloidal Gold-Labeled Proteins. In *Bioconjugate Techniques (Second Edition)*, Academic Press: New York, 2007; pp 924-935.
110. Åkerman, M. E.; Chan, W. C. W.; Laakkonen, P.; Bhatia, S. N.; Ruoslahti, E., Nanocrystal targeting in vivo. *Proceedings of the National Academy of Sciences of the United States of America* **2002**, 99, (20), 12617-12621.
111. Mirkin, C. A.; Letsinger, R. L.; Mucic, R. C.; Storhoff, J. J., A DNA-based method for rationally assembling nanoparticles into macroscopic materials. *Nature* **1996**, 382, (6592), 607-609.
112. Zanchet, D.; Micheel, C. M.; Parak, W. J.; Gerion, D.; Alivisatos, A. P., Electrophoretic Isolation of Discrete Au Nanocrystal/DNA Conjugates. *Nano Letters* **2000**, 1, (1), 32-35.
113. Clapp, A. R.; Medintz, I. L.; Mauro, J. M.; Fisher, B. R.; Bawendi, M. G.; Mattoussi, H., Fluorescence Resonance Energy Transfer Between Quantum Dot Donors and Dye-Labeled Protein Acceptors. *Journal of the American Chemical Society* **2003**, 126, (1), 301-310.
114. Ding, S.-Y.; Jones, M.; Tucker, M. P.; Nedeljkovic, J. M.; Wall, J.; Simon, M. N.; Rumbles, G.; Himmel, M. E., Quantum Dot Molecules Assembled with Genetically Engineered Proteins. *Nano Letters* **2003**, 3, (11), 1581-1585.
115. Delehanty, J. B.; Medintz, I. L.; Pons, T.; Brunel, F. M.; Dawson, P. E.; Mattoussi, H., Self-Assembled Quantum Dot-Peptide Bioconjugates for Selective Intracellular Delivery. *Bioconjugate Chemistry* **2006**, 17, (4), 920-927.
116. Medintz, I. L.; Clapp, A. R.; Mattoussi, H.; Goldman, E. R.; Fisher, B.; Mauro, J. M., Self-assembled nanoscale biosensors based on quantum dot FRET donors. *Nature Materials* **2003**, 2, (9), 630-638.
117. Tan, W. B.; Jiang, S.; Zhang, Y., Quantum-dot based nanoparticles for targeted silencing of HER2/neu gene via RNA interference. *Biomaterials* **2007**, 28, (8), 1565-1571.
118. Jiang, S.; Zhang, Y., Upconversion Nanoparticle-Based FRET System for Study of siRNA in Live Cells. *Langmuir* **2010**, 26, (9), 6689-6694.
119. Goldman, E. R.; Anderson, G. P.; Tran, P. T.; Mattoussi, H.; Charles, P. T.; Mauro, J. M., Conjugation of Luminescent Quantum Dots with Antibodies Using an Engineered Adaptor Protein To Provide New Reagents for Fluoroimmunoassays. *Analytical Chemistry* **2002**, 74, (4), 841-847.
120. Derfus, A. M.; Chan, W. C. W.; Bhatia, S. N., Probing the Cytotoxicity of Semiconductor Quantum Dots. *Nano Letters* **2003**, 4, (1), 11-18.
121. Wu, X.; Liu, H.; Liu, J.; Haley, K. N.; Treadway, J. A.; Larson, J. P.; Ge, N.; Peale, F.; Bruchez, M. P., Immunofluorescent labeling of cancer marker Her2 and

- other cellular targets with semiconductor quantum dots. *Nat Biotech* **2003**, 21, (1), 41-46.
122. Winter, J. O.; Liu, T. Y.; Korgel, B. A.; Schmidt, C. E., Recognition Molecule Directed Interfacing Between Semiconductor Quantum Dots and Nerve Cells. *Advanced Materials* **2001**, 13, (22), 1673-1677.
  123. Gao, X.; Cui, Y.; Levenson, R. M.; Chung, L. W. K.; Nie, S., In vivo cancer targeting and imaging with semiconductor quantum dots. *Nature Biotechnology* **2004**, 22, (8), 969-976.
  124. Agrawal, A.; Zhang, C.; Byassee, T.; Tripp, R. A.; Nie, S., Counting Single Native Biomolecules and Intact Viruses with Color-Coded Nanoparticles. *Analytical Chemistry* **2006**, 78, (4), 1061-1070.
  125. Liu, Y.; Brandon, R.; Cate, M.; Peng, X.; Stony, R.; Johnson, M., Detection of Pathogens Using Luminescent CdSe/ZnS Dendron Nanocrystals and a Porous Membrane Immunofilter. *Analytical Chemistry* **2007**, 79, (22), 8796-8802.
  126. Bagalkot, V.; Zhang, L.; Levy-Nissenbaum, E.; Jon, S.; Kantoff, P. W.; Langer, R.; Farokhzad, O. C., Quantum Dot-Aptamer Conjugates for Synchronous Cancer Imaging, Therapy, and Sensing of Drug Delivery Based on Bi-Fluorescence Resonance Energy Transfer. *Nano Letters* **2007**, 7, (10), 3065-3070.
  127. Kell, A. J.; Stewart, G.; Ryan, S.; Peytavi, R.; Boissinot, M.; Huletsky, A.; Bergeron, M. G.; Simard, B., Vancomycin-Modified Nanoparticles for Efficient Targeting and Preconcentration of Gram-Positive and Gram-Negative Bacteria. *ACS Nano* **2008**, 2, (9), 1777-1788.
  128. Chang, E.; Miller, J. S.; Sun, J.; Yu, W. W.; Colvin, V. L.; Drezek, R.; West, J. L., Protease-activated quantum dot probes. *Biochemical and Biophysical Research Communications* **2005**, 334, (4), 1317-1321.
  129. Hermanson, G. T., Chapter 3 - Zero-Length Crosslinkers. In *Bioconjugate Techniques (Second Edition)*, Academic Press: New York, 2008; pp 213-233.
  130. Lin, P.-C.; Chou, P.-H.; Chen, S.-H.; Liao, H.-K.; Wang, K.-Y.; Chen, Y.-J.; Lin, C.-C., Ethylene Glycol-Protected Magnetic Nanoparticles for a Multiplexed Immunoassay in Human Plasma. *Small* **2006**, 2, (4), 485-489.
  131. Petkova, G.; Zaruba, K.; Zvatora, P.; Kral, V., Gold and silver nanoparticles for biomolecule immobilization and enzymatic catalysis. In Vol. 7, p 287.
  132. Tessmer, I.; Kaur, P.; Lin, J.; Wang, H., Investigating bioconjugation by atomic force microscopy. *Journal of Nanobiotechnology* **2013**, 11, (1), 25.
  133. Alliegro, M. C., Effects of Dithiothreitol on Protein Activity Unrelated to Thiol-Disulfide Exchange: For Consideration in the Analysis of Protein Function with Cleland's Reagent. *Analytical Biochemistry* **2000**, 282, (1), 102-106.
  134. Brinkley, M., A brief survey of methods for preparing protein conjugates with dyes, haptens and crosslinking reagents. *Bioconjugate Chemistry* **1992**, 3, (1), 2-13.
  135. Cai, W.; Shin, D.-W.; Chen, K.; Gheysens, O.; Cao, Q.; Wang, S. X.; Gambhir, S. S.; Chen, X., Peptide-Labeled Near-Infrared Quantum Dots for Imaging Tumor Vasculature in Living Subjects. *Nano Letters* **2006**, 6, (4), 669-676.
  136. Chen, G.; Ohulchanskyy, T. Y.; Kumar, R.; Ågren, H.; Prasad, P. N., Ultrasmall Monodisperse NaYF<sub>4</sub>:Yb<sup>3+</sup>/Tm<sup>3+</sup> Nanocrystals with Enhanced Near-Infrared to

- Near-Infrared Upconversion Photoluminescence. *ACS Nano* **2010**, 4, (6), 3163-3168.
137. Gerion, D.; Parak, W. J.; Williams, S. C.; Zanchet, D.; Micheel, C. M.; Alivisatos, A. P., Sorting Fluorescent Nanocrystals with DNA. *Journal of the American Chemical Society* **2002**, 124, (24), 7070-7074.
  138. Parak, W. J.; Gerion, D.; Zanchet, D.; Woerz, A. S.; Pellegrino, T.; Micheel, C.; Williams, S. C.; Seitz, M.; Bruehl, R. E.; Bryant, Z.; Bustamante, C.; Bertozzi, C. R.; Alivisatos, A. P., Conjugation of DNA to Silanized Colloidal Semiconductor Nanocrystalline Quantum Dots. *Chemistry of Materials* **2002**, 14, (5), 2113-2119.
  139. Tian, L.; Shi, C.; Zhu, J., Reversible formation of hybrid nanostructures via an organic linkage. *Chemical Communications* **2007**, (37), 3850-3852.
  140. El-Sayed, M. E. H.; Hoffman, A. S.; Stayton, P. S., Rational design of composition and activity correlations for pH-sensitive and glutathione-reactive polymer therapeutics. *Journal of Controlled Release* **2005**, 101, 47-58.
  141. White, M. A.; Johnson, J. A.; Koberstein, J. T.; Turro, N. J., Toward the Syntheses of Universal Ligands for Metal Oxide Surfaces: Controlling Surface Functionality through Click Chemistry. *Journal of the American Chemical Society* **2006**, 128, (35), 11356-11357.
  142. Fleming, D. A.; Thode, C. J.; Williams, M. E., Triazole Cycloaddition as a General Route for Functionalization of Au Nanoparticles. *Chemistry of Materials* **2006**, 18, (9), 2327-2334.
  143. Sun, X.-L.; Stabler, C. L.; Cazalis, C. S.; Chaikof, E. L., Carbohydrate and Protein Immobilization onto Solid Surfaces by Sequential Diels-Alder and Azide-Alkyne Cycloadditions. *Bioconjugate Chemistry* **2005**, 17, (1), 52-57.
  144. <https://www.clickchemistrytools.com/>
  145. Whitehead, K. A.; Langer, R.; Anderson, D. G., Knocking down barriers: advances in siRNA delivery. *Nature Reviews Drug Discovery* **2009**, 8, (2), 129-138.
  146. Giljohann, D. A.; Seferos, D. S.; Prigodich, A. E.; Patel, P. C.; Mirkin, C. A., Gene Regulation with Polyvalent siRNA-Nanoparticle Conjugates. *Journal of the American Chemical Society* **2009**, 131, (6), 2072-2073.
  147. Liu, J.; Lu, Y., Preparation of aptamer-linked gold nanoparticle purple aggregates for colorimetric sensing of analytes. *Nature Protocols* **2006**, 1, (1), 246-252.
  148. Ho, K.-C.; Tsai, P.-J.; Lin, Y.-S.; Chen, Y.-C., Using Biofunctionalized Nanoparticles To Probe Pathogenic Bacteria. *Analytical Chemistry* **2004**, 76, (24), 7162-7168.
  149. Gao, X.; Cui, Y.; Levenson, R. M.; Chung, L. W. K.; Nie, S., In vivo cancer targeting and imaging with semiconductor quantum dots. *Nat Biotech* **2004**, 22, (8), 969-976.
  150. Liu, W.; Howarth, M.; Greytak, A. B.; Zheng, Y.; Nocera, D. G.; Ting, A. Y.; Bawendi, M. G., Compact Biocompatible Quantum Dots Functionalized for Cellular Imaging. *Journal of the American Chemical Society* **2008**, 130, (4), 1274-1284.
  151. Fu, A.; Micheel, C. M.; Cha, J.; Chang, H.; Yang, H.; Alivisatos, A. P., Discrete Nanostructures of Quantum Dots/Au with DNA. *Journal of the American Chemical Society* **2004**, 126, (35), 10832-10833.



152. Chen, F.; Gerion, D., Fluorescent CdSe/ZnS Nanocrystal-Peptide Conjugates for Long-term, Nontoxic Imaging and Nuclear Targeting in Living Cells. *Nano Letters* **2004**, 4, (10), 1827-1832.
153. Flavell, R. R.; Muir, T. W., Expressed Protein Ligation (EPL) in the Study of Signal Transduction, Ion Conduction, And Chromatin Biology. *Accounts of Chemical Research* **2008**, 42, (1), 107-116.
154. Reulen, S. W. A.; Brusselaars, W. W. T.; Langereis, S.; Mulder, W. J. M.; Breurken, M.; Merks, M., Protein-liposome Conjugates Using Cysteine-Lipids And Native Chemical Ligation. *Bioconjugate Chemistry* **2007**, 18, (2), 590-596.
155. Xia, Z.; Xing, Y.; So, M.-K.; Koh, A. L.; Sinclair, R.; Rao, J., Multiplex Detection of Protease Activity with Quantum Dot Nanosensors Prepared by Intein-Mediated Specific Bioconjugation. *Analytical Chemistry* **2008**, 80, (22), 8649-8655.
156. Elias, D. R.; Cheng, Z.; Tsourkas, A., An Intein-Mediated Site-Specific Click Conjugation Strategy for Improved Tumor Targeting of Nanoparticle Systems. *Small* **2010**, 6, (21), 2460-2468.
157. Kim, Y.-P.; Daniel, W. L.; Xia, Z.; Xie, H.; Mirkin, C. A.; Rao, J., Bioluminescent nanosensors for protease detection based upon gold nanoparticle-luciferase conjugates. *Chemical Communications* **2010**, 46, (1), 76-78.

**CHAPTER 3**

**DEVELOPMENT OF BIOCOMPATIBLE LUMINESCENT  
NANOPARTICLES FOR BIOIMAGING APPLICATIONS**

### 3.1 Introduction

Group II-VI semiconductor nanocrystals, referred as quantum dots (QDs), have been extensively studied as light-emitting materials for biological labeling over last decade, because of their strong size-tunable bandgap luminescence.<sup>1-4</sup> Cadmium Selenide (CdSe) QDs are one of the most attractive QDs in bio-imaging due to their size-dependent emission in a visible region as well as the high photoluminescence (PL) quantum yield.<sup>5, 6</sup> However, CdSe QDs show the inherent biological toxicity<sup>7, 8</sup> and instability in aqueous solution,<sup>9</sup> which limit their *in vitro* and *in vivo* biomedical applications. A variety of materials have been used to cap or re-cap QDs, including amphiphilic molecules,<sup>2, 10-14</sup> polymers<sup>15, 16</sup> and inorganic silica shells,<sup>1, 17, 18</sup> to enhance the stability and biocompatibility of QDs. In particular, encapsulation of QDs in biopolymer not only protects QDs from oxidation, but also provides a biocompatible layer to avoid the direct interaction between living cells and the Cd- and Se- containing QDs core. In addition, a great variety of functional groups could offer new chemical functionalities to QDs by grafting bio-molecules.

Gelatin is a natural biocompatible biopolymer derived from collagen. Gelatin nanoparticles (GNPs) have been used in gene delivery.<sup>19-21</sup> Most recently, fluorescent GNPs-encapsulating demonstrates the potential applications in drug delivery and bio-imaging at the same time.<sup>22-27</sup> Unlike loading organic dye, loading quantum dots (QDs) within GNPs may improve the biocompatible of QDs and fluorescence properties of GNPs. The two-step desolvation process initially developed by Coester *et. al.* is able to produce well-tailored GNPs in terms of uniform size and narrow size distribution.<sup>20, 28</sup> Previous reports indicate that the pH value above 3.0 may result in early agglomeration of gelatin chains in the second-step of desolvation method.<sup>28, 29</sup> However, it should be noted that the PL properties of QDs in terms of PL intensity and lifetime normally decay in acidic conditions, pH < 5, due to acid etching<sup>10, 30</sup> and/or surface state energies modification.<sup>31-33</sup> In this case, encapsulating QDs into GNPs by the desolvation method might result in the quenching of QDs because of low pH value in the second desolvation step. In addition, other defects such as colloidal instability and low quantum yields (QY)

are hardly avoided in reported methods, e.g. in situ loading QDs onto GNPs in aqueous media.<sup>22, 26</sup>

In this chapter, two approaches were presented for preparing hybrid CdSe QDs-gelatin nanoparticles (QDs-GNP) nanosystem. In the first method, nanosystem QDs-GNP1 is prepared by directly encapsulating hydrophilic CdSe QDs in NPs ( ) via desolvation method through carefully controlling of the medium pH. Fluorescent property and biocompatibility were investigated. To improve the stability of QDs photoluminescence, a second approach involving an electrostatic layer-by-layer (LBL) deposition process was developed to prepare a novel multilayer gelatin/QDs core/shell NPs by assembly of hydrophilic CdSe QDs on the surface of gelatin nanoparticles (i.e. nanosystem QDs-GNP2). The advantage of using electrostatic LBL deposition method is that it has been known as one of the simple and cost-effective methods for multilayer coatings.<sup>34-38</sup> The sequentially assembled polymers with opposite charges onto micro/nanoparticle templates have demonstrated a great potential in fabrication of multifunctional core-shell structures.<sup>34</sup> The morphology, structure, pH stability in term of PL property, biocompatibility, and potential applications in bio-imaging of the nanocomposites were further investigated, respectively. The PL properties of the core-shell nanoparticles as a function of the pH value are studied. In addition, the cytotoxicity of the luminescent QDs-GNP2 has been investigated by using NIH/3T3 mouse fibroblast cell line. It is expected that the new fluorescent core-shell QDs-GNPs can be an alternative fluorescent contrast agent with stable photostability and superior biocompatibility.

## 3.2 Experimental procedures

### 3.2.1 Materials and Reagents

Type A gelatin from porcine skin (~300 g Bloom), cadmium acetate hydrate, selenium powder (99.5%), trioctylphosphine Oxide (90%, TOPO), trioctylphosphine (TOP, 90%, Aldrich), 11-Mercaptoundecanoic acid (MUA), tetramethylammonium hydroxide pentahydrate (TMAHP, 97%, Sigma), ethyl acetate, ether, poly(sodium 4-styrenesulfonate) (PSS), polydiallyldimethyl ammonium chloride (PDAC), glutaraldehyde (25%), 2-(4-amidinophenyl)-1H-indole-6-carboxamide (DAPI), and

phosphate buffered saline (PBS, tablet) were purchased from Sigma-Aldrich (ST, Louis MO). MultiTox-Fluor multiplex cytotoxicity kit was ordered from Promega (Madison, WI). For cell culture, Gibco® Dulbecco's Modified Eagle's medium (DMEM) and FBS were supplied by Invitrogen (Grand Island, NY). Glass bottom petridishes were supplied by MaTek Inc (MA, USA).

### 3.2.2 Preparation of hydrophilic CdSe QDs

TOPO capped CdSe QDs were synthesized following a modification of procedure described by Aldana *et. Al.*<sup>39</sup> In brief, 0.5 g cadmium acetate hydrate mixed with 40 g TOPO was heated to 330 °C under argon flow. A selenium stock solution consisting of 0.8 g selenium powder, 20 g TOP and 0.35 g anhydrous toluene was then injected rapidly into the above mixture. The temperature was cooled down to 270 °C and maintained for 4 min. After that, the solution was cooled down to 30-50 °C. Excess amount of methanol was added to the mixture to precipitate the QDs. The QDs were then centrifuged at 8000 rpm for 15 min. After repeating washing with methanol and acetone, the hydrophobic CdSe QDs were dissolved in hexane and kept under dark.

The hydrophilic CdSe QDs were prepared by replacing TOPO from the surface of QDs with MUA. In a typical experiment, 20 mg of MUA was mixed with 15 mL methanol under dark conditions and argon flow. The pH of the mixture was then adjusted to 10.3 by addition of 200 mg TMAHP. Following that, 20 mg of the as-synthesized CdSe QDs were added into the mixture. The mixture was further heated to 65 °C. After overnight refluxing, the mixture was cooled down to room temperature. The QDs were then precipitated by addition of excess amounts of ethyl acetate and ether (1:1). The QDs were further washed and purified by centrifugation (5800 rpm for 5 min). Finally, the QDs were re-dissolved in distilled water.

### 3.2.3 Preparation of gelatin NPs

Gelatin NPs were made by a two-step desolvation approach with slight modification.<sup>28</sup> Briefly, 1.25g of gelatin type A powder was dissolved in 25 mL nanopure water under constant heating at 40 °C. In order to achieve the desolvation of gelatin, 25 mL of acetone was then added rapidly to this solution. The supernatant was discarded and the remaining

high molecular weight (HMW) gelatin was re-dissolved by adding another 25 mL of nanopure water at 40 °C. The pH of this solution was adjusted to 2.5. The gelatin was then desolvated again by dropwise addition of 75 mL acetone during 15 min under this constant heating. A white milk-like solution appears when 55 to 60 mL of acetone was introduced into the mixture. After 10 min of stirring, 0.5 mL of 25% glutaraldehyde solution (Sigma-Aldrich) was added to crosslink the particles. After another 30 min of stirring, the dispersion was centrifuged at 6500 rpm for 10 min. The particles were purified by repeating re-dispersion with acetone (30%) and centrifugation. After the final centrifugation, the particles were freezing-dried overnight and kept at 4 °C for further studies.

### 3.2.4 Preparation of QDs-GNP1 by direct encapsulation of QDs in GNPs.

Figure 3.1 is a schematic illustration of the preparation of QDs-GNP1. Briefly, 1.25 g of the gelatin powder was first dissolved in water (25 mL) and acetone (25 mL) at 40 °C, followed by centrifugation. The extracted gelatin was then re-dissolved in 40 mL of an acidic water solution (pH 2.5). Hydrophilic MUA-QDs (1.0 mL; 0.25 mg/mL) were added to the gelatin mixture at this point. Acetone was added (drop wise) to the solution to form NPs. After 30 min of stirring, 0.5 mL of glutaraldehyde solution (25% v/v) was added as a cross-linker to stabilize the NPs. The particles were then purified and washed using an ethanol and acetone mixture, and freeze-dried overnight.

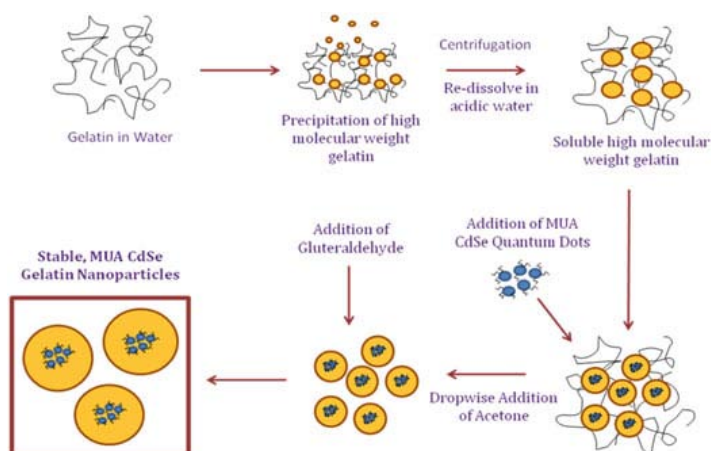


Figure 3.1 Schematic illustration of preparation of QD-GNP1

### 3.2.5 Preparation of QDs-GNP2

Figure 3.2 shows the scheme of preparation of multilayer QDs-GNP2 by LBL deposition method. LBL coating process starts from coating of two stabilized bi-layer of PSS and PDAC at pH 6.0. In brief, a supporting film consisting of two PE bilayers by the alternate adsorption of PSS solution (0.3 mg/mL in nanopure water, pH 6.0) and PDAC (0.3 mg/mL in nanopure water, pH 6.0) twice first covered the surface of as-prepared GNPs (~200 mg). The polyanion PSS was deposited as the first layer on the positive GNPs. After formation of two supporting bilayers, MUA-QDs (0.5 mg/mL in nanopure water, pH 9.0) were deposited toward the PDAC layer, followed by the cycle of PSS/PDAC/MUA-QDs adsorption. For adsorption of each layer, the suspending was allowed for 15 min under vigorous shaking. Followed that, the particles were washed with nanopure water and collected through centrifugation (5000 g for 5 min). The cycle was run repeatedly until the formation of four layers of MUA-QDs on the GNPs. After adsorption of the final MUA-QDs layer, the particles were protected by depositing a layer of PSS. The multilayer NPs were then purified, freeze-dried and stored at 4 °C ready for use.

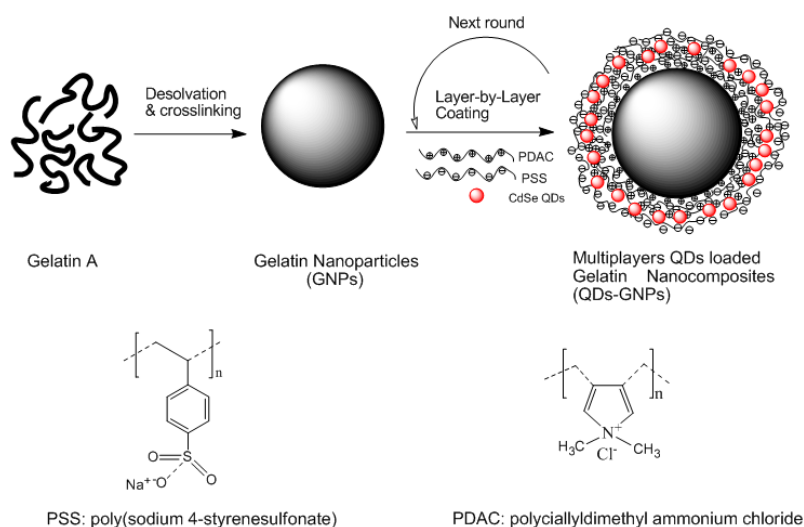


Figure 3.2. Schematic illustration of preparation of QDs-GNPs by LBL technique.

### 3.2.6 Characterization

Transmission electron microscopy (TEM) and scanning electron microscopy (SEM) coupled with energy-dispersive X-ray spectroscopy (EDX) were used to analyze the morphology and composition of all the NPs. The TEM images were obtained using a Philips CM-10 microscopy operating at 100 kV. A high resolution TEM (HRTEM, JEOL 2010 F, operating at 200 kV) was used to analyze the crystalline structure of MUA-QDs. The SEM analysis was taken by a Hitachi 3400s SEM coupled with EDX. The average diameter of the multiple layer NPs was calculated from TEM images by analyzing at least 200 NPs for each sample using ImageJ software (National Institutes of Health, USA).

The Zeta ( $\zeta$ ) potentials of the GNs with and without LBL coatings were measured by Malvern Zetasizer 3000HSA, and calculated as the mean of five individual measurements. The functional groups of nanomaterials were studied by using Fourier transform infrared (FTIR) spectrophotometer (Bruker FTIR-IFS 55, Germany). UV-visible absorption spectra were recorded by UV-3600 spectrophotometer (Shimadzu, Japan). PL spectra and quantum yields were measured by a QuantaMaster™ 40 Spectrofluorometer (Photon Technology International Inc., London, ON).

### 3.2.7 Analysis of pH effect in photostability

The pH effect on the PL stability of MUA-QDs and QDs-GNP2 were investigated further under the excitation wavelength ( $\lambda_{\text{ex}}$ ) at 470 nm. Corresponding amounts of MUA-QDs and QDs-GNs were suspended in distilled water with different pH values, i.e., 1, 4, 7, and 9, respectively. The pH value of the aqueous media was adjusted by using HCl and NaOH. Each measurement was repeated at least three times. The light source is a pulsed dye laser pumped by a pulsed nitrogen laser with the dye wavelength set at 480 nm (the bandwidth of the dye laser output is about 0.04 nm). The emission was measured with a monochromator set at 620 nm. Furthermore, there was a 550 nm long-pass filter used on the emission side so that no excitation light can enter the detector, that is, the scattering effect is ruled out. The PTI-patterned Strobe technique measures fluorescence decay curves (i.e., fluorescence intensity as a function of time) directly. It is considered a faster measurement than TCSPC (Time-Correlation Single Photon Counting) by using a



nonlinear detection time scale to record the fluorescence intensity. The data analysis was performed with Felix GX analytical software package using a 1-to-4 exponential fitting function by  $\chi^2$  minimization employing Marquardt-Levenberg algorithm with iterative reconvolution. In order to carry out reconvolution, an instrument response function (IRF) was measured by using a scattering suspension of Ludox in deionized water. The PL decays required either a single or double-exponential function to fulfill fitting criteria, such as the value and the randomness of residuals. For double exponential decays the intensity-weighted average lifetimes were calculated using the following equation (Equation 3.1),<sup>40</sup>

$$\tau_{ave} = \sum a_i \tau_i^2 / \sum a_i \tau_i \quad (\text{Equation 3.1})$$

where  $a_i$  are the pre-exponential weights and  $\tau_i$  the decay times obtained in the multi-exponential fitting.

### 3.2.8 Cell viability/cytotoxicity study

The toxic effects of nanomaterials studied in this chapter on NIH/3T3 mouse cells (ATCC) was tested by a commercial kit (MultiTox-Fluor cytotoxicity assay). The assay was done following the manufacturer's instruction. Briefly, 10,000 cells per well (of 96-well) of the 3T3 cells were cultured in DMEM medium supplemented with 10% FBS at 37 °C, 5% CO<sub>2</sub>. After 24 hrs of culture, the medium was replaced with fresh medium containing 5-fold serial diluted QDs-GNPs and MUA-QDs ranging from 25 mg/mL to 0.2 mg/mL, and from 6.25 mg/mL to 0.05 mg/mL, respectively. Cells without any treatment were used as controls. After another 24 hrs, 20  $\mu$ L of 2 X MultiTox-Fluor multiplex cytotoxicity assay reagent was added to each well. An Omega microplate reader (BMG Labtech, Ortenberg, Germany) at an excitation of 400 nm and an emission of 505 nm was used in this study.

### 3.2.9 *In vitro* fluorescence imaging

NIH/3T3 mouse fibroblast cells ( $2 \times 10^5$  per petridish, glass bottom petridishes), were cultured in DMEM medium supplemented with 10 % FBS at 37 °C, 5 % CO<sub>2</sub>, for 24 hrs. The cells were then rinsed by PBS, and subsequently treated with DMEM mediums

spiked with 0.1 mg/mL MUA-QDs, QDs-GNP2 and GNPs, respectively, and incubated for 24 hrs. The treated cells were washed by PBS for three times and fixed using a PBS solution containing 2.5% glutaraldehyde under for 30 min under mild shaking. After that, the cells were washed for another three times by PBS and incubated with a PBS mounting solution containing DAPI solution for 30 min. Afterwards the cells were washed with PBS for another five times and were examined by a LSM Zeiss 510 Duo Confocal microscopy.

### 3.3 Results and Discussion (I)

The initial work using QDs-GNP1 are presented and discussed in this section.

#### 3.3.1 Characterization

The diameter of the MUA-QDs is estimated to be  $5 \pm 1$  nm by TEM and HRTEM, as shown in Figure 3.3a. The well-resolved lattice fringes on the HRTEM micrographs are typical crystalline structures of CdSe QDs. Figure 3.3b shows spherical QDs-GNP1 with average diameters of  $150 \pm 10$  nm. In addition, TEM shows that free MUA-QDs are generally not found outside GNPs.

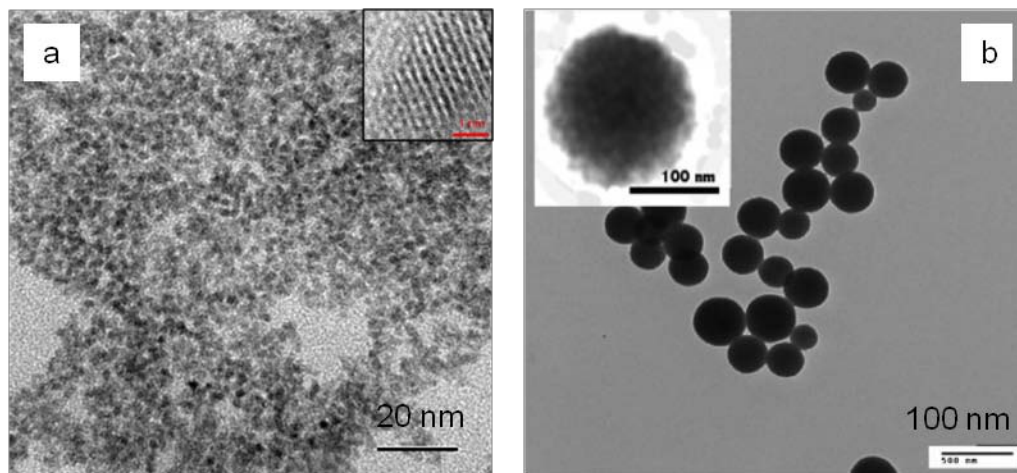


Figure 3.3 TEM micrograph of MUA-CdSe QDs (a) and (b) QD-GNP1.

FTIR was then carried out to investigate the encapsulation of MUA-QDs in GNPs. Figure 3.4 shows FTIR spectra of MUA-QDs, GNPs and QDs-GNP1. C=O stretching can be found in both GNPs and MUA occurring at  $\sim 1660$   $\text{cm}^{-1}$ . GNPs in the FTIR spectrum

show -NH bending between  $1550\text{ cm}^{-1}$  and  $1500\text{ cm}^{-1}$ . Peaks at  $1660\text{ cm}^{-1}$  are assigned to the imide C–N group formed via a cross-linking reaction between gelatin and glutaraldehyde, which is close to -C=O stretching. For MUA-QDs, previous studies have shown that the carboxyl group of MUA may participate in the hydrogen-bonding processes. The absorption band at  $1200\text{ cm}^{-1}$  is attributed to the C–OH stretching of MUA. The band at  $1430\text{ cm}^{-1}$  can be found in both and is assigned to a combination of the symmetric COO<sup>-</sup> stretching band of the carboxylate anion and the -CH<sub>2</sub> scissors deformation of the carboxylic acid.<sup>41</sup> Unfortunately, they are quite weak, and could not be identified in QDs-GNP1. Also, most of characteristic peaks of MUA-QDs (stretches of -C=O, -CH<sub>2</sub> and -OH groups) are observable in GNPs.

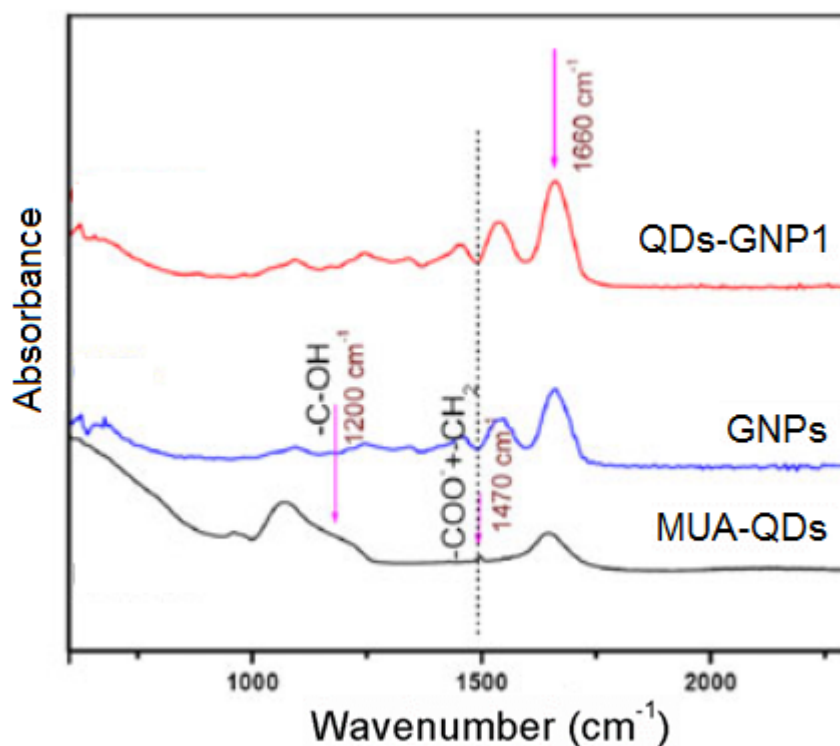


Figure 3.4 FTIR spectra of MUA-QDs, GNPs and QD-GNP1

A fluorospectrometer was then used to study the encapsulation of MUA-QDs in GNPs (Figure 3.5). The maximum fluorescent emission peak ( $\lambda_{\text{em max}}$ ) is found at 630 nm for

MUA-QDs under an excitation wavelength ( $\lambda_{\text{ex}}$ ) of 460 nm. As expected, there is no emission from the plain GNPs. There is a 24-nm red-shift in  $\lambda_{\text{em max}}$  while MUA-QDs were encapsulated into GNPs. Previous reports indicate a blue-shift of  $\lambda_{\text{em max}}$  for the gelatin encapsulating PbS QDs, which was claimed to be due to the polar environment of gelatin on the dipole interaction of PbS QDs.<sup>24</sup> However, it should be mentioned that the PbS QDs used previously were synthesized by a hydrothermal method without the protection of a stabilizer. In the other words, the surface of PbS QDs would be very sensitive to environmental conditions. In our case, CdSe QDs were capped by long-chain MUA molecules, which protect the surface atoms of QDs from direct interaction with solution. The red-shift at the emission wavelength might be caused by extension of the exciton wavefunction of CdSe QDs to the outer organic ligands. This results in a decrease in the confinement energy of the exciton and the wavelength red-shift.<sup>39</sup>

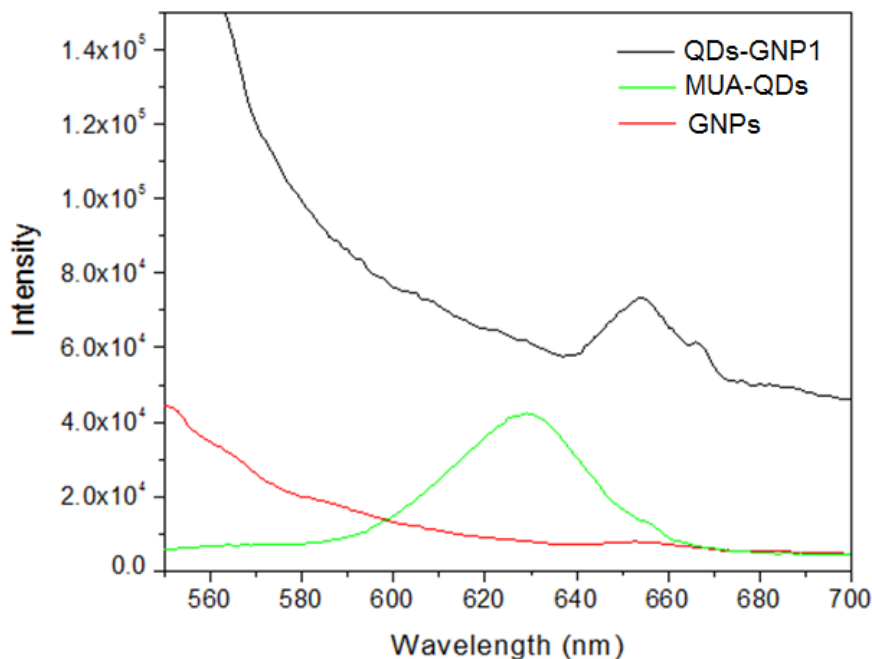


Figure 3.5 Fluorescent spectra of MUA-QDs, GNPs and QD-GNP1

The QDs-GNP1 was further studied by using confocal laser scanning microscopy (Figure 3.6). The inset shows agglomerated NPs under the bright field. When the excitation,  $\lambda_{\text{ex}}$ , was 460 nm, a bright photoluminescent signal could be captured from the NPs (green dots in Figure 3.6). This further demonstrates that MUA-QDs can be successfully loaded

into GNPs. No free MUA-QDs after the encapsulation are identified by confocal laser scanning microscopy. It is noted that the isoelectric point (PI) for MUA is  $\sim 6$ , and the acid pH (2.5) in the second desolvation may cause protonization of MUA-QDs, resulting in slight aggregation. As shown in Figure 3.6, the photoluminescence was well distributed around those QDs-GNP1; it seems that the possible slight aggregation did not affect the homogenous encapsulation process. In addition,  $\sim 1$  g of QDs-GNP1 could be produced in each process. The amount of QDs incorporated inside of NPs can be adjustable.

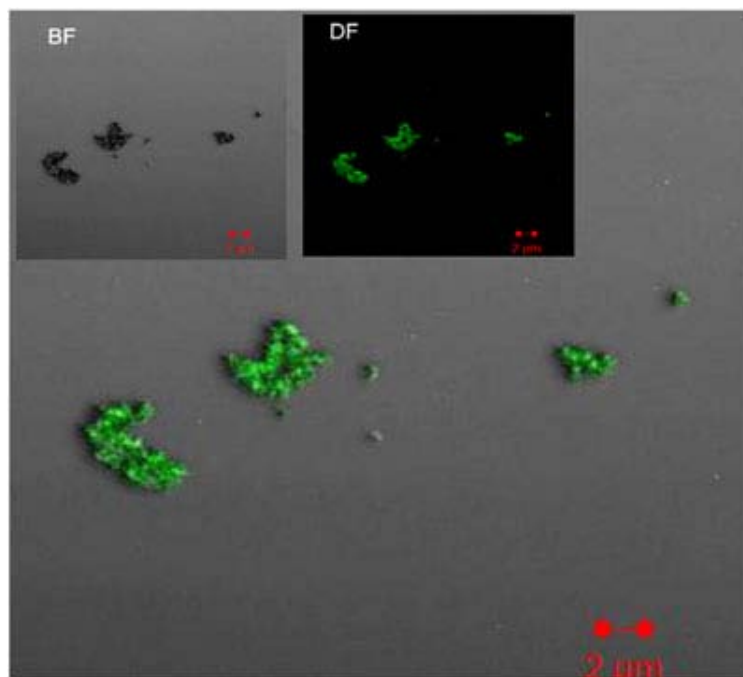


Figure 3.6 Confocal fluorescent of microscopy images of QD-GNP1. BF indicates bright field and DF indicates the dark field, respectively.

### 3.3.2 Cytotoxicity

The cytotoxicity effects of the GNPs, CdSe QDs and QDs-GNP1 were studied using NIH/3T3 mouse fibroblast cells. Cells were cultured to confluence. Different samples were mixed with cells in medium and were continually cultured for 24 h. Figure 3.7 shows that MUA-QDs not encapsulated in GNPs have a significant adverse effect on cell

viability when the concentration of MUA-QDs increases from 0.01 to 0.05 mg/mL. Whereas GNPs and QDs-GNP1, at concentrations up to 5 mg/mL, are not toxic to cells. In addition, no QDs released from GNPs have been found over a period of 5 days.

In sum, we initially used nature polymer gelatin as coating material for QDs to produce luminescent NPs. The luminescent NPs, i.e. QDs-GNP1, exhibit good biocompatibility. However, as we discussed above, the optimum pH ranges (2.5-4) for formation of GNPs can cause aggregation of MUA-QDs, and may result in photobleaching. Further improvement in photostability of gelatin-QDs system is required for its use in bioimaging.

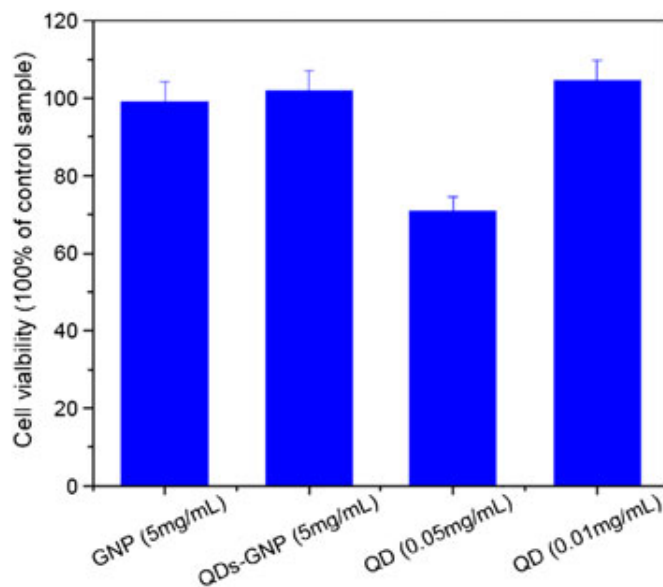


Figure 3.7 Cytotoxicity analysis of GNPs, MUA-QDs and QD-GNP1.

### 3.4 Results and Discussion (II)

This section presents the results for preparation of a new type of gelatin-QDs hybrid NPs system (i.e. QDs-GNP2) with bright luminescence, good photostability and biocompatibility for potential cell imaging use.

### 3.4.1 Materials characterization

The average diameter of the core-shell QDs-GNP2 is estimated at  $484 \pm 40$  nm through SEM and TEM results (Figure 3.8 a). TEM micrograph (Figure 3.8 b) clearly shows the multiple layers of dense dark dots on the shell, which are attributed to the assembled CdSe QDs verified by a high-resolution TEM. Element analysis carried by EDX (Figure 3.8 c) indicates the existing of elements S, Cd and Se on the layers, which are attributed to the capping molecule MUA and two main compositions of the QDs.

The  $\zeta$  potential of GNPs, MUA-QDs, and QDs-GNP2 are  $24.1 \pm 0.4$  mV,  $-29.9 \pm 0.48$  mV, and  $-16 \pm 0.4$  mV, respectively. The surface of the core-shell QDs -GNP2 is negatively charged. Two specific bands located at  $1020\text{ cm}^{-1}$  and  $1130\text{ cm}^{-1}$  are found in the FTIR spectra (Figure 3.9), which are assigned to the PSS characterization stretches (Figure 3.9 b). The results indicate that the MUA-QDs have been successfully assembled onto the GNPs with the assistance of PE layers. In addition, it is estimated that there are 0.25 mg QDs per 1 mg core-shell QDs-GNP2 (1:4 w/w) by comparing with the PL intensities of QDs and QDs-GNP2 as mentioned in experimental section (Figure A1, see appendix 1).

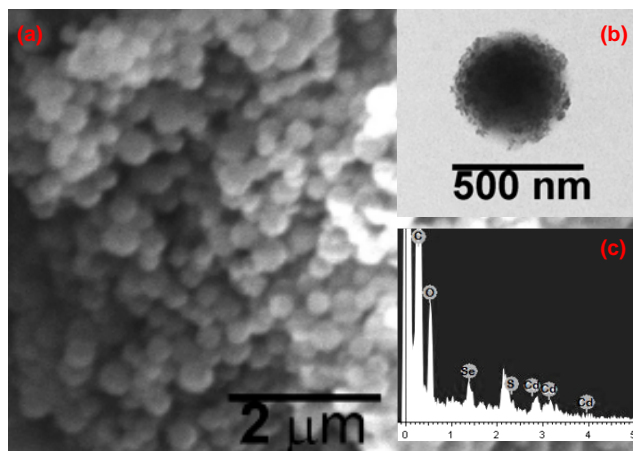


Figure 3.8. Characterization of QDs-GNP2 by electron microscopy.

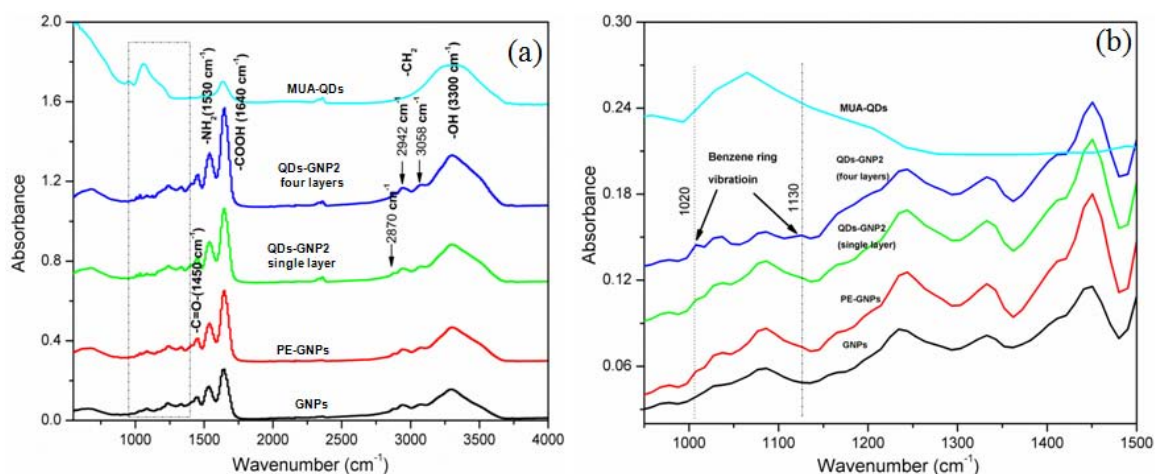
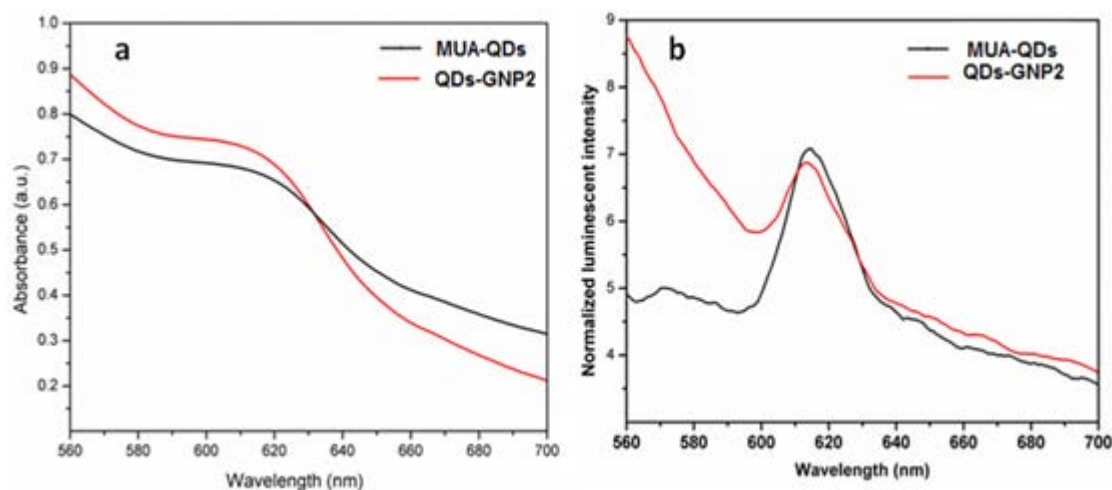


Figure 3.9. FTIR spectra of (i) bare GNPs, (ii) PE coating GNPs, (iii) single layer QDs coating GNPs, (iv) multilayer QDs coating GNPs, and (v) free MUA-QDs.

### 3.4.2 Absorbance and PL spectra

Figure 3.10 displays the absorbance and PL emission spectra of MUA-QDs and QDs-GNP2, respectively. It indicates that the first exciton absorption peak ( $\lambda_{ab}$ ) of MUA-QDs is around 600 nm, and the maximum PL is occurred with the emission wavelength ( $\lambda_{em}$ ) at 617 nm. It is noted that a very slight blue shift ( $3 \pm 1$  nm) occurs to both  $\lambda_{ab}$  and  $\lambda_{em}$  of QDs-GNP2 as comparing to those of MUA-QDs. PL emission of small semiconductor QDs are known to be dependent on either band-to-band recombination in the nanocrystal core<sup>30, 42</sup> or radiative surface states.<sup>31-33</sup> In our study, the blue-shift could be attributed to the latter mechanism because PE matrix assisting the assembly of MUA-QDs layers may offer a higher degree of surface passivation of charges via interacting with surface atoms of QDs.<sup>31</sup> Our results also indicate that the relative quantum yield (QY) of QDs-GNP2 is 1.8-fold higher than that of the free MUA-QDs. Thus, PE matrix may minimize the surface nonradiative recombination and increase confinement of charge carrier, which consequently cause higher band-gap energy, shorter wavelengths and higher quantum yields (QY).<sup>31, 32</sup>





**Figure 3.10.** (a) Absorbance and (b) PL spectra for MUA-QDs and corresponding QDs-GNP2.

### 3.4.3 The pH effects on photostability

The photoquenching of luminescence at low pH value limits the application of QDs in bio-imaging *in vitro* and *in vivo*,<sup>37, 42</sup> for some important physiological cells normally live in low pH values (<7), including endosomes and lysosomes inside cells (pH 5-6.5) and some tumor cells (pH 6-6.9).<sup>43, 44</sup> Here, we further studied the proton-resistant capability of QDs-GNP2 in different pH values with the comparison of MUA-QDs. The weight ratio of MUA-QDs to QDs-GNP2 is 1:4 to maintain the same amount of QDs in both samples. Figure 3.11a shows that the PL intensity of MUA-QDs decreases with decreasing of pH value from 9 to 1, whereas the PL intensity of QDs-GNP2 is relatively stable, independent- pH value. It shows that the PL intensity of QDs-GNP2 is two times higher than that of MUA-QDs at pH 1.0. The decreasing behavior of PL intensity could result from the aggregation of free MUA-QDs at low pH, which could be caused by the protonation of capping material MUA molecule. Agglomerations were observed in low pH levels (data not shown).

In addition, the average lifetime ( $\tau_{ave}$ ) of MUA-QDs and QDs-GNP2 as a function of pH value (pH at 1, 4, 7, and 9) were measured using the TM-30 Laser Strobe time-resolved

fluorometer, as shown in the Figure A1 (see appendix), in which the experimental data are shown as dots, and numerical fits as lines.

As per equation 3.1, the calculated average lifetime ( $\tau_{ave}$ ) of QDs-GNP2 is about  $889 \pm 23$  ps, which is 3-fold longer than that of MUA-QDs ( $263 \pm 10$  ps) at pH 7.0. It is noted that most reported lifetime for CdSe QDs is 3 to 20 ns. Our short calculated average lifetimes of produced QDs could be related to the defects of the produced QDs caused by oxidation. The PL decay of MUA-QDs is pH- dependent as shown in Figure 3.11b, which is in agreement with previous reports.<sup>45</sup> The average lifetime ( $\tau_{ave}$ ) for free MUA-QDs decreases dramatically from 285 ps to 112 ps with decreasing pH value from 9.0 to 1.0. In contrast, the  $\tau_{ave}$  of QDs-GNP2 (775 ps ~ 914 ps) does not change significantly along with the change of pH value from 9 to 1. Acid etching results in the changes of nanocrystal semiconductive structures, and lead to the decreases of the PL intensity and lifetime of QDs.<sup>31</sup>

Here, the negatively charged PSS layer may neutralize the surrounding protons in acidic conditions, and, therefore, against the potential proton effect on the PL photostability of the core-shell QDs-GNP2. In addition, the immobilization of QDs on GNP2 prevents QDs with negative charges from aggregations caused by the addition of protons. As a result, the PL signals of QDs-GNP2 are relatively stable in a broad range of pH value from 9 to 1.

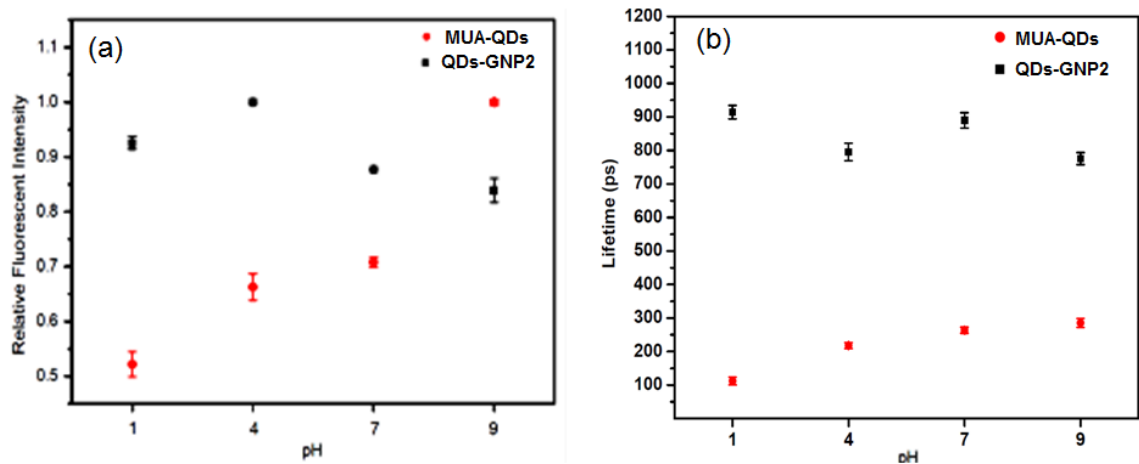


Figure 3.11. The pH effects on (a) PL intensity and (b) average lifetimes

### 3.4.4 Cytotoxicity analysis of QDs-GNP2

We further investigated the cytotoxicity of the QDs-GNP2 with the comparison of MUA-QDs. NIH/3T3 mouse fibroblast cell line was treated by free MUA-QDs and QDs-GNP2 with weight ratio of 1 to 4 to maintain the same amount of QDs in both samples. MultiTox-Fluor assay was used to analyze the cell viability. When the concentration of QDs-GNP2 increases from 5 mg/mL to 0.2 mg/mL, the relative cell viability (%) increases up to 140% as compared to the control samples (Figure 3.12). It is noted that GNPs may enhance the cell proliferation.<sup>46</sup> As indicated by above result (Figure 3.6), no significant toxic effect was imposed on cells when the concentration of GNP2 is up to 5 mg/mL. Whereas the relative cell viability (%) decreases from 100% to 82% when the concentration of MUA-QDs increases from 0.05 mg/mL to 1.25 mg/mL. With further increasing concentration of MUA-QDs up to 6.25 mg/mL, the cell viability dramatically decreases to 20%. Meanwhile, the relative cell viability percentage dramatically drops to 50% when the concentration of QDs-GNP2 increases up to 25 mg/mL, which might be related to the negative interference of florescent detection caused by the high concentration of non-transparent QDs-GNP2.

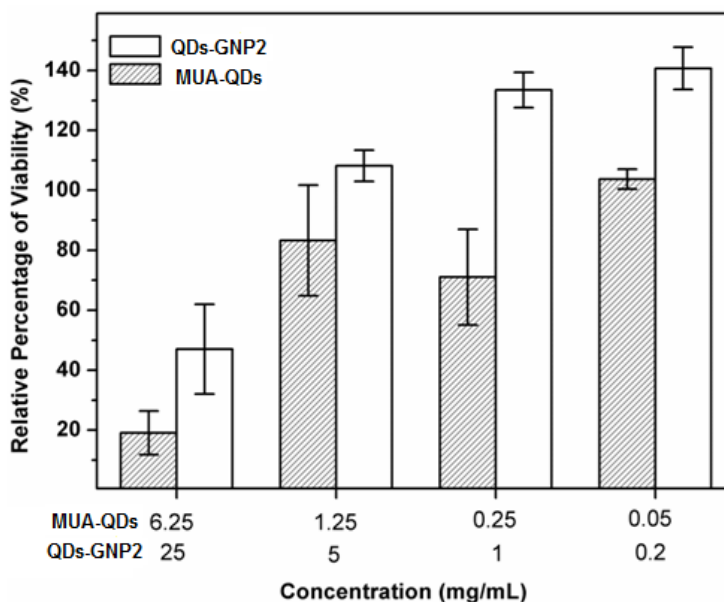
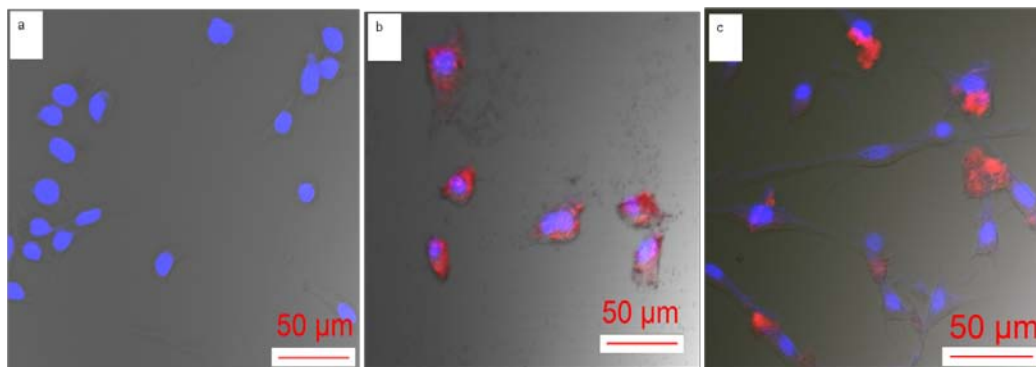


Figure 3.12. Cytotoxicity profile of MUA-QDs and corresponding QDs-GNP2 after 24 hrs incubation with 3T3 cells. Percent viability is expressed relative to control cells (n=3)

### 3.4.5 *In vitro* bio-imaging application

We subsequently investigated the core shell QDs-GNP2 *in vitro* bio-imaging applications by using confocal microscopy. The NIH/3T3 mouse fibroblast cell line was applied and incubated with 0.1 mg/mL MUA-QDs and 0.4 mg/mL QDs-GNP2 for 24 hrs, respectively. Figure 3.13a indicates that the cells are alive with mixing GNPs (0.3 mg/mL). As shown in Figure 3.13b, MUA-QDs are observed on the surface of most of cells (red color), which is in agreement with previous reports.<sup>8</sup> Very few MUA-QDs are suspended in the culture media. The nonspecific cellular uptake of MUA-QDs results from passive endocytosis due to its very small particle size.<sup>8, 47-49</sup> In addition, the produced QDs-GNP2 with high photostability (red color) are preferred to attach on the surface of the cells (Figure 3.13c). It is unlikely that NIH/3T3 mouse fibroblast cells could naturally uptake of large QDs-GNP2 with average diameter of  $480 \pm 40$  nm. The internalization of NPs with such a large diameter through passive endocytosis could merely be possible to specialized mammalian cells (such as monocytes, macrophages and neutrophils) via phagocytosis.<sup>50</sup> Previous reports indicate that the negatively charged surfaces (PSS dominated) are favorable to cell adhesion and spreading.<sup>51</sup> In addition, the advantage of using PSS as an out layer may lead to longer circulation time *in vivo*.<sup>52</sup>



**Figure 3.13** Confocal microscopy images of (a) GNPs (0.3 mg/mL), (b) MUA-QDs (0.1 mg/mL), and (c) QDs-GNP2 (0.4 mg/mL) after co-incubation with NIH/3T3 mouse fibroblast cells. All nucleuses were labeled with DAPI (blue).

Consequently, our biocompatible and fluorescent QDs-GNP2 are favorable to attach onto the cell surface, and can be used as an alternative fluorescent imaging agent for cell

labeling, especially in acidic conditions. It is also noted that the QDs-GNP2 interact with cells through the electrostatic interaction (nonspecific interaction). Further efforts will be taken to modify the surface of the hybrid nanospheres for targeted cell

### 3.5 Conclusions and Prospects

In conclusion, we have prepared two different biocompatible quantum dots-GNPs systems (QD-GNPs) for bioimaging application. The first system involves utilizing gelatin for directly embedding quantum dots (QD-GNP1) to form a quantum dots/gelatine core/shell structure. TEM result show QD-GNP1 has an average diameter of 200 nm with QD embedded. QD-GNP1 exhibits bright fluorescence with maximum emission wavelength at 613 nm. The results from cytotoxicity test indicate good biocompatibility of QD-GNP1. To improve photostability of QD-GNPs system, we further prepared a new system consist of a QDs embedded polyelectrolytes (PE) shell coated gelatin nanoparticles (QD-GNP2) through a LBL process. Electronic microscopy results show the QD-GNP2 has a gelatin core and PE shell, with an averaged diameter of ~480 nm. Four layers of CdSe QDs were showed embedded in the PE shell. The nanocomposites exhibit good dispersibility and extremely bright and stable PL property in aqueous solution under a wide pH range. The quantum yield and lifetime of encapsulated QDs are found improved due to the multilayer PE protection. Good biocompatibility of the as-prepared NPs is further demonstrated by cytotoxicity study. The bright PL allows the NPs for detecting and labeling living 3T3 cells, which indicates the QDs-GNPs system could be a suitable candidate for bio-imaging application. We believe that our QDs-GNPs systems could be used for in situ real-time monitoring/imaging drug delivery in future.

### 3.6 References

1. Bruchez, M.; Moronne, M.; Gin, P.; Weiss, S.; Alivisatos, A. P., Semiconductor Nanocrystals as Fluorescent Biological Labels. *Science* **1998**, 281, (5385), 2013-2016.
2. Chan, W. C. W.; Nie, S., Quantum Dot Bioconjugates for Ultrasensitive Nonisotopic Detection. *Science* **1998**, 281, (5385), 2016-2018.
3. Michalet, X.; Pinaud, F. F.; Bentolila, L. A.; Tsay, J. M.; Doose, S.; Li, J. J.; Sundaresan, G.; Wu, A. M.; Gambhir, S. S.; Weiss, S., Quantum Dots for Live Cells, in Vivo Imaging, and Diagnostics. *Science* **2005**, 307, (5709), 538-544.

4. Mamedova, N. N.; Kotov, N. A.; Rogach, A. L.; Studer, J., Albumin-CdTe Nanoparticle Bioconjugates: Preparation, Structure, and Interunit Energy Transfer with Antenna Effect. *Nano Letters* **2001**, 1, (6), 281-286.
5. Chan, W. C. W.; Maxwell, D. J.; Gao, X.; Bailey, R. E.; Han, M.; Nie, S., Luminescent quantum dots for multiplexed biological detection and imaging. *Current Opinion in Biotechnology* **2002**, 13, (1), 40-46.
6. Xing, B.; Li, W.; Dou, H.; Zhang, P.; Sun, K., Systematic Study of the Properties of CdSe Quantum Dots Synthesized in Paraffin Liquid with Potential Application in Multiplexed Bioassays. *The Journal of Physical Chemistry C* **2008**, 112, (37), 14318-14323.
7. Chang, E.; Thekkekk, N.; Yu, W. W.; Colvin, V. L.; Drezek, R., Evaluation of Quantum Dot Cytotoxicity Based on Intracellular Uptake. *Small* **2006**, 2, (12), 1412-1417.
8. Derfus, A. M.; Chan, W. C. W.; Bhatia, S. N., Probing the Cytotoxicity of Semiconductor Quantum Dots. *Nano Letters* **2003**, 4, (1), 11-18.
9. Yu, W. W.; Chang, E.; Drezek, R.; Colvin, V. L., Water-soluble quantum dots for biomedical applications. *Biochemical and Biophysical Research Communications* **2006**, 348, (3), 781-786.
10. Guo, W.; Li, J. J.; Wang, Y. A.; Peng, X., Conjugation Chemistry and Bioapplications of Semiconductor Box Nanocrystals Prepared via Dendrimer Bridging. *Chemistry of Materials* **2003**, 15, (16), 3125-3133.
11. Kim, S.; Bawendi, M. G., Oligomeric Ligands for Luminescent and Stable Nanocrystal Quantum Dots. *Journal of the American Chemical Society* **2003**, 125, (48), 14652-14653.
12. Osaki, F.; Kanamori, T.; Sando, S.; Sera, T.; Aoyama, Y., A Quantum Dot Conjugated Sugar Ball and Its Cellular Uptake. On the Size Effects of Endocytosis in the Subviral Region. *Journal of the American Chemical Society* **2004**, 126, (21), 6520-6521.
13. Pathak, S.; Choi, S.-K.; Arnheim, N.; Thompson, M. E., Hydroxylated Quantum Dots as Luminescent Probes for in Situ Hybridization. *Journal of the American Chemical Society* **2001**, 123, (17), 4103-4104.
14. Pinaud, F.; King, D.; Moore, H.-P.; Weiss, S., Bioactivation and Cell Targeting of Semiconductor CdSe/ZnS Nanocrystals with Phytochelatin-Related Peptides. *Journal of the American Chemical Society* **2004**, 126, (19), 6115-6123.
15. Gao, X.; Cui, Y.; Levenson, R. M.; Chung, L. W. K.; Nie, S., In vivo cancer targeting and imaging with semiconductor quantum dots. *Nat Biotech* **2004**, 22, (8), 969-976.
16. Pellegrino, T.; Manna, L.; Kudera, S.; Liedl, T.; Koktysh, D.; Rogach, A. L.; Keller, S.; Rädler, J.; Natile, G.; Parak, W. J., Hydrophobic Nanocrystals Coated with an Amphiphilic Polymer Shell: A General Route to Water Soluble Nanocrystals. *Nano Letters* **2004**, 4, (4), 703-707.
17. Gerion, D.; Pinaud, F.; Williams, S. C.; Parak, W. J.; Zanchet, D.; Weiss, S.; Alivisatos, A. P., Synthesis and Properties of Biocompatible Water-Soluble Silica-Coated CdSe/ZnS Semiconductor Quantum Dots. *The Journal of Physical Chemistry B* **2001**, 105, (37), 8861-8871.

18. Selvan, S. T.; Tan, T. T.; Ying, J. Y., Robust, Non-Cytotoxic, Silica-Coated CdSe Quantum Dots with Efficient Photoluminescence. *Advanced Materials* **2005**, 17, (13), 1620-1625.
19. Balthasar, S.; Michaelis, K.; Dinauer, N.; von Briesen, H.; Kreuter, J. r.; Langer, K., Preparation and characterisation of antibody modified gelatin nanoparticles as drug carrier system for uptake in lymphocytes. *Biomaterials* **2005**, 26, (15), 2723-2732.
20. Coester, C. J.; Langer, K.; Briesen, H. V.; Kreuter, J., Gelatin nanoparticles by two step desolvation a new preparation method, surface modifications and cell uptake. *Journal of Microencapsulation* **2000**, 17, (2), 187-193.
21. Kumari, A.; Yadav, S. K.; Yadav, S. C., Biodegradable polymeric nanoparticles based drug delivery systems. *Colloids and Surfaces B: Biointerfaces* **2010**, 75, (1), 1-18.
22. Byrne, S. J.; Williams, Y.; Davies, A.; Corr, S. A.; Rakovich, A.; Gun'ko, Y. K.; Rakovich, Y. P.; Donegan, J. F.; Volkov, Y., "Jelly Dots": Synthesis and Cytotoxicity Studies of CdTe Quantum Dot-Gelatin Nanocomposites. *Small* **2007**, 3, (7), 1152-1156.
23. Wang, Y.; Chen, H.; Ye, C.; Hu, Y., Synthesis and characterization of CdTe quantum dots embedded gelatin nanoparticles via a two-step desolvation method. *Materials Letters* **2008**, 62, (19), 3382-3384.
24. Mozafari, M.; Moztarzadeh, F., Controllable synthesis, characterization and optical properties of colloidal PbS/gelatin core-shell nanocrystals. *Journal of Colloid and Interface Science* **2010**, 351, (2), 442-448.
25. Raevskaya, A. E.; Stroyuk, A. L.; Kuchmiy, S. Y.; Azhniuk, Y. M.; Dzhagan, V. M.; Yuhymchuk, V. O.; Valakh, M. Y., Growth and spectroscopic characterization of CdSe nanoparticles synthesized from CdCl<sub>2</sub> and Na<sub>2</sub>SeSO<sub>3</sub> in aqueous gelatine solutions. *Colloids and Surfaces A: Physicochemical and Engineering Aspects* **2006**, 290, (1-3), 304-309.
26. Wang, Y.; Ye, C.; Wu, L.; Hu, Y., Synthesis and characterization of self-assembled CdHgTe/gelatin nanospheres as stable near infrared fluorescent probes in vivo. *Journal of Pharmaceutical and Biomedical Analysis* **2010**, 53, (3), 235-242.
27. Xu, L.; Chen, K.; El-Khair, H. M.; Li, M.; Huang, X., Enhancement of band-edge luminescence and photo-stability in colloidal CdSe quantum dots by various surface passivation technologies. *Applied Surface Science* **2001**, 172, (1-2), 84-88.
28. Azarmi, S.; Huang, Y.; Chen, H.; McQuarrie, S.; Abrams, D.; Roa, W.; Finlay, W. H.; Miller, G. G.; Lobenberg, R., Optimization of a two-step desolvation method for preparing gelatin nanoparticles and cell uptake studies in 143B osteosarcoma cancer cells. *J Pharm Pharm Sci* **2006**, 9, (1), 124-32.
29. Shutava, T. G.; Balkundi, S. S.; Vangala, P.; Steffan, J. J.; Bigelow, R. L.; Cardelli, J. A.; O'Neal, D. P.; Lvov, Y. M., Layer-by-Layer-Coated Gelatin Nanoparticles as a Vehicle for Delivery of Natural Polyphenols. *ACS Nano* **2009**, 3, (7), 1877-1885.

30. Jiang, W.; Mardyani, S.; Fischer, H.; Chan, W. C. W., Design and Characterization of Lysine Cross-Linked Mercapto-Acid Biocompatible Quantum Dots. *Chemistry of Materials* **2006**, 18, (4), 872-878.
31. Komarala, V. K.; Rakovich, Y. P.; Bradley, A. L.; Byrne, S. J.; Corr, S. A.; Gun'ko, Y. K., Emission properties of colloidal quantum dots on polyelectrolyte multilayers. *Nanotechnology* **2006**, 17, (16), 4117-22.
32. Maule, C.; Gonçalves, H.; Mendonça, C.; Sampaio, P.; Esteves da Silva, J. C. G.; Jorge, P., Wavelength encoded analytical imaging and fiber optic sensing with pH sensitive CdTe quantum dots. *Talanta* **2010**, 80, (5), 1932-1938.
33. Wang, Y.; Tang, Z.; Correa-Duarte, M. A.; Pastoriza-Santos, I.; Giersig, M.; Kotov, N. A.; Liz-Marzán, L. M., Mechanism of Strong Luminescence Photoactivation of Citrate-Stabilized Water-Soluble Nanoparticles with CdSe Cores. *The Journal of Physical Chemistry B* **2004**, 108, (40), 15461-15469.
34. Ai, H.; Jones, S.; Lvov, Y., Biomedical applications of electrostatic layer-by-layer nano-assembly of polymers, enzymes, and nanoparticles. *Cell Biochemistry and Biophysics* **2003**, 39, (1), 23-43.
35. He, J.-A.; Valluzzi, R.; Yang, K.; Dolukhanyan, T.; Sung, C.; Kumar, J.; Tripathy, S. K.; Samuelson, L.; Balogh, L.; Tomalia, D. A., Electrostatic Multilayer Deposition of a Gold-Dendrimer Nanocomposite. *Chemistry of Materials* **1999**, 11, (11), 3268-3274.
36. Kim, J.; Wang, H.-C.; Kumar, J.; Tripathy, S. K.; Chittibabu, K. G.; Cazeca, M. J.; Kim, W., Novel Layer-by-layer Complexation Technique and Properties of the Fabricated Films. *Chemistry of Materials* **1999**, 11, (8), 2250-2256.
37. Lvov, Y.; Ariga, K.; Ichinose, I.; Kunitake, T., Assembly of Multicomponent Protein Films by Means of Electrostatic Layer-by-Layer Adsorption. *Journal of the American Chemical Society* **1995**, 117, (22), 6117-6123.
38. Ostrander, J. W.; Mamedov, A. A.; Kotov, N. A., Two Modes of Linear Layer-by-Layer Growth of Nanoparticle-Polyelectrolyte Multilayers and Different Interactions in the Layer-by-layer Deposition. *Journal of the American Chemical Society* **2001**, 123, (6), 1101-1110.
39. Aldana, J.; Wang, Y. A.; Peng, X., Photochemical Instability of CdSe Nanocrystals Coated by Hydrophilic Thiols. *Journal of the American Chemical Society* **2001**, 123, (36), 8844-8850.
40. Lakowicz, J., Frequency-Domain Lifetime Measurements. In *Principles of Fluorescence Spectroscopy*, Springer US: 2006; pp 157-204.
41. Yuan, C.; Chou, W.; Chuu, D.; Chang, W. H.; Lin, H.; Ruaan, R., Fluorescence properties of colloidal CdSe/ZnS quantum dots with various surface modifications. *Journal of Medical and Biological Engineering* **2006**, 26, (3), 131-135.
42. Guo, W.; Li, J. J.; Wang, Y. A.; Peng, X., Luminescent CdSe/CdS Core/Shell Nanocrystals in Dendron Boxes: Superior Chemical, Photochemical and Thermal Stability. *Journal of the American Chemical Society* **2003**, 125, (13), 3901-3909.
43. Ganta, S.; Devalapally, H.; Shahiwala, A.; Amiji, M., A review of stimuli-responsive nanocarriers for drug and gene delivery. *Journal of Controlled Release* **2008**, 126, (3), 187-204.



44. Wan, X.; Wang, D.; Liu, S., Fluorescent pH-Sensing Organic/Inorganic Hybrid Mesoporous Silica Nanoparticles with Tunable Redox-Responsive Release Capability. *Langmuir* **2010**, 26, (19), 15574-15579.
45. Ruedas-Rama, M. J.; Orte, A.; Hall, E. A. H.; Alvarez-Pez, J. M.; Talavera, E. M., Quantum dot photoluminescence lifetime-based pH nanosensor. *Chemical Communications* **2011**, 47, (10), 2898-2900.
46. Gupta, A. K.; Gupta, M.; Yarwood, S. J.; Curtis, A. S. G., Effect of cellular uptake of gelatin nanoparticles on adhesion, morphology and cytoskeleton organisation of human fibroblasts. *Journal of Controlled Release* **2004**, 95, (2), 197-207.
47. Hanaki, K.-i.; Momo, A.; Oku, T.; Komoto, A.; Maenosono, S.; Yamaguchi, Y.; Yamamoto, K., Semiconductor quantum dot/albumin complex is a long-life and highly photostable endosome marker. *Biochemical and Biophysical Research Communications* **2003**, 302, (3), 496-501.
48. Hoshino, A.; Hanaki, K.-i.; Suzuki, K.; Yamamoto, K., Applications of T-lymphoma labeled with fluorescent quantum dots to cell tracing markers in mouse body. *Biochemical and Biophysical Research Communications* **2004**, 314, (1), 46-53.
49. Jaiswal, J. K.; Mattoussi, H.; Mauro, J. M.; Simon, S. M., Long-term multiple color imaging of live cells using quantum dot bioconjugates. *Nat Biotech* **2003**, 21, (1), 47-51.
50. Zhao, F.; Zhao, Y.; Liu, Y.; Chang, X.; Chen, C.; Zhao, Y., Cellular Uptake, Intracellular Trafficking, and Cytotoxicity of Nanomaterials. *Small* **2011**, 7, (10), 1322-1337.
51. Han, L.; Mao, Z.; Wu, J.; Zhang, Y.; Gao, C., Influences of surface chemistry and swelling of salt-treated polyelectrolyte multilayers on migration of smooth muscle cells. *J. R. Soc. Interface* **2012**, 9, (77), 3455-3468.
52. Yong Serk, P.; Maruyama, K.; Huang, L., Some negatively charged phospholipid derivatives prolong the liposome circulation in vivo. *Biochimica et Biophysica Acta (BBA) - Biomembranes* **1992**, 1108, (2), 257-260.

## **CHAPTER 4**

### **DEVELOPMENT OF BIOCONJUGATED MAGNETIC LUMINESCENT NANOMATERIALS FOR BACTERIAL CAPTURE, DETECTION AND ANTIBACTERIAL APPLICATIONS**

## 4.1 Introduction

Bacteria can lead to serious infectious diseases and environmental contamination, and bring a huge public health burden.<sup>1</sup> In particular, gram-negative bacterium *Escherichia coli* and gram-positive bacterium *Staphylococcus aureus* are known as two of the leading causes in food borne diseases in the world.<sup>2, 3</sup> In addition, bacterial infections are also found in the skin, soft-tissue, bone, joint, and endovascular disorders.<sup>4, 5</sup> Antibiotics have been developed to treat bacterial infections, but the effective dosage is not well controlled. In addition, the unique cell wall made of highly cross-linked peptidoglycan offer a rigid shell to protect the gram-positive bacteria from osmotic pressure, external hazard macromolecules permeability and antibacterial enzyme digesting, which make the treatment of their infections with much difficulty.<sup>6</sup> Laboratory diagnosis of bacterial infectious disease depends mainly on techniques such as cell culture, enzyme-linked immunosorbent assay (ELISA) and polymerase chain reaction (PCR), while they are normally time-consuming and involved with multiple steps that affect the assay efficiency.<sup>7, 8</sup> In addition, very few bacterial cells may cause disease as they can double their population less than 20 min.<sup>9</sup> Therefore, rapid capture, detection, and decontamination of bacteria are strongly demanded to avoid or minimize contamination of the environment, food, and infections.

In recent, engineered magnetic nanoparticles (MNPs) conjugated with biomolecules have shown promises in applications in drug delivery, magnetic separation,<sup>10, 11</sup> sensor, cell-tracking,<sup>12</sup> and bio-imaging,<sup>13, 14</sup> because of their inducible magnetization, tunable size, nontoxic and biodegradable. Bio-molecules, such as antibody,<sup>15</sup> antibiotics,<sup>16-19</sup> carbohydrate,<sup>20</sup> and small organic molecules,<sup>21</sup> have been reported to conjugate MNPs for bacterial labelling and detection. In particular, bio-conjugated antibiotics to nanostructure can offer a novel manner to simultaneously separate and kill the bacteria from contaminated source at the early stage. For example, Xu and co-workers conjugated FePt-based magnetic NPs with vancomycin, and through peptide binding captured *E. coli* at a low concentration of  $3 \times 10^4$  cells/mL.<sup>16, 17, 19</sup> El-Boubbou *et. al.* conjugated lectin to MNPs and used mannose to bind, capture and kill *E. coli*.<sup>20</sup>

To improve the efficiency and versatility of nanoparticles (NPs) in numerous applications, multiple functionalities have been incorporated to form hybrid MNPs. In particular, optical properties such as fluorescence allow sensitive and quantitative detection of bacteria<sup>22</sup> and visualization of cell structure.<sup>23</sup> Thereby, it is of advantage to develop of fluorescent magnetic nanoparticles (FMNPs) that posse both fluorescent and magnetic properties, regard to detection, imaging and cell tracking. Typically, FMNPs include a core-shell structure, i.e. a magnetic core coated with a fluorescent shell. The fluorescent shell can be composed of polymers and inorganic materials loaded with organic dye,<sup>24-26</sup> quantum dots,<sup>27</sup> or other complexes.<sup>28, 29</sup> Silica is one of the well-studied materials that can act as a shell due to its functional surface, and its unique porous nature.<sup>30-32</sup> Previous studies demonstrated that fluorophore-loaded mesoporous SiO<sub>2</sub> NPs are 20 times brighter than semiconductor quantum dots.<sup>33, 34</sup> They can be taken up by dendritic cells for cell tracking and cancer treatment.<sup>35, 36</sup> The magnetic cores of most FMNPs are intended to be Fe<sub>2</sub>O<sub>3</sub>-rich materials.<sup>37</sup> However, compared to hematite (Fe<sub>2</sub>O<sub>3</sub>) and other magnetic materials, magnetite (Fe<sub>3</sub>O<sub>4</sub>) shows higher magnetization, about 65 emu/g<sup>32, 38</sup> and has various applications in biosensing and imaging.<sup>39, 40</sup>

The common method for preparation of silica coated iron oxide nanoparticles (SMNPs) involves two steps, i.e. synthesis of iron oxide nanoparticles (IONPs) and post coating of silica on the surface. Several methods have been developed to synthesize IONPs, including co-precipitation, hydrothermal and thermal decomposition method. Co-precipitation process is one of the most preferred ways to produce magnetite and maghemite, which involves co-precipitation of Fe<sup>2+</sup> and Fe<sup>3+</sup> in aqueous solution by addition of base. The reaction runs under mild condition (room temperature) and the products are hydrophilic and ready for further silanation. However, the drawbacks are poor crystalline of the particles and difficulty in controlling of the size distribution. The other two approaches, in particular thermal decomposition method, require high temperature and thus can produce particles in good crystalline structure and narrow size distribution. However, the NPs are usually coated by hydrophobic ligands for thermal decomposition method. Thus additional surface modification such as ligand exchange to bring NPs into aqueous solution is required prior for further coating with silica shell. For silica coating, there are two widely used methods. The first one is based on the Stöber

process,<sup>41</sup> which comprises the hydrolysis and condensation of a sol-gel precursor such as TEOS. In the second method, silica shell is produced via the microemulsion process, where reverse micelles are used to confine and control the condensation of TEOS.<sup>42</sup> In both methods, fluorescent dyes can be conjugated to silane (such as APTS) before condensation of TEOS, to form fluorescent shell.

Alternative strategy for preparation of FMNPs is one-pot synthesis scheme. In our group, we previously developed a one-pot synthesis to produce dye labeling silica-coated magnetite NPs. The process simplifies the reaction by co-precipitation of iron salt directly in an oil-water micelle, followed by condensation of TEOS on the IONPs surface in the same solution. Improved fluorescent properties and magnetic properties have been reported.

In this chapter, we reported preparation of a new bioconjugation of FMNPs with antibiotic gentamicin for ubiquitous capture, detection and decontamination of bacteria applications. We introduced and compared two approaches in preparation of the FMNPs, i.e. one-pot co-precipitation way and two-step decomposition method. The as-made NPs are thus named FMNP1 and FMNP2, respectively. In addition, gentamicin (Gm) is a FDA approved thermal-resistant antibiotic for the treatment of infection caused by gram-negative bacteria and susceptible gram-positive bacteria. The amino groups of Gm show positive charges through protonation in physiologic solutions, which contribute to the interaction of Gm with lipopolysaccharides (LPS) on the surface of Gram-negative bacteria and phospholipids and teichoic acid on the surface of Gram-positive bacteria, respectively.<sup>43, 44</sup> We thoroughly investigate the interaction between bacteria and FMNPs with/without Gm-bioconjugation. Meanwhile, the detection sensitivity and toxic effect are also investigated.

## 4.2 Experimental

Unless otherwise stated, chemicals were obtained from Sigma-Aldrich.

The scheme in Figure 4.1 illustrates the preparation and bio-conjugation of FMNPs for bacterial capture. The experimental details are described below.

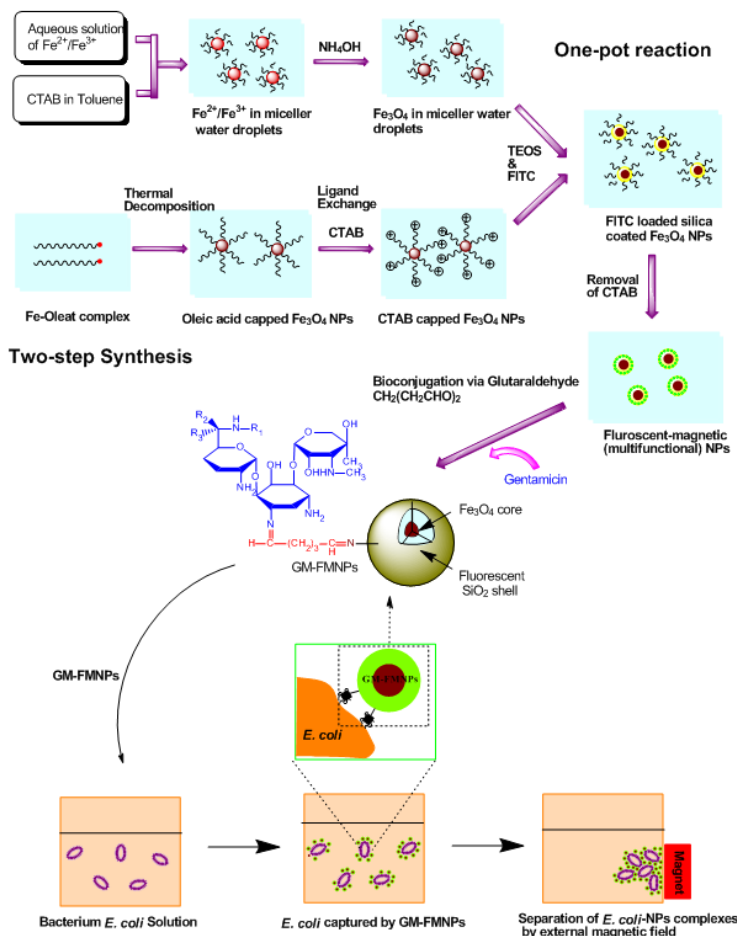


Figure 4.1 Schematic illustration of the synthesis of FMNPs used for *E. coli* capture and magnetic separation in solution

#### 4.2.1 Preparation of FMNP1 by one-pot method

The FMNP1 were produced by an one-pot reaction involving a process of base-catalyzed precipitation of  $\text{Fe}^{2+}/\text{Fe}^{3+}$ , followed by the condensation of tetraethylorthosilicate (TEOS, 99%), and the in situ encapsulation of fluorescein isothiocyanate (FITC, 90%) in the shell as shown in Figure 4.1. Briefly, 7.3 g of cetyl-trimethylammonium bromide (CTAB) (98%) was added to 100 mL of toluene (99.8%). The mixture was stirred at 600 rpm for 4

h, followed by the slow addition of an aqueous solution of  $\text{FeCl}_2/\text{FeCl}_3$  (0.22 g/0.56 g, 7.3 mL;  $\text{FeCl}_2$ , 98%,  $\text{FeCl}_3$ , 97%). The mixture (solution A) was stirred vigorously for 8 h. Then, 1 mL  $\text{NH}_4\text{OH}$  solution (28%) was added drop-wise to the solution. Solution A was stirred for another 4 h. Meanwhile, 5.5 mg fluorescein isothiocyanate (FITC) and 25  $\mu\text{L}$  aminopropyltriethoxysilane (APTS, 98%) were mixed to form *N*-1-(3-triethoxysilylpropyl)-*N'*-fluoresceyl thiourea (FITC-APTS). After 2 h, 2.5 mL of TEOS was added to the FITC-APTS solution. This mixture (solution B) was stirred continuously for an additional 3 h using aluminum foil to protect the dye conjugate from light. Solution B was then added drop-wise to the main reaction of the solution A pot and continuously stirred for 5 days. All reactions were kept under  $\text{N}_2$  atmosphere. Aluminum foil was used to cover the reactor to protect the products from photo-degradation. Finally, the reaction was stopped by addition of 20 mL ethanol. The particles were washed with a mixture of ethanol/acetone (1:1, v/v) and purified by repeat centrifugation. The as-made FMNP1 were then freeze-dried and stored in the dark.

#### 4.2.2 Preparation of FMNP2 by two-step coating method

The FMNP2 were prepared by a two-step process. Firstly, monodisperse IONPs were synthesized through a modified thermal decomposition method.<sup>45</sup> In brief, 1.32 g of  $\text{FeCl}_3$  and 7.4 g of sodium oleate (TCI, 95%) were dissolved in a mixture of 16.3 mL of absolute ethanol, 13.08 mL of water and 28.5 mL of hexane (95%). The solution was refluxed at 60 °C for 4 h, followed by washing with a solution of ethanol and water (1:1, v/v) five times. The resultant iron-oleate precursor was then dried under vacuum overnight at 70 °C. Afterwards, 1 g of wax-like precursor was re-dissolved in a solution of 177.3  $\mu\text{L}$  oleic acid (99%) and 7.1 mL triethylamine (98%). The solution was stirred vigorously and heated to 360 °C rapidly under argon atmosphere, and then aged for 1 h. After that the solution was cooled down, washed with hexane and ethanol (1:3, v/v) mixture and purified by centrifugation for three times. The particles were finally dissolved in chloroform and kept at room temperature.

Silica coating of IONPs were carried out through a modified sol-gel method.<sup>46</sup> Firstly, 1 mg of fluorescein isothiocyanate was dissolved in 0.5 mL of absolute ethanol, followed by addition of 10  $\mu\text{L}$  of APTS. The solution was stirred for 2 h. In another vessel, 50 mg

of IONPs were mixed in 20 ml of an aqueous solution of 2% CTAB. The mixture was stirred vigorously and heated to 70 °C to boil off chloroform. The NPs mixture was further filtered through a 0.45 µm syringe filter to remove large aggregates. Next, 5 mL of the filtered mixture was added into a solution of 43 mL water and 350 µL NaOH (2 M) and heated to 70°C. The mixture of 0.5 mL of TEOS and 10 µL of APTES-FITC solution was then slowly added to the CTAB aqueous solution. After 15 min, 127 µL of trihydroxysilylpropylmethylphosphonate (THPMP) (42%) was added to the solution and stirred for another 2 h under dark. Then, the as-synthesized FMNP2 were precipitated by adding excess methanol and collected by centrifugation. To remove CTAB, the FMNP2 were further re-dispersed and heated at 60 °C for 15 min in a solution containing 160 mg NH<sub>4</sub>NO<sub>3</sub> and 60 mL 95% ethanol. Afterwards, the NPs were purified by repeating centrifugation and washing with ethanol. Finally, the FMNP2 were freeze-dried overnight and kept under dark ready for use.

#### 4.2.3 Bioconjugation of FMNPs with Gm

For bioconjugation of Gm, both FMNP1 and FMNP2 at 2.5 mg/mL in water were reacted with a glutaraldehyde solution (Glu, Grade I, a final concentration of 3% in water) overnight in the dark, respectively. The mixture was then purified by centrifugation (5800 rpm for 5 min) to remove the supernatant, and further re-suspended in water. The purification process was repeated twice, and the Glu conjugated FMNPs were then freeze-dried. To immobilize Gm onto the surface of the FMNPs, a solution containing gentamicin sulfate (1 mg/mL) and 2.5 mg/mL FMNPs was mixed and stirred overnight under dark. The unbound Gm was removed by repeated centrifugation and washing, as described above. The solution was then mixed with 1% bovine serum albumin (BSA, 96%) solution for 1 h to block free formyl group onto the surface of the FMNPs. Finally, the purified Gm-FMNPs were freeze-dried and stored in the dark at 4 °C. In addition to the negative control samples of bare FMNPs and Glu-FMNPs, another negative control sample used to evaluate the Gm-bioconjugation was ethanolamine (EA, 98%). The conjugation of EA to FMNPs followed with the same procedure described above.



#### 4.2.4 Characterization

The morphology of NPs and their interaction with bacteria was examined by TEM and TEM-energy dispersive X-ray spectrometry (TEM/EDX). The TEM images were obtained using a Philips CM-10 microscope operating at 80 kV. The magnetic properties of both IONPs and MNPs were measured by Vibrating Sample Magnetometer 7404 (VSM, Lakeshore Inc.). The hysteresis loop was measured at room temperature under 1 kOe (1 T). A superconducting quantum interference device (SQUID, Quantum Design) was used for measuring of blocking temperature of FMNPs. The zero-field-cooled (ZFC) and field-cooled (FC) magnetization curves of the FMNPs were recorded at 50 Oe over a temperature range of 5 to 300 K. The sample capsule was diamagnetic and did not contribute to the measured result.

The Fe K-edge X-ray absorption near edge structure spectroscopy (XANES) study was conducted to investigate the composition of NPs by using the Soft X-ray Microcharacterization Beamline (SXRMB) at the Canadian Light Source (CLS). The specimens were placed on the sample manipulator in a vacuum chamber ( $\sim 10^{-8}$  Torr). XANES were collected in Total Electron Yield (TEY) by measuring the specimen current in the presence of a voltage bias. In addition, the XANES spectra have been normalized to  $I_0$ , the intensity of the incoming photon beam.

Fluorescence microscopy (Zeiss Axio Imager Z1) analysis was conducted to study the interaction between the bacterial cells and FMNP1 with and without Gm bioconjugation by placing glass slides of the samples under an excitation wavelength ( $\lambda_{\text{ex}}$ ) of 492 nm. In addition, the fluorescent emission signals of the FMNP1 were detected by fluorophotometry (QuantaMaster<sup>TM</sup> 30, PTI) with an excitation wavelength ( $\lambda_{\text{ex}}$ ) of 492 nm. Fourier transform infrared (FTIR) transmittance spectrometry was carried out to identify the Gm bioconjugation. A Bruker Vector 22 was used in the range of 600–4500  $\text{cm}^{-1}$  with a resolution of 4  $\text{cm}^{-1}$  and 64 scans.

#### 4.2.5 Bacteria Capture

In a typical experiment, bacteria *E. coli* (K-12, sub-strain W3110) and *S. aureus* (ATCC 33807) were grown at 37 °C for 24 h in broth media, respectively. The optical density

(O.D.) of this culture was adjusted to having a concentration of approximately  $1 \times 10^7$  CFU/mL. The cells were harvested by centrifugation (8000 rpm, 5 min) and further re-suspended in phosphate buffered saline (PBS, 0.01 M, pH 7.4) buffer containing Gm-FMNPs (final concentration of 0.1 mg/mL). The mixtures were further incubated for 20 and 60 min, respectively. Two samples with different interaction times (t) were separated from the solution using magnetic confinement. Both samples were washed three times, and then re-suspended in PBS for TEM analysis. The mixture was then applied in an external magnetic field (0.2 T) for 1 min. After washing twice, the magnetic confined complex was re-suspended with PBS.

#### 4.2.6 Analysis of the antibacterial effect

The antibacterial property of Gm-FMNP1 to *E. coli* was analyzed by using plate counting technique. Typically, 200  $\mu$ L of the above bacterial solution and NPs mixture were spread homogeneously onto agar plates. All the agar plates were then incubated overnight at 37 °C. The number of CFU of the bacteria was calculated following the incubation.

The antimicrobial efficiency of Gm-FMNPs to *E. coli* was further investigated by standard agar disc diffusion. Briefly, one isolated *E. coli* colony was incubated overnight in fresh broth at room temperature to reach a bacterial culture of  $\sim 10^7$  CFU/mL. A 200  $\mu$ L aliquot of this culture ( $\sim 10^5$  CFU/mL) was spread onto agar plates. Sterile filter paper discs (7 mm) immersed in 1 mL PBS containing different standard concentrations of free Gm and FMNP1 solution samples (both conjugated with or without Gm) were then applied to the plates and incubated for 18 h at 37 °C. The antibacterial efficiency of the Gm-FMNPs was then determined as a function of *E. coli* colony inhibition diameters based on the calibration exponential curve obtained in experiments with known concentrations of the standard solutions.

#### 4.2.7 Determine the concentration of gentamicin on the FMNP1

The amount of gentamicin conjugated on the GM-FMNPs was determined via an o-phthalaldehyde assay reported by C. Lecárocz with slight modification.<sup>47</sup> In brief, the o-phthalaldehyde reagent was formulated by adding 25 mg of o-phthalaldehyde, 625  $\mu$ L of methanol and 30  $\mu$ L of mercaptoethanol to 5.6 mL of sodium borate (0.04 M, pH 9.7)

under dark for at least 24 h at room temperature. This reagent should be used in 48 h. Standard concentrations of gentamicin sulfate were prepared by serial dilution with borate buffer at concentrations of 50, 25, 12.5, 6.25, 3.1, and 1.5  $\mu\text{g/mL}$ . The concentrations of gentamicin in the GM-FMNPs were measured by spiking the NPs in the borate buffer (1 mg/mL). Then, o-phthalaldehyde reagent, gentamicin solutions (standard solutions and NPs solutions), and isopropanol were mixed in similar proportions and stored for 30 min at room temperature. The amount of gentamicin was evaluated by measuring the adsorptions at 292 nm (Shimadzu 3600 UV-visible spectrophotometer) to obtain a standard adsorption curve relating to gentamicin concentration. The concentrations of gentamicin in the NPs solution were calculated by means of the standard curve.

#### 4.2.8 Preparation of thin section samples for TEM analysis

In the initial experiment, thin section treated samples were prepared for TEM/EDX to confirm the interaction of Gm-FMNP1 with bacteria *E. coli*. The samples were prepared by fixing the above bacteria-NPs complex (*E. coli* incubated with and without Gm-FMNPs for 20 min and 60 min, respectively) with 2.5% (v/v) glutaraldehyde in sodium cacodylate buffer (0.1 M, pH 7.4). After 2.5 h fixation, the cells were washed three times in cacodylate buffer with centrifugation ( $\sim 4500\text{ g}$  for 6 min), and further fixed with 1% osmium tetroxide in a cacodylate buffer solution for 1 h. The samples were washed again, and the final pellets were placed in drops of 5% Noble agar. The samples were further fixed in 2% uranyl acetate for 2 h, followed by dehydration in an ethanol solution with ascending gradients of strength (50%, 70%, 85%, 95% with two changes in absolute ethanol, 15 min each). The specimens were then washed in propylene oxide twice and infiltrated with an EPON resin: propylene oxide mixture (ratio 1: 1 and 3: 1, placed in each once) and twice in pure EPON resin. Sample resin blocks were prepared by embedding the samples in resin and polymerizing them at 60  $^{\circ}\text{C}$  for 2 days. The resin blocks were then trimmed and sectioned (80–100 nm) on a Reichert Om-U3 ultramicrotome with a diamond knife. Ultrathin sections were placed on 200-mesh formvar/carbon-coated nickel (Ni) grids for further TEM/EDX analysis.

## 4.3 Results and Discussion

### 4.3.1 Characterization

The morphology of both FMNPs was characterized by TEM as shown in Figure 4.2. An obvious boundary between the core and the shell is observed in most of the particles. For FMNP1, the average diameter of the iron oxide core is estimated to be  $50 \pm 8$  nm, while the thickness of the silica shell is estimated to be  $12 \pm 5$  nm (Figure 4.2a). The mean particle size is approximately  $65 \pm 8$  nm. For FMNP2, the average diameter of monodispersed IONPs is  $18 \pm 2$  nm (Figure 4.2b). The average diameter of the core-shell FMNP2 is about  $30 \pm 5$  nm, and the shell is estimated at  $5 \pm 2$  nm.

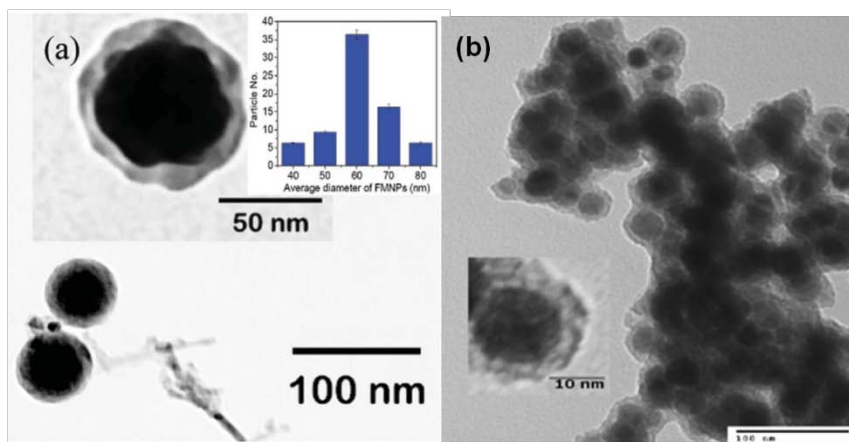


Figure 4.2 TEM micrograph of the core-shell structures of FMNP1 (a) and FMNP2 (b).

The core-shell structured both FMNPs was further investigated through the XRD. As shown in Figure 4.3, the typical peak of semi-crystalline  $\text{SiO}_2$  is broad and can be found around  $23^\circ$  ( $2\theta$ ). The other positions (labelled) and intensity of the peaks are coincident with XRD pattern for bulk  $\text{Fe}_3\text{O}_4$  or  $\alpha\text{-Fe}_2\text{O}_3$  phase with cubic inverse spinel structure (JCPDS file 39-1346 and 190629, respectively). Thus, combining the TEM images, the semi-crystalline  $\text{SiO}_2$  shell has a lighter color in the TEM micrograph, whereas the  $\text{Fe}_3\text{O}_4$  or  $\alpha\text{-Fe}_2\text{O}_3$  core has higher electron density, and therefore, has a darker color. For FMNP2, we also examine the oxidation status of FMNP2 by XANES. The results show the Fe K-edge in the XANES spectra of the standard  $\text{Fe}_3\text{O}_4$  sample and FMNPs (Figure A3, from Appendix 3). The Fe K-edge excitation threshold ( $E_0$ ) is the maximum of the first derivative of the XANES spectra. Clearly, the FMNPs have the same  $E_0$  as that of  $\text{Fe}_3\text{O}_4$ . Thus, the core of the FMNPs is attributed to  $\text{Fe}_3\text{O}_4$ .

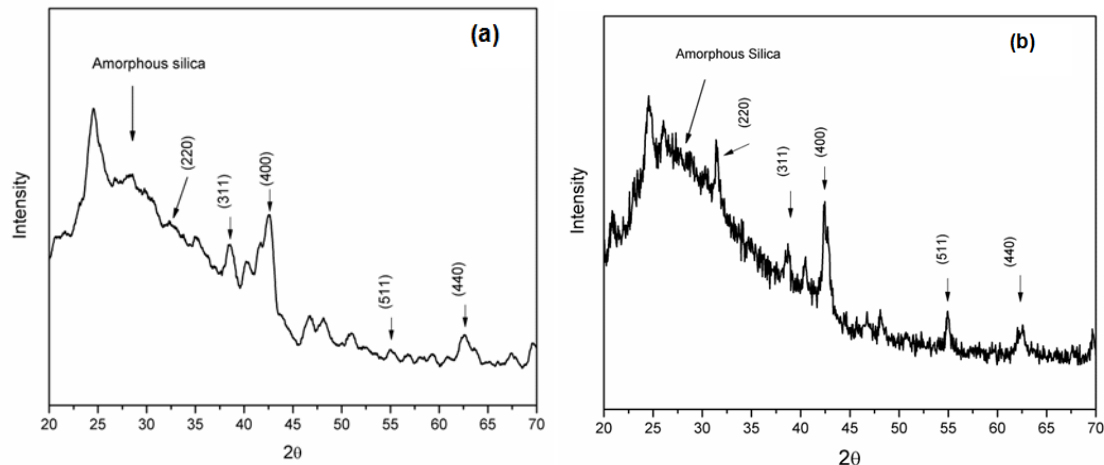


Figure 4.3 XRD profiles of the core-shell structured (a) FMNP1 and (b) FMNP2

Magnetite ( $\text{Fe}_3\text{O}_4$ ) NPs are known for their unique superparamagnetic property at room temperature<sup>48</sup>. As shown in Figure 4.4, typical hysteretic loops for superparamagnet are found for both FMNPs by VSM analysis, which indicate both particles exhibit superparamagnetic property. Our calculation shows the saturation magnetization ( $M_s$ ) at room temperature of FMNP1 and FMNP2 are 2.512 emu/g and 1.5955 emu/g, respectively. In comparison with other Fe-based magnetic materials,  $\text{Fe}_3\text{O}_4$  has high thermal stability with a high Curie temperature ( $T_c$ ) of 858 K. Figure 4.4 shows the superparamagnetic behavior of the FMNPs during field cooling (FC) and zero-field cooling (ZFC) from SQUID analysis. The results indicate the blocking temperatures of FMNP1 and FMNP2 are at 120 K and 115 K, respectively.

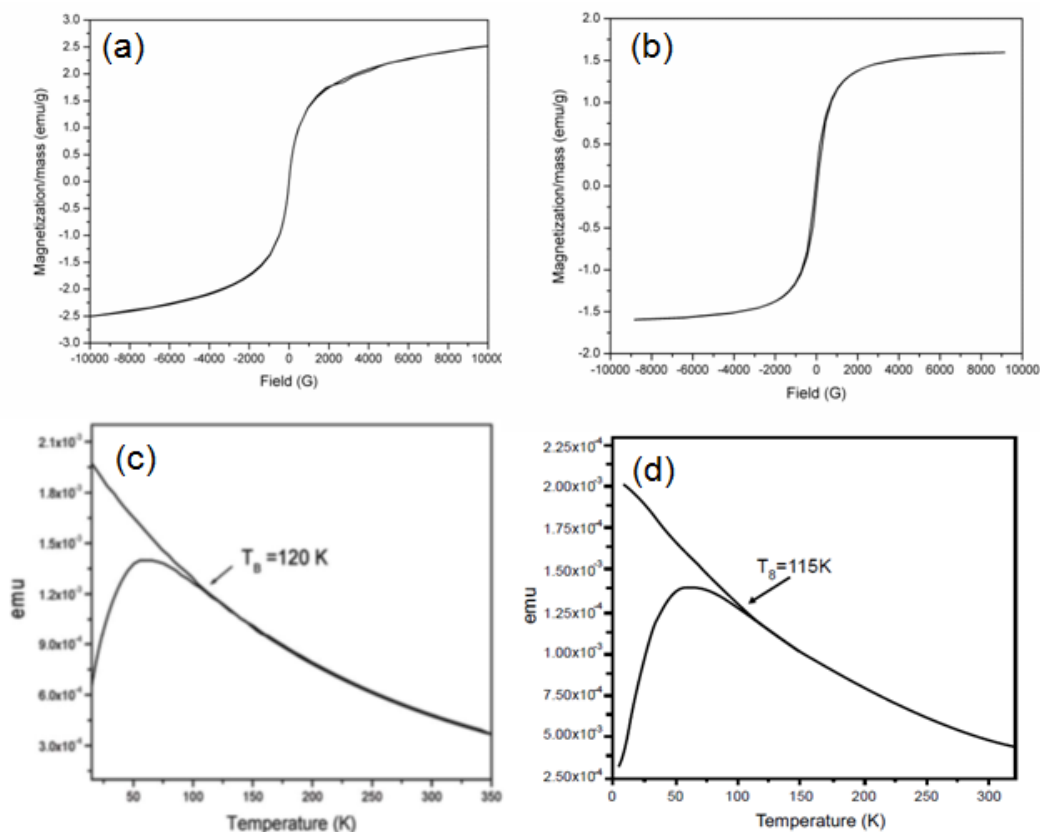


Figure 4.4 Characterization of magnetic property. VSM measurement of hysteresis loops of FMNP1 (a) and FMNP2 (b); SQUID analysis of zero-field-cooled (ZFC) magnetization curve of FMNP1 (c) and FMNP2 (d) at 50 Oe.

Fourier Transform Infrared Spectroscopy (FTIR) was further carried out to confirm the formation of silica shell and bioconjugation of Gm to FMNP1. As shown in Figure 4.5, Si-O-Si stretch is found at  $1070\text{ cm}^{-1}$ . Furthermore, the typical  $-\text{CH}_2$  stretch at  $2930\text{ cm}^{-1}$ , the  $-\text{C}=\text{N}$  stretch of the imine group, and  $-\text{C}=\text{N}-\text{R}$  at  $1640\text{ cm}^{-1}$  appears in the spectrum of Gm-FMNP1. No  $-\text{C}=\text{O}$  stretch at  $1760\text{ cm}^{-1}$  is found after Glu linking the FMNPs and Gm. Similar results were also found for Gm-FMNP2 (data not shown).

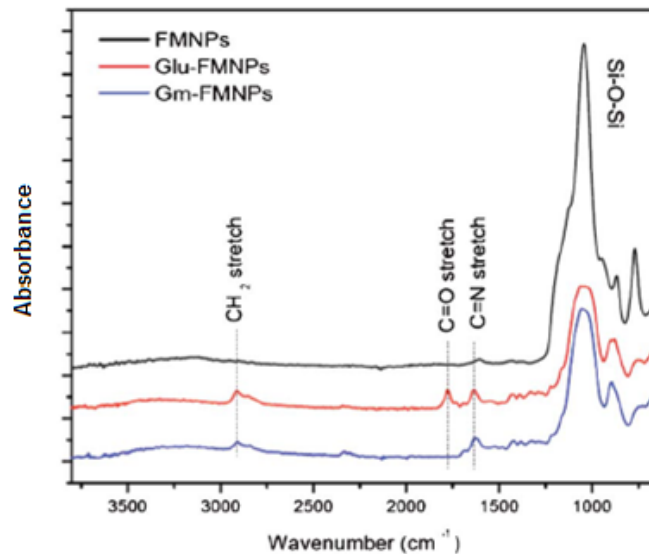


Figure 4.5 FTIR absorption spectra of FMNP1, glutaraldehyde (Glu) modified FMNP1 (Glu-FMNP1), and Gm-FMNP.

#### 4.3.2 Capture, detection and decontamination of *E. coli* by Gm-FMNP1

It should be noted that, in our initial experiment, Gm-FMNP1 was prepared for capturing bacteria *E. coli*. As shown in Figure 4.6, Gm-FMNP1 (1 mg) are found to capture and remove *E. coli* cells ( $1 \times 10^7$  CFU/mL) under an external magnetic field of 0.2 T. Specifically, approximately 90% of the Gm-FMNP1 can be separated from the solution within 6 min, and almost no *E. coli* cell is found in the suspension after 20 min of magnetic confinement.



Figure 4.6 Magnetic capture of bacterium *E. coli* under external magnetic field.



We further used fluorometer and fluorescent microscopy to confirm the capability of Gm-FMNP1 for bacteria capture. For Gm-FMNP1, the maximum fluorescent emission ( $\lambda_{em}$ ) measured by a fluorometer is at 517 nm with an excitation wavelength of 492 nm, while free FITC with  $\lambda_{em} = 513$  is shown in Figure 4.7a. After mixing with *E. coli* cells for 20 min ( $1 \times 10^3$  CFU/mL), a broad emission peak with a substantial decrease in intensity is observed for Gm-FMNPs. It is also found that the peak has a slight red-shift to  $\lambda_{em}$  at 528 nm. No significant change is observed over time. This decreasing in fluorescent intensity and red shift could be attributed to formation of aggregation between NPs and bacterial cells, which cause inner filter effect to suppress the blue side of emission spectrum by re-absorption of photons.<sup>49</sup> Through fluorescent microscopy, we can further confirm the formation of aggregation. Figure 4.7b-2 shows clearly that *E. coli* cells attached to Gm-FMNPs are aggregated in solution, while there is no aggregation when the *E. coli* were incubated with FMNPs alone (Figure 4.7b-1). Therefore, it clearly shows that Gm-conjugated with FMNPs are able to recognize very low concentrations of *E. coli*.

We then used TEM to study the capability of Gm-FMNP1 to capture *E. coli*. FMNP1 without Gm were used as the negative controls, including FMNP1, glutaraldehyde (Glu)-FMNP1, and ethanolamine (EA)-FMNP1. From Figure 4.8, we found that the bacterial cells were attached with the aggregation of dark dots in the mixture of Gm-FMNP1 and *E. coli*. It is interesting that instead of the central cylindrical region of the cell, the cell poles (dark hemispheres) are more aggressively attacked by Gm-FMNP1. No interaction between *E. coli* cells and the negative control samples was found (Figure 4.8). TEM-EDX analysis of thin section samples (Figure 4.8e) clearly shows that the dark dots interacting with *E. coli* contain iron (Fe) from the core of the FMNP1 and silicon (Si) from the mesoporous silica shell. The peaks of nickel (Ni) stem from the TEM sample grid. Thus, these dark dots are attributed to FMNP1 (Figure 4.8 d). It is believed Gm has strong interaction with lipopolysaccharides on the Gram-negative bacterial cell wall,<sup>50, 51</sup> while EA is inert towards *E. coli*. We can conclude that Gm-FMNP1 can recognize and attach with the surface of *E. coli* cell because of the linkage of Gm to *E. coli* cell surface. This attachment mediates the capturing of bacterial cells.

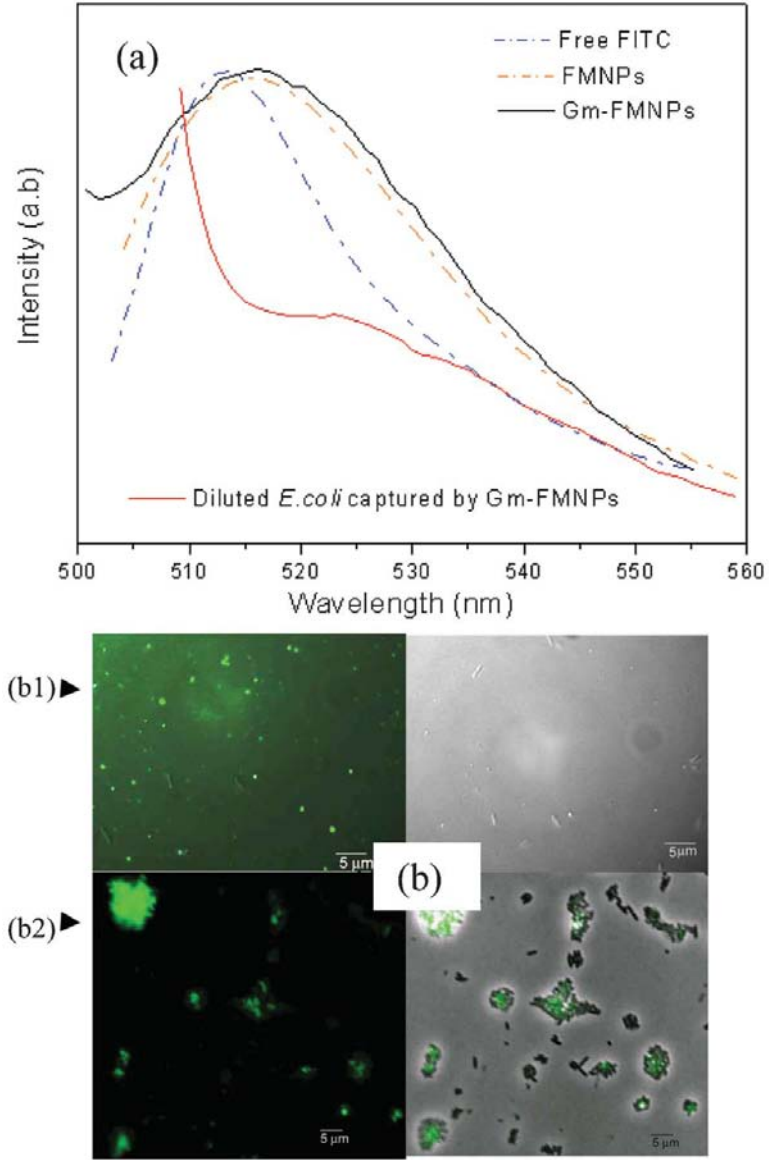


Figure 4.7 (a) Fluorescent spectra of free FITC, FMNP1, and the Gm-FMNP1 before/after detecting *E. coli* cells ( $1 \times 10^3$  CFU/mL); (b1) FMNP1 mixing with *E. coli*,  $1 \times 10^3$  CFU/mL, (with dark field (DF, left) and bright field (BF, right)); (b2) *E. coli* interacting with Gm-FMNP1 with dark field (DF, left) and bright field (BF, right) when  $t = 20$  min.

To further investigate the interaction between Gm-FMNP1 and *E. coli*, we measured the samples of bacteria and NPs which were cultured for 20 min and 60 min as shown in Figure 4.8b and c, respectively. The interaction between Gm-FMNP1 and *E. coli* cells is observed (indicated by a blue arrow) when the interaction time (t) is 20 min, maintaining the integral “envelope” structure. However, the areas of the cell wall to which the Gm-FMNP1 attach exhibit texture changes (see the small insert in Figure 4.8b). Significant disruption of the membrane and cell lysis occur with an increase in the interaction time from 20 to 60 min. Figure 4.7c shows that the bacterial cell membranes are broken and the cytoplasmic matrix appears to be leaking out. Such phenomena are not observed in samples of bacteria mixed with negative control samples, i.e. FMNP1 (Figure 4.8a), Glu-FMNP1, and EA-FMNP1, respectively. Furthermore, no bacterial cells with an integral structure are observed using TEM when the sample was incubated for 3 h. Previous report indicated that the polycationic from gentamicin could induce strong cell wall-adsorption at an early stage.<sup>51</sup> After that, cationic Gm may rearrange the lipopolysaccharide packing order through ionic bonding, consequently disrupting bacteria’s outer membrane and promoting membrane permeability.<sup>52, 53</sup> Thus, in our study, it is likely that the Gm- FMNP1 attach and damage the cell wall first, and are then adsorbed within the cell.

The response of *E. coli* to the Gm-FMNP1 was further studied by calculating the colony-forming units (CFU) of both supernatants and precipitates. A cultured *E. coli* sample was used as a positive control. Negative controls are FMNP1 without Gm, i.e. FMNP1, Glu-FMNP1, EA-FMNP1. Diluted *E. coli* cells were incubated with Gm-FMNP1 and negative controls for 30 min, respectively. We found no significant precipitation is observed in the *E. coli* suspensions mixed with negative controls: FMNP1s, Glu-FMNP1, and EA-FMNP1, respectively. However, obvious precipitation can be found in the *E. coli* suspension mixed with Gm-FMNP1. To evaluate the antibacterial activity of Gm-FMNP1, all samples were washed and freeze-dried several times to remove free Gm from the sample.

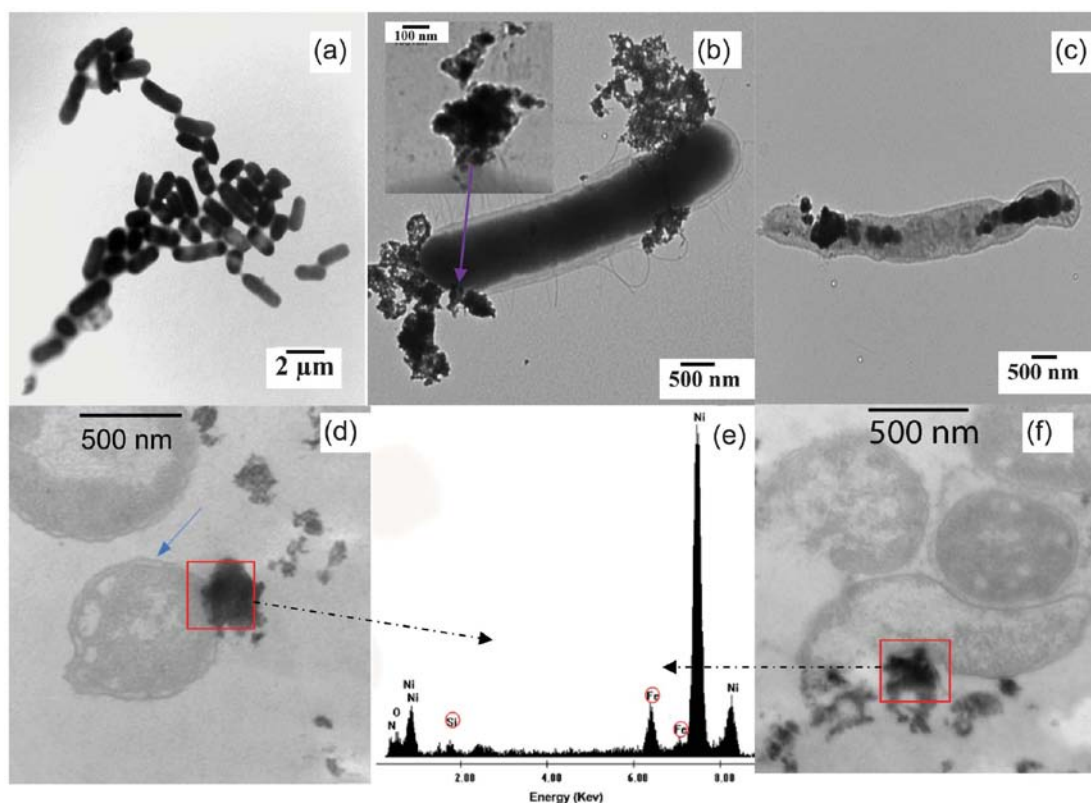


Figure 4.8 Analysis of the interaction between NPs and bacterium *E. coli*. (a), TEM image of *E. coli* mixing with FMNP1 without Gm conjugation. (b) *E. coli* mixing with Gm-FMNP1 with less than 20 min of interaction time (t). (c) *E. coli* interacting with Gm-FMNP1 when  $t = 60$  min. (d) Thin section TEM analysis of *E. coli* mixing with Gm-FMNP1 when  $t = 20$  min. (e) The TEM-EDX spectrum of the Gm-FMNP1. (f) Thin section TEM analysis of *E. coli* mixing with Gm-FMNP1 when  $t = 60$  min.

Figure 4.9 shows photographs of the resulting colonies in agar plates for all samples. The cultured *E. coli* mixed with FMNP1 (Figure 4.9a-A2), Glu-FMNP1 (Figure 4.9a-A3), and EA-FMNP1 (Figure 4.9a- A4), respectively, show a similar result with the positive control (Figure 4.9a-A1); whereas Gm-FMNP1 (0.1 mg) significantly inhibit the growth of *E. coli*. No living cells can be found throughout the suspension of *E. coli* mixed with Gm-FMNP1 as shown in (Figure 4.9a-A5 and -A6). Further analysis indicates that the bacterial concentration of those FMNP1 without Gm is  $0.8 \times 10^3$  CFU/mL, which is similar to the positive control ( $1.0 \times 10^3$  CFU/mL). However, the bacterial concentration decreases dramatically in the sample of Gm-FMNP1 as shown in Figure 4.9b. The results confirm that Gm-conjugation is playing the key role to allow the FMNP1 to interact with *E. coli*. The antimicrobial susceptibility of *E. coli* to Gm-FMNP1 was further determined by the agar disk diffusion method with the comparison of the calibration curve obtained by testing pure Gm (Figure 4.9c). Here, 0.1 mg of Gm-FMNP1 shows a similar antimicrobial efficiency to 12–15 mg of pure Gm. Our experimental results indicate that  $\sim 8 \mu\text{g}$  of Gm could be conjugated on 0.1 mg FMNP1 (Figure A4 and Table A1, from Appendix 4). Furthermore, Gm- FMNP1 are able to maintain their bioactivity, even when stored at 6 °C for 3 months.

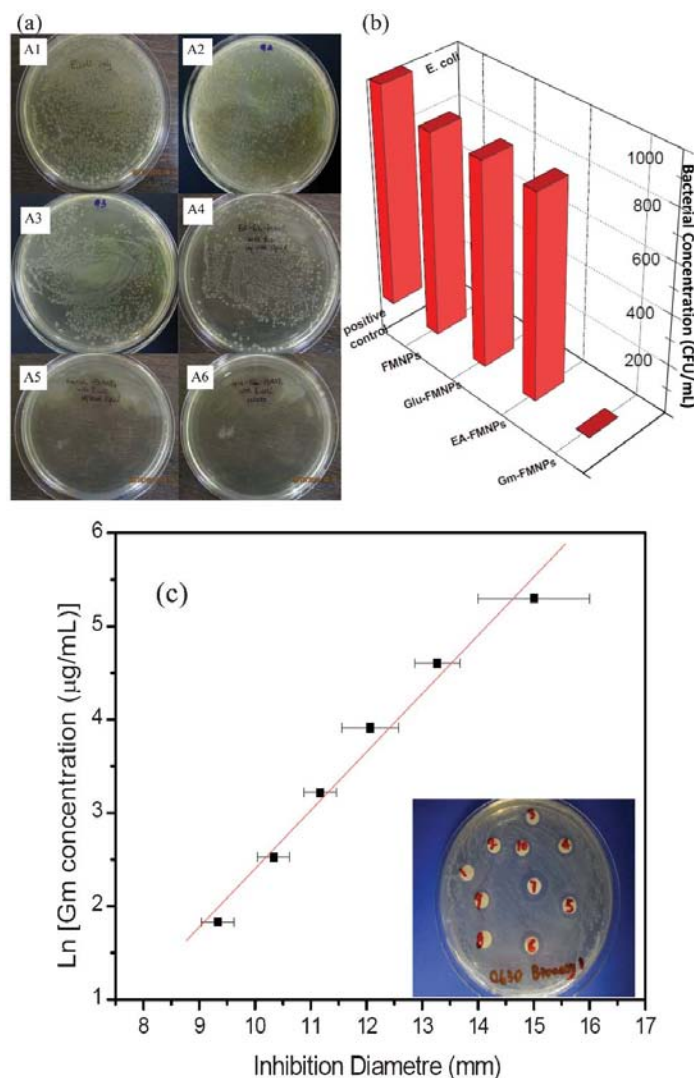


Figure 4.9 Antimicrobial efficiency of Gm-FMNP1 (0.1 mg/mL) with *E. coli* ( $\sim 1.0 \times 10^3$  CFU/mL) in 1 mL solution. (a) Plate counting of (A1) *E. coli* alone, (A2) *E. coli* mixed with FMNP1, (A3) Glu-FMNP1, (A4) EA-FMNP1, (A5) the upper-level liquid of Gm-FMNP1 interacting with *E. coli*, and (A6) the precipitate of *E. coli* mixed with Gm-FMNP1; (b) calculation the number of colony-forming unit (CFU) of all samples. (c) The agar-diffusion assay. In the small inset image, No. 2 to No. 7 represent a 2-fold serial dilution of Gm solutions (from 6.25 to 200 mg/mL). No. 1, No. 8, No. 9 and No. 10 refer to the negative controls with PBS solution, EA-FMNP1 solution and Gm-FMNP1 solution stored in a fridge for 3 months, Gm-FMNP1 were freshly prepared. In all cases, the concentration of NPs is 0.1 mg/mL.

### 4.3.3 Ubiquitous capture of bacteria by Gm-FMNP2

We further developed an updated Gm modified NPs (Gm-FMNP2) for ubiquitous capture of bacteria. We first mixed Gm-FMNP2 with bacterium *E. coli*. As expected, TEM image shows clearly the attachment of NPs with bacterial cells (Figure 4.10a). We further analyze the ability of Gm-FMNP2 for capturing Gram-positive bacterium *S. aureus*. As discussed above, Gm is known to be uptaken by susceptible Gram positive bacteria such as *S. aureus* strain and kill the bacterium under the regulation of membrane potential and electrochemical gradient.<sup>54, 55</sup> The uptake of gentamicin by *S. aureus* is reported involving of ionic adherence to the cell surface and subsequently binding to a membrane aerobic energization complex.<sup>43</sup> Phospholipids and teichoic acid on the surface of Gram-positive bacteria were supposed to be the initial binding site for aminoglycoside antibiotic.<sup>56, 57</sup> Thus it is expected that our Gm modified NPs can interact with *S. aureus*, and hence capture and separate bacterial cells from solution under external magnetic field. As shown in Figure 4.10b, TEM image shows Gm-FMNP2 were found to bind on the surface of the *S. aureus*. Furthermore, in the EA-FMNP2 and *S. aureus* group, we did not find the interaction between the particles and bacteria.

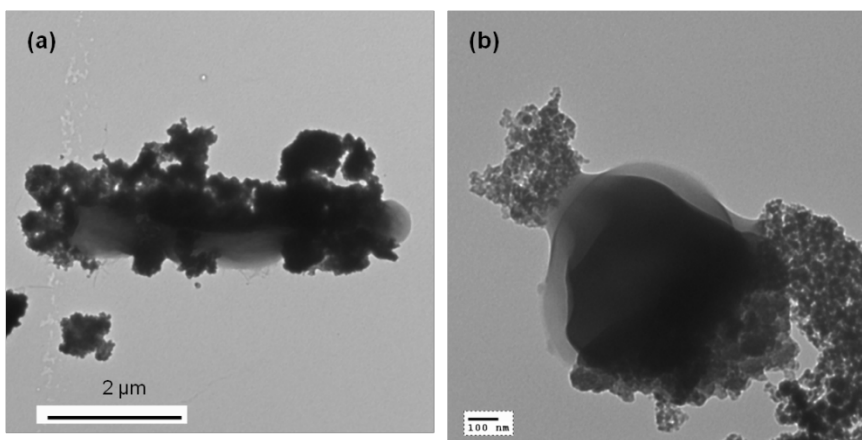


Figure 4.10 TEM micrographs of capture of bacteria *E. coli* and *S. aureus* by Gm-FMNP2.



In our study, the bacteria capture experiment in our study was done by mixing Gm-FMNPs with *S. aureus* for desired time. Although one hour incubation Gm-FMNP2 with bacteria could reach maximum capture effect, we could also find a few bacteria even after 10 min mixing through optical microscopy. In addition, as discussed above, the Gm-FMNP2 exhibit a smaller hydro-diameter and better magnetic property, due to a smaller core with good crystalline structure and thinner silica shell. Good magnetization can result in fast confinement of particles. Consistently, we observed the bacterium-NPs complex (aggregation) can be confined even in 1 min under external magnetic field of 0.2 T. Using the optical microscopy, we found that the diluted *S. aureus* with the concentration as low as  $0.5 \times 10^3$  CFU/mL can be separated from the solution by the core-shell MNPs in 1 min. Further quantitative analysis of the capture efficiency, detection limitation and possible toxic effect of Gm-FMNP2 to *S. aureus* are under study.

## 4.4 Conclusion

In sum, we have demonstrated an efficient and fast way for ubiquitous capture, detection and decontamination of bacteria, by conjugating antibiotic gentamicin to fluorescent magnetic nanoparticles (FMNPs). Two different methods were developed for synthesis of FMNPs, including a one-pot co-precipitation approach and two-step thermal decomposition method. TEM results show that the FMNPs prepared by both methods comprise of a  $\text{Fe}_3\text{O}_4$  core and a silica ( $\text{SiO}_2$ ) shell. Both Gm conjugated FMNPs show a typical superparamagnetic property. Preliminary results show that Gm-FMNP1 can capture bacterium *E. coli* up 90 % of bacterium cells in a concentration of  $1 \times 10^7$  CFU/mL within 20 min. The detection limit was found to be as low as to a concentration of  $1 \times 10^3$  CFU/ mL through optical microscopy analysis. The antibacterial effect of Gm-FMNP1 to *E. coli* was further demonstrated by plate counting technique and the efficiency was found 20 % enhanced. Furthermore, Gm-FMNP2 prepared by two-step method with a better crystalline structure and magnetization, show higher capture efficiency for capturing both gram-negative bacterium *E. coli* and Gm sensitive Gram-positive bacterium *S. aureus*. By improvement of particles stability through efficient functionalization, we estimate that the Gm-FMNPs can be a promising platform for



simultaneous rapid capture, sensitive detection, and decontamination of bacteria for disease control in clinic and wastewater treatment.

## 4.5 References

1. Woodford, N.; Livermore, D. M., Infections caused by Gram-positive bacteria: a review of the global challenge. *Journal of Infection* 2009, 59, Supplement 1, (0), S4-S16.
2. Solomon, E. B.; Yaron, S.; Matthews, K. R., Transmission of *Escherichia coli* O157:H7 from Contaminated Manure and Irrigation Water to Lettuce Plant Tissue and Its Subsequent Internalization. *Applied and Environmental Microbiology* 2002, 68, (1), 397-400.
3. Dinges, M. M.; Orwin, P. M.; Schlievert, P. M., Exotoxins of *Staphylococcus aureus*. *Clinical Microbiology Reviews* 2000, 13, (1), 16-34.
4. Shockman, G. D.; Barren, J. F., Structure, Function, and Assembly of Cell Walls of Gram-Positive Bacteria. *Annual Review of Microbiology* 1983, 37, (1), 501-527.
5. Lowy, F. D., *Staphylococcus aureus* Infections. *New England Journal of Medicine* 1998, 339, (8), 520-532.
6. Fong, W. K.; Modrusan, Z.; McNevin, J. P.; Marostenmaki, J.; Zin, B.; Bekkaoui, F., Rapid Solid-Phase Immunoassay for Detection of Methicillin-Resistant *Staphylococcus aureus* Using Cycling Probe Technology. *Journal of Clinical Microbiology* 2000, 38, (7), 2525-2529.
7. Noble, R. T.; Weisberg, S. B., A review of technologies for rapid detection of bacteria in recreational waters. *Journal of water and health* 2005, 3, (4), 381-392.
8. Acharya, G.; Chang, C.-L.; Savran, C., An Optical Biosensor for Rapid and Label-Free Detection of Cells. *Journal of the American Chemical Society* 2006, 128, (12), 3862-3863.
9. Contois, D. E., Kinetics of Bacterial Growth: Relationship between Population Density and Specific Growth Rate of Continuous Cultures. *Journal of General Microbiology* 1959, 21, (1), 40-50.
10. Safarik, I.; Safarikova, M., Magnetic techniques for the isolation and purification of proteins and peptides. *Biomagnetic Research and Technology* 2004, 2, (1), 7.
11. Zilai Zhao, Z. B. L. C. X. H. Y. W., Synthesis and Surface-Modifications of Iron Oxide Magnetic Nanoparticles and Applications on Separation and Analysis. *Biomaterials* 2006, 18, (10), 1288-1297.
12. Tsai, Z.-T.; Wang, J.-F.; Kuo, H.-Y.; Shen, C.-R.; Wang, J.-J.; Yen, T.-C., In situ preparation of high relaxivity iron oxide nanoparticles by coating with chitosan: A potential MRI contrast agent useful for cell tracking. *Journal of Magnetism and Magnetic Materials* 2010, 322, (2), 208-213.
13. Lobatto, M. E.; Fuster, V.; Fayad, Z. A.; Mulder, W. J. M., Perspectives and opportunities for nanomedicine in the management of atherosclerosis. *Nat Rev Drug Discov* 2011, 10, (11), 835-852.
14. Pinaud, F.; Michalet, X.; Bentolila, L. A.; Tsay, J. M.; Doose, S.; Li, J. J.; Iyer, G.; Weiss, S., Advances in fluorescence imaging with quantum dot bio-probes. *Biomaterials* 2006, 27, (9), 1679-1687.

15. Edwards, C.; Porter, J.; Pickup, R., Magnetic Particle-Based Separation Techniques for Monitoring Bacteria from Natural Environments. In *Environmental Monitoring of Bacteria*, Humana Press: 1999; Vol. 12, pp 75-96.
16. Gu, H.; Ho, P.-L.; Tsang, K. W. T.; Wang, L.; Xu, B., Using Biofunctional Magnetic Nanoparticles to Capture Vancomycin-Resistant *Enterococci* and Other Gram-Positive Bacteria at Ultralow Concentration. *Journal of the American Chemical Society* 2003, 125, (51), 15702-15703.
17. Gu, H.; Ho, P.-L.; Wt Tsang, K.; Yu, C.-W.; Xu, B., Using biofunctional magnetic nanoparticles to capture Gram-negative bacteria at an ultra-low concentration. *Chemical Communications* 2003, (15), 1966-1967.
18. Kell, A. J.; Stewart, G.; Ryan, S.; Peytavi, R.; Boissinot, M.; Huletsky, A.; Bergeron, M. G.; Simard, B., Vancomycin-Modified Nanoparticles for Efficient Targeting and Preconcentration of Gram-Positive and Gram-Negative Bacteria. *ACS Nano* 2008, 2, (9), 1777-1788.
19. Gao, J.; Li, L.; Ho, P. L.; Mak, G. C.; Gu, H.; Xu, B., Combining Fluorescent Probes and Biofunctional Magnetic Nanoparticles for Rapid Detection of Bacteria in Human Blood. *Advanced Materials* 2006, 18, (23), 3145-3148.
20. El-Boubbou, K.; Gruden, C.; Huang, X., Magnetic Glyco-nanoparticles: A Unique Tool for Rapid Pathogen Detection, Decontamination, and Strain Differentiation. *Journal of the American Chemical Society* 2007, 129, (44), 13392-13393.
21. Huang, Y.-F.; Wang, Y.-F.; Yan, X.-P., Amine-Functionalized Magnetic Nanoparticles for Rapid Capture and Removal of Bacterial Pathogens. *Environmental Science & Technology* 2010, 44, (20), 7908-7913.
22. Zhao, X.; Hilliard, L. R.; Mechery, S. J.; Wang, Y.; Bagwe, R. P.; Jin, S.; Tan, W., A rapid bioassay for single bacterial cell quantitation using bioconjugated nanoparticles. *Proceedings of the National Academy of Sciences* 2004, 101, (42), 15027-15032.
23. Bertorelle, F.; Wilhelm, C.; Roger, J.; Gazeau, F.; M茅nager, C.; Cabuil, V., Fluorescence-Modified Superparamagnetic Nanoparticles: Intracellular Uptake and Use in Cellular Imaging. *Langmuir* 2006, 22, (12), 5385-5391.
24. Shashwat, S. B. a. D.-H. C., A multifunctional magnetic nanocarrier bearing fluorescent dye for targeted drug delivery by enhanced two-photon triggered release. *Nanotechnology* 2009, 20, (18), 185103.
25. Lee, J.-H.; Schneider, B.; Jordan, E. K.; Liu, W.; Frank, J. A., Synthesis of Complexable Fluorescent Superparamagnetic Iron Oxide Nanoparticles (FL SPIONs) and Cell Labeling for Clinical Application. *Advanced Materials* 2008, 20, (13), 2512-2516.
26. Corr, S. A.; O' Byrne, A.; Gun'ko, Y. K.; Ghosh, S.; Brougham, D. F.; Mitchell, S.; Volkov, Y.; Prina-Mello, A., Magnetic-fluorescent nanocomposites for biomedical multitasking. *Chemical Communications* 2006, (43), 4474-4476.
27. Li, L.; Li, H.; Chen, D.; Liu, H.; Tang, F.; Zhang, Y.; Ren, J.; Li, Y., Preparation and Characterization of Quantum Dots Coated Magnetic Hollow Spheres for Magnetic Fluorescent Multimodal Imaging and Drug Delivery. *Journal of Nanoscience and Nanotechnology* 2009, 9, (4), 2540-2545.

28. Ma, Z. Y.; Dosev, D.; Nichkova, M.; Gee, S. J.; Hammock, B. D.; Kennedy, I. M., Synthesis and bio-functionalization of multifunctional magnetic Fe<sub>3</sub>O<sub>4</sub>@Y<sub>2</sub>O<sub>3</sub>:Eu nanocomposites. *Journal of Materials Chemistry* 2009, 19, (27), 4695-4700.
29. Prucek, R.; Tuček, J.; Kilianová, M.; Panáček, A.; Kvítek, L.; Filip, J.; Kolář, M.; Tománková, K.; Zbořil, R., The targeted antibacterial and antifungal properties of magnetic nanocomposite of iron oxide and silver nanoparticles. *Biomaterials* 2011, 32, (21), 4704-4713.
30. Torney, F.; Trewyn, B. G.; Lin, V. S. Y.; Wang, K., Mesoporous silica nanoparticles deliver DNA and chemicals into plants. *Nature Nanotechnology* 2007, 2, (5), 295-300.
31. Zhao, X.; Tapecc-Dytioco, R.; Tan, W., Ultrasensitive DNA Detection Using Highly Fluorescent Bioconjugated Nanoparticles. *Journal of the American Chemical Society* 2003, 125, (38), 11474-11475.
32. Chekina, N.; Horak, D.; Jendelova, P.; Trchova, M.; Benes, M. J.; Hruby, M.; Herynek, V.; Turnovcova, K.; Sykova, E., Fluorescent magnetic nanoparticles for biomedical applications. *Journal of Materials Chemistry* 2011, 21, (21), 7630-7639.
33. Burns, A. A.; Vider, J.; Ow, H.; Herz, E.; Penate-Medina, O.; Baumgart, M.; Larson, S. M.; Wiesner, U.; Bradbury, M., Fluorescent Silica Nanoparticles with Efficient Urinary Excretion for Nanomedicine. *Nano Letters* 2008, 9, (1), 442-448.
34. Ow, H.; Larson, D. R.; Srivastava, M.; Baird, B. A.; Webb, W. W.; Wiesner, U., Bright and Stable Core-shell Fluorescent Silica Nanoparticles. *Nano Letters* 2004, 5, (1), 113-117.
35. Mumin, A. M.; Barrett, J. W.; Dekaban, G. A.; Zhang, J., Dendritic cell internalization of foam-structured fluorescent mesoporous silica nanoparticles. *Journal of Colloid and Interface Science* 2011, 353, (1), 156-162.
36. Cho, N.-H.; Cheong, T.-C.; Min, J. H.; Wu, J. H.; Lee, S. J.; Kim, D.; Yang, J.-S.; Kim, S.; Kim, Y. K.; Seong, S.-Y., A multifunctional core-shell nanoparticle for dendritic cell-based cancer immunotherapy. *Nature Nanotechnology* 2011, 6, (10), 675-682.
37. Tsang, S. C.; Yu, C. H.; Gao, X.; Tam, K., Silica-Encapsulated Nanomagnetic Particle as a New Recoverable Biocatalyst Carrier. *The Journal of Physical Chemistry B* 2006, 110, (34), 16914-16922.
38. Clauter, D. A.; Schmidt, V. A., Shifts in blocking temperature spectra for magnetite powders as a function of grain size and applied magnetic field. *Physics of the Earth and Planetary Interiors* 1981, 26, (1-2), 81-92.
39. Bruce, I. J.; Sen, T., Surface Modification of Magnetic Nanoparticles with Alkoxysilanes and Their Application in Magnetic Bioseparations. *Langmuir* 2005, 21, (15), 7029-7035.
40. Gupta, A. K.; Gupta, M., Synthesis and surface engineering of iron oxide nanoparticles for biomedical applications. *Biomaterials* 2005, 26, (18), 3995-4021.

41. Ohmori, M.; Matijević, E., Preparation and properties of uniform coated colloidal particles. VII. Silica on hematite. *Journal of Colloid and Interface Science* 1992, 150, (2), 594-598.
42. Moore, A.; Marecos, E.; Bogdanov, A.; Weissleder, R., Tumoral Distribution of Long-circulating Dextran-coated Iron Oxide Nanoparticles in a Rodent Model1. *Radiology* 2000, 214, (2), 568-574.
43. Miller, M. H.; Edberg, S. C.; Mandel, L. J.; Behar, C. F.; Steigbigel, N. H., Gentamicin Uptake in Wild-Type and Aminoglycoside-Resistant Small-Colony Mutants of *Staphylococcus aureus*. *Antimicrobial Agents and Chemotherapy* 1980, 18, (5), 722-729.
44. Taber, H. W.; Mueller, J. P.; Miller, P. F.; Arrow, A. S., Bacterial uptake of aminoglycoside antibiotics. In 1987; Vol. 51, pp 439-457.
45. Park, J.; An, K.; Hwang, Y.; Park, J.-G.; Noh, H.-J.; Kim, J.-Y.; Park, J.-H.; Hwang, N.-M.; Hyeon, T., Ultra-large-scale syntheses of monodisperse nanocrystals. *Nature Materials* 2004, 3, (12), 891-895.
46. Liong, M.; Lu, J.; Kovochich, M.; Xia, T.; Ruehm, S. G.; Nel, A. E.; Tamanoi, F.; Zink, J. I., Multifunctional Inorganic Nanoparticles for Imaging, Targeting, and Drug Delivery. *ACS Nano* 2008, 2, (5), 889-896.
47. Lecároz, C.; Campanero, M. A.; Gamazo, C.; Blanco-Prieto, M. J., Determination of gentamicin in different matrices by a new sensitive high-performance liquid chromatography-mass spectrometric method. *Journal of Antimicrobial Chemotherapy* 2006, 58, (3), 557-563.
48. Cornell, R. M.; Schwertmann, U., Electronic, Electrical and Magnetic Properties and Colour. In *The Iron Oxides*, Wiley-VCH Verlag GmbH & Co. KGaA: 2004; pp 111-137.
49. Imhof, A.; Megens, M.; Engelberts, J. J.; de Lang, D. T. N.; Sprik, R.; Vos, W. L., Spectroscopy of Fluorescein (FITC) Dyed Colloidal Silica Spheres. *The Journal of Physical Chemistry B* 1999, 103, (9), 1408-1415.
50. Hancock, R. E. W., Alterations in Outer Membrane Permeability. *Annual Review of Microbiology* 1984, 38, (1), 237-264.
51. Martin, N. L.; Beveridge, T. J., Gentamicin interaction with *Pseudomonas aeruginosa* cell envelope. *Antimicrobial Agents and Chemotherapy* 1986, 29, (6), 1079-1087.
52. Kadurugamuwa, J. L.; Lam, J. S.; Beveridge, T. J., Interaction of gentamicin with the A band and B band lipopolysaccharides of *Pseudomonas aeruginosa* and its possible lethal effect. *Antimicrobial Agents and Chemotherapy* 1993, 37, (4), 715-721.
53. Hancock, R. E. W.; Bell, A., Antibiotic uptake into gram-negative bacteria. *European Journal of Clinical Microbiology and Infectious Diseases* 1988, 7, (6), 713-720.
54. Polyfunctional Antibiotics Affecting Bacterial Membrane Dynamics. *Anti-Infective Agents in Medicinal Chemistry (Formerly `Current Medicinal Chemistry - Anti-Infective Agents)* 2009, 8, 3-16.
55. Tam, V. H.; Kabbara, S.; Vo, G.; Schilling, A. N.; Coyle, E. A., Comparative Pharmacodynamics of Gentamicin against *Staphylococcus aureus* and *Pseudomonas aeruginosa*. In 2006; Vol. 50, pp 2626-2631.

56. Tam, V. H.; Kabbara, S.; Vo, G.; Schilling, A. N.; Coyle, E. A., Comparative Pharmacodynamics of Gentamicin against *Staphylococcus aureus* and *Pseudomonas aeruginosa*. *Antimicrobial Agents and Chemotherapy* 2006, 50, (8), 2626-2631.
57. Taber, H. W.; Mueller, J. P.; Miller, P. F.; Arrow, A. S., Bacterial uptake of aminoglycoside antibiotics. *Microbiological Reviews* 1987, 51, (4), 439-457.

**CHAPTER 5**

**DEVELOPMENT OF LUCIFERASE CONJUGATED  
GOLD NANOPARTICLES IN DETECTION OF  
THROMBIN**

## 5.1 Introduction

Fluorescent labels have been widely used in modern biotechnology. For example, directly labelling of biomolecules with fluorophore can locate molecules inside cell or provide signal for immunoassay. However, biological activities are often involved in dynamic processes, including protein interactions, ligand-receptor binding, changes of proteins and nucleic acid conformation in response to stimulus. One signal obtained by simple labelling is hard to provide more information. In this case, extensive using of fluorescent labels in the form of Förster/fluorescence resonance energy transfer (FRET) provides a powerful tool to probe those biological processes.

FRET is a process in which nonradiative energy is transferred from an excited luminescent fluorophore (sever as a donor) to a proximal ground state fluorophore (sever as an acceptor, typically in a few nanometers away).<sup>1</sup> The energy transfer efficiency (E), which is defined as the fraction of energy transfer event occurring per fluorophore donor excitation event, is thus distance dependent, as shown in the equation (5.1) below,

$$E = \frac{1}{1 + \left(\frac{r}{R_0}\right)^6} \quad (5.1)$$

where  $r$  is the distance between two partners and  $R_0$  is the distance at which the resonance energy transfer (RET) efficiency is 50% and represents a characteristic parameter for the given partners. As a result, this process can be used as a “molecular ruler”, allowing one to determine the distance between partners by measuring the changes of fluorescent signal from the donors or acceptors.

FRET is a very sensitive and reliable technique widely used in biosensing. In particular, detecting analytes can be achieved by using the ratio of the two different fluorescent intensities. This could eliminate most ambiguities in the detection caused by external assay factors such as excitation source fluctuations and sensor concentration.<sup>2, 3</sup>

In conventional FRET system, both the donor and the acceptor are fluorescent agents. However, the process of RET can also involve bioluminescent and chemiluminescent donor, or nonluminescent acceptors. In particular, bioluminescence resonance energy

transfer (BRET) which is operated by biochemical energy generated by bioluminescent protein to excite fluorophore offer additional advantages over FRET, including intrinsic low background, less signal interference and no photobleaching issue. The reason for those aspects is that BRET does not require external light source. In addition, BRET possesses less harmful to biological system comparing to FRET and chemiluminescence resonance energy transfer (CRET), as the reaction to produce light is a nature biochemical process.

Traditionally, fluorophores such as fluorescent dyes are used in RET systems. However, fluorescent dyes have several drawbacks such as photobleaching and high sensitivity to environmental factors. In recent, a number of studies have incorporated nanoparticle into the design of RET system with enhanced RET performance and flexibility in the selection of excitation source. Nanoparticles (NPs), such as gold nanoparticles (Au NPs) and quantum dots (QDs), possess unique optical properties and can act either a quencher (a special acceptor) a fluorescent donor (and acceptor), respectively.

Au NPs can serve as excellent fluorescence quenchers (acceptor) for RET based assay because of their extraordinary molar extinction coefficients and broad energy absorption bandwidth in the visible range.<sup>4, 5</sup> In addition, the unique chemical reactivity of gold allows Au NPs to be a suitable platform to selectively binding of a wide range of organic or biological fluorescent ligands for detecting small molecules and biological targets. The most common set-up for Au NPs based RET assay is the fluorescence quenching-based switch on/off. For example, fluorescence (or bioluminescence) of the donor is quenched on attaching with Au NPs. The presence of analytes results in release (or extends the usable distances) of donor from Au NPs and hence restores the fluorescence (or bioluminescence), of which the intensity is proportional to the amount (concentration) of analytes. In the last decades, a number of innovative approaches using Au NPs as quencher in RET system have been developed for the detection of metal ions,<sup>6-8</sup> small molecules,<sup>9, 10</sup> nucleic acids<sup>11</sup> and enzymes.<sup>12, 13</sup>

Bioconjugated nanoparticles have proven to be extremely convenient and invaluable tools for biomedical applications over last decades. Apart from using as excellent drug/gene



delivery cargoes and bio-imaging agents, bioconjugated nanoparticles have also been used to create nanosensors of extremely sensitivity and highly specificity in analysis of a variety of biological analytes. Among the most important biological analytes are protease, a group of enzymes that selectively cleave peptide bonds in proteins and polypeptides via hydrolysis.<sup>14-17</sup> Proteases not only play a crucial role in a number of biological processes, including hormone activation, blood coagulation and apoptosis, but also are involved in many diseases, such as viral infection, cancer, and inflammatory disease. The development of approaches for detecting and real time monitoring of protease is of great interest as they can be biomarker for certain disease.<sup>17</sup>

One of important proteases is thrombin. Thrombin is a serine protease that plays a central role in haemostasis by converting soluble fibrinogen to fibrin clot.<sup>18, 19</sup> Thrombin has been reported involved in variety of diseases, such as rheumatoid arthritis,<sup>20</sup> pulmonary fibrosis<sup>21</sup> and glomerulonephritis.<sup>22</sup> The concentration of thrombin in both blood and urine of health bodies is almost undetectable, as it exhibits in the form of prothrombin (or thrombin-antithrombin complex).<sup>23, 24</sup> However, it can reach to low micromolar level during coagulation process and early haemostatic process in plasma.<sup>23</sup> In the urine samples from glomerulonephritis patients, even low level of thrombin has been generated.<sup>24</sup> A number of strategies have thus been developed for sensing and monitoring thrombin, including antibody based radioimmunoassay/ELISA,<sup>23</sup> fluorophore labelled substrate bound sensor,<sup>25-28</sup> and recent developed nucleic acid probes based aptamersensor.<sup>29-31</sup> Among them, peptide substrate reporters offer a lot advantages, as they response only to the active thrombin and thus avoid false positive from prothrombin. In addition, fluorophore labelled peptide substrate can be further incorporated into NPs based RET system to enhance the sensitivity and reduce assay time.

In this section, we report the development of a nanosensor based on luciferase conjugated gold nanoparticles for sensing thrombin in both buffer and urine samples. The advantage of using urine samples is that urine samples can be easily and repetitively obtained avoiding problems and risks associated with blood sampling. In addition, as the presence of thrombin activity in urine is reported to be associated with glomerulonephritis, it is possible to provide useful information for diagnosis of diseases related to kidney.<sup>24</sup>

## 5.2 Experimental section

### 5.2.1 Design of the pRluc-Au NPs nanosensor

In this study, the design of the nanosensor for detection of thrombin concentration is shown in Figure 5.1. The nanosensor is composed of a conjugate of alkanethiol ligand stabilized gold nanoparticles (Au NPs) and a recombinant protein pRluc that containing a domain of *Renilla* luciferase (Rluc) and a short peptide as the sensing element. Au NPs have been demonstrated for its strong quenching effect for emission from proximate organic fluorophores,<sup>32</sup> fluorescent proteins,<sup>33</sup> QDs<sup>34</sup> and even bioluminescence<sup>35</sup> in RET system. Thus, in this system, the initial bioluminescence generated by the pRluc is quenched due to proximal conjugation with Au NPs. However, in the presence of thrombin, the sensing peptide is cleavage, which result in release of Rluc from nanoparticles and hence generate bioluminescence.

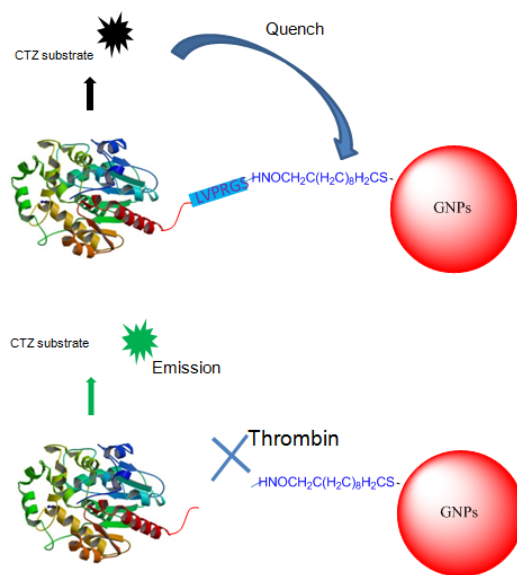


Figure 5.1 Schematic diagram of detection of thrombin via pRluc conjugated gold nanoparticles

The details of the experiment are described below. Unless otherwise stated, chemicals were obtained from Sigma-Aldrich. Only NANOpure water ( $p=18.2 \text{ M}\Omega$ ) was used.

### 5.2.2 Dihydrolipoic acid (DHLA) synthesis

DHLA was synthesized by reduction of thioctic acid (TA) according to a published procedure.<sup>36</sup> Briefly, NaBH<sub>4</sub> (1.2 g) was added by small portions into an aqueous solution of TA (6 g in 117 mL of 0.25 M sodium bicarbonate solution). The mixture was stirred vigorously under cold bath (~ 4 °C) for 30 min. Afterwards, the mixture was acidified to ~ pH 1.0 by addition of HCl. DHLA was extracted three times from the crude product by 20 mL of toluene. The organic phase was washed by water and dried under vacuum oven. The purified DHLA was stored at room temperature under vacuum.

### 5.2.3 Synthesis and functionalization of Gold Nanoparticles

Gold nanoparticles were prepared via the sodium citrate reduction of HAuCl<sub>4</sub>·3H<sub>2</sub>O as described by Frens *et. al.*<sup>37</sup> with slight modification. In brief, one hundred millilitres of 1 mM HAuCl<sub>4</sub>·3H<sub>2</sub>O in water was heated until refluxing under stirring. Following that, 5 mL of 38.8 mM sodium citrate tribasic dehydrate with water was added quickly into the solution under vigorously stirring. The mixture was then kept under refluxing for another 15 min. The color of the solution turned from yellow to clear, black, purple and to deep red eventually. Afterwards, the mixture was removed from heating and cool to room temperature. The resultant solution was then filter through 0.45-μm acetate filter to remove large agglomerates and stored at room temperature under dark.

Citrate-stabilized gold nanoparticles were further functionalized by alkanethiols, i.e. 11-mercaptoundecanoic acid (MUA) and DHLA. In following experiment, only MUA is used in description of the procedure. Typically, a solution of 3 mL of the above citrate-stabilized gold nanoparticles (15 nM, pH adjusted to 10.0 by 0.5 M NaOH) was mixed with 0.5 mL ethanol. Afterwards, a solution of 0.5 mL ethanol dissolved with MUA (10 mM) was added in the gold solution and stirred for 19 h. The mixture was then filtered through 0.45-μm acetate filter. The MUA modified gold nanoparticles were further purified by amicon ultral filters (Ultra-0.5 mL). Finally, the MUA modified particles were re-suspended in 1 mL DDW (~ 60 nM).

#### 5.2.4 Plasmid constructions

A recombinant protein containing *Renilla* luciferase (Rluc) and a short peptide sequence as thrombin substrate was constructed as following. Firstly, Rluc gene from the plasmid pRL-null (Promega, Inc) was cloned into the MCS site of pET 32-a (Merck Millipore Inc.) plasmid under two restriction sites (BamH I and Xho I). Two primers were designed for the cloning (forward: 5' AAAGGATCCAGCGGTGGTGGTGGTAGCATGACTTCGAAAGTTTATGATCCAG; reverse: 5' TGTGCTCGAGTTGTTTCATTTTGA GAACTCGCTC 3'). As shown in Figure A5 (Appendix5), thrombin substrate originally from pET 32-a plasmid is thus located at upstream (N-terminal) of Rluc gene. A trx region from pET 32-a coding for thioredoxin protein is kept to maintain high level of recombinant protein expression.<sup>38</sup> The bold underline in the forward primer indicates a six amino acid linker (SGGGGS) was inserted after Bam H I site to leave a flexible space for proper folding of Rluc protein.

In a typical experiment, the PCR products and the plasmid were digested with relating restriction enzyme and purified through agarose gel, respectively. The digested DNA insert was ligated into the relating MCS site at the plasmid. The ligation product was transformed into *E. coli* BL21 cells. The successful construction of the plasmid was confirmed by DNA sequencing (Robarts Institute, Western University).

#### 5.2.5 Protein Expression and Purification

The above bacterial cells with recombinant plasmid were grown overnight at 37 °C in 5 mL of Luria Bertani (LB) broth containing 100 µg/mL ampicillin. This culture was used to further inoculate 500 mL of broth containing 100 µg/ml of ampicillin, and this was grown at 37 °C. When the culture reached an OD<sub>600</sub> of 0.375, Isopropyl β-D-1-thiogalactopyranoside (IPTG) was added to 1 mM final concentration to induce the expression of recombinant protein pRluc and the bacteria were left to grow for 4 h at room temperature. The cells were harvested by centrifugation at 12,000 rpm for 5 min at 4 °C. The pellet was resuspended in a binding solution (BS) of 20 mM Tris/HCl, pH 7.4, 500 mM NaCl and 5 mM imidazole and sonicated on ice using 15-s bursts followed by 30-s rest for 30 cycles using a Mandel Scientific Q500 sonicator (Guelph, Canada). The

suspension was centrifuged at 10,000 rpm at 4 °C for 30 min to collect the supernatant from bacterial cell pellet. The protein was purified via His-trap HP columns (GE lifescience, Inc.) by a syringe pump. The column was first equilibrated with BS. The supernatant containing the protein was loaded on the column, and the column was washed with 10 column volumes of the BS. The protein was eluted using BS with a gradient of imidazole from 20 mM to 200 mM) over 10 column volumes. Five milliliters fractions were collected. An SDS-PAGE was run to verify the fractions containing the fusion protein, which were pooled together. Excess imidazole was removed from the combined fractions by buffer exchange with excess amount of 10 mM Tris/HCl, pH 7.4 using an amicon Ultra centrifugal filter (ultra-15, MWCO 10 kDa, Millipore Inc). The resultant pRluc protein solution was stored in aliquot at -20 °C. The concentration of the protein was determined by bicinchoninic acid (BCA) protein assay (Thermo scientific Inc).

#### 5.2.6 Bioconjugation of Au NPs by pRluc protein

The bioconjugation was mediated 1-Ethyl-3-(3-dimethylaminopropyl) carbodiimide (EDC). In a typical experiment, MUA or DHLA modified Au NPs (10 µL at 60 nM), pRluc (10 µL at 0.2 mM) and EDC (10 µL at 1 mM) were mixed in 270 µL of water. The mixture was incubated at room temperature for 2 h under gently shaking. Afterwards, 10 µL of ethanolamine was added to stop the reaction. The pRluc Au NPs were further purified by amicon ultra-0.5 filter.

#### 5.2.7 Characterization

Transmission electron microscopy (TEM) was used to analyze the morphology of the as-made nanoparticles. The TEM images were obtained using a Philips CM-10 microscopy operating at 100 kv. The modification of nanoparticles by PE and QDs were verified by using Fourier transform infrared (FTIR) spectrophotometer (Bruker FTIR-IFS 55, Germany). UV-visible absorption spectra were recorded by UV-3600 spectrophotometer (Shimadzu, Japan).

### 5.2.8 Thrombin assay

The pRluc-Au NPs conjugate (50  $\mu$ L at 15 mM) was mixed with 10 mM Tris buffer (TBS, 240  $\mu$ L, pH 7.4). The assay was initiated by addition of thrombin (from human plasma, 1000 NIH U/mg, 1 NIH unit is approximate equal to 0.3  $\mu$ g in amount, 10  $\mu$ L of each stock solution), giving final concentrations ranging from 3 ng/mL to 300  $\mu$ g/mL. In a typical experiment, the reaction was incubated at room temperature for 1 h. Bioluminescence emission spectra were collected immediately following addition of 1  $\mu$ L of CTZ (10 mg/mL in ethanol) to the digestion solution, by a QuantaMaster™ 40 Spectrofluorometer (PTI Inc., London, ON).

For detecting the thrombin in urine, a fraction of fresh urine solution from health body (provided by Mr. GeYi Bao from St. Joseph's Hospital) were first pretreated by centrifugation (6000 rpm, 15 min) and filtration (0.2  $\mu$ m filter). The thrombin with different concentrations was then spiked into a solution of pretreated urine (10% in TBS). The pRluc-Au NPs conjugate (50  $\mu$ L at 15 mM) was added into this solution. After 1 h, bioluminescence emission spectra were collected as described above.

## 5.3 Results and Discussion

### 5.3.1 Characterization of the pRluc-Au NP conjugate

In our study, citrate stabilized Au NPs with an average diameter around 13 nm (Figure A6a, from Appendix 6) was first synthesized, followed by surface functionalized with alkanethiol molecules (MUA and DHLA in this study). The carboxyl group presented on the surface of nanoparticles is then used to conjugate with the purified pRluc (MW ~ 60 kDa, Figure A6b at Appendix 6) via EDC mediated carbodiimide chemistry. Figure 5.2a shows the UV-visible spectra of unconjugated and pRluc conjugated Au NPs. The maximum absorption wavelength ( $\lambda_{ab \text{ max}}$ ) for both citrate capped Au NPs and DHLA modified Au NPs are found at 520 nm as expected. Meanwhile, MUA-Au NPs exhibits a 30-nm red shift in  $\lambda_{ab \text{ max}}$ , which indicates the formation of a slight aggregation of the NPs. Au NPs are favorable for chemical absorption of alkanethiol. However, the monothiol ligands modified colloidal gold can undergo irreversible aggregation, partially due to the desorption of thiol from NPs surface.<sup>39</sup> In addition, in a partially formed self-

assembled monothiol layer, long methylene groups of alkanethiol ligands render the NPs with hydrophobic character, thereby promoting their aggregation.<sup>40</sup> However, the disulfide group from DHLA offers higher affinity for the ligand to bind and stabilize Au NPs, resulting in a homogenous colloidal solution. Conjugation of pRluc to MUA-Au NPs causes a slight red shift of  $\lambda_{ab\ max}$  and a broader absorption spectrum, which might be due to the cross-link of a pRluc molecule with several Au NPs.

We further used FTIR to investigate the conjugation of pRluc with Au NPs. As shown in Figure 5.2b, citrate capped Au NPs shows a strong –OH stretch at 3500  $\text{cm}^{-1}$ . After modification with alkanethiol ligands (only MUA modified Au NPs was showed here), a peak is found around 1700  $\text{cm}^{-1}$ , which is attributed to –COOH group. A new band at 1640  $\text{cm}^{-1}$  is found in the pRluc-Au NPs sample, which is due to the stretch of peptide bond –CO-NH-. Thereby, we can conclude the pRluc is successful conjugated to Au NPs.

### 5.3.2 Assay optimization

We first tested the feasibility of the assay for detecting thrombin. Figure 5.3 shows that the bioluminescence is quenched while conjugating pRluc onto Au NPs. It should be note that, the RET only occurs when two partners approach very close to each other.<sup>41</sup> Thus, we did not observed any quenching of bioluminescence found in a mixture of pRluc and Au NPs, without conjugation (data not shown). Furthermore, we found the recovery of bioluminescence while adding thrombin to pRluc-Au NPs. It is expected this recovery of bioluminescence is related to the concentration of thrombin, as more thrombin will free more pRluc from Au NPs surface. In order to obtain a best correlation of the bioluminescence signal to the analyte amount, we then test the factors that may affect the assay performance.

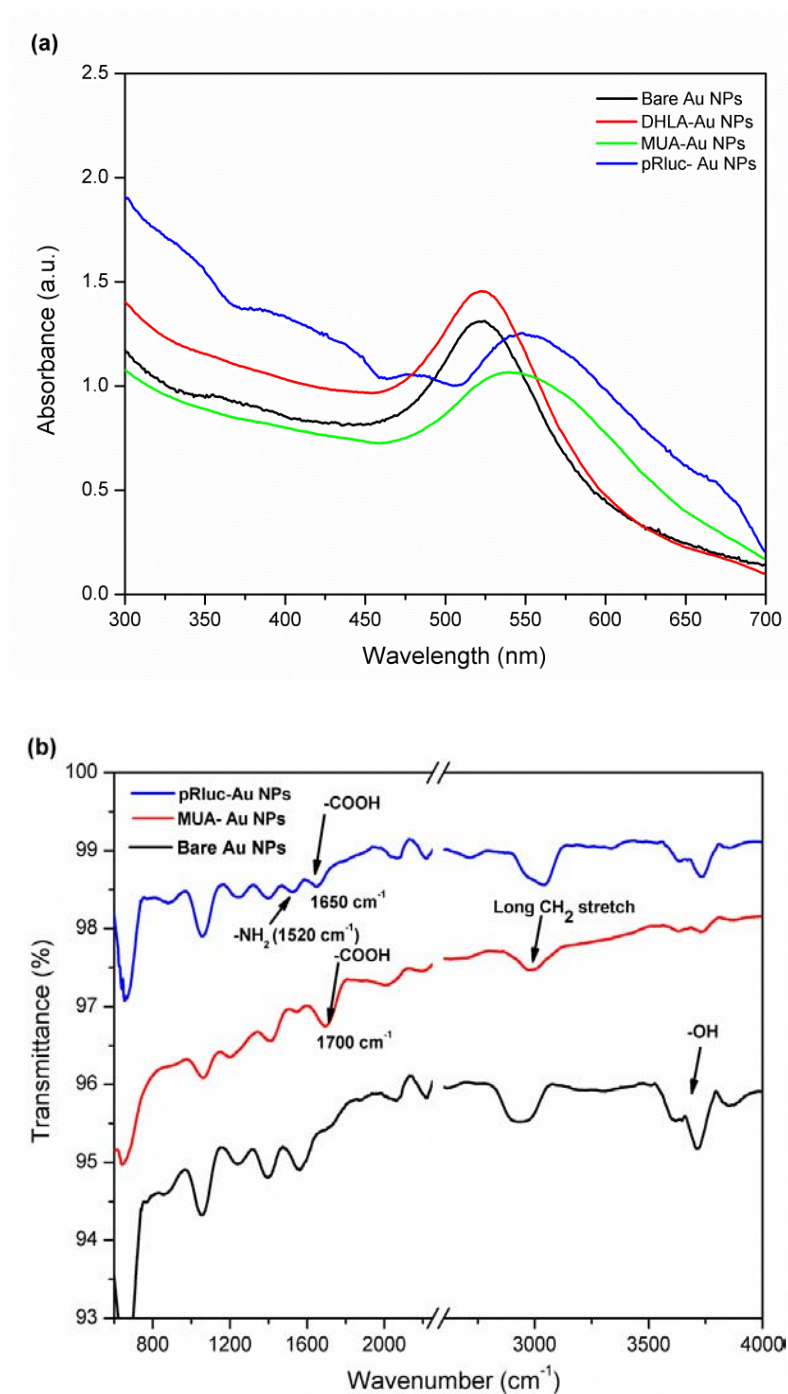


Figure 5.2 (a) UV-visible spectra and (b) FTIR spectra of bare Au NPs, alkanethiol acid functionalized Au NPs and pRluc conjugated Au NPs



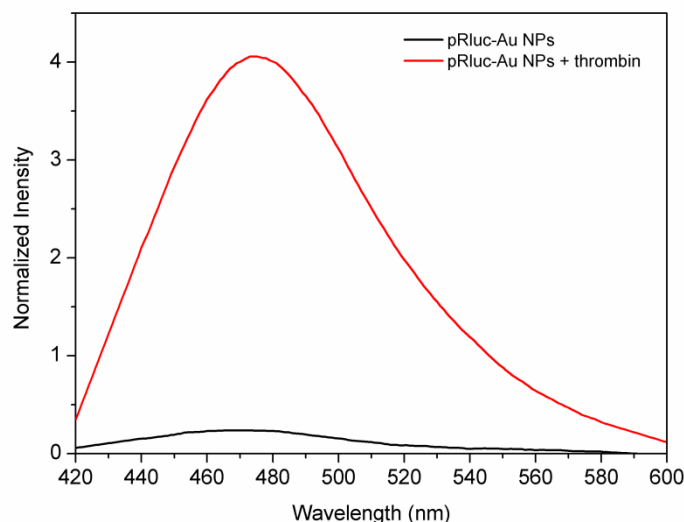


Figure 5.3 Bioluminescent spectra of pRluc-Au NPs conjugates.

We first test the alkanethiol ligands length effect. In our study, alkanethiol ligands MUA (11 C) and DHLA (5 C) are used to control the distance between pRluc and Au NPs, respectively. As described above, RET ratio is reverse-proportional with distance between fluorophores.<sup>41</sup> Thus, it is expected that the shorter linker of DHLA could have better quenching effect and result in higher recovered BL. However, our result (Figure 5.4a) shows the recovered BL intensity from MUA (11 C) linker is 2-fold higher than that from DHLA. Two factors may contribute to the result. The first one might be more pRluc molecules released from NPs by thrombin in MUA modified Au NPs, as long chain of MUA gives more freedom between NP and protein for the access of thrombin to its substrate peptides. The other factor may be the dramatic loss of enzyme activity in the DHLA modified Au NPs due to conformation changes. Au NPs has been reported to cause the loss activity for enzymes absorbed to NPs surface by change their conformation.<sup>42, 43</sup> Despite of lower stability of MUA Au NPs, the long chain of MUA may offer a steric barrier preventing the direct interaction between enzymes and Au NPs. On basis of this result, we then only use MUA modified Au NPs to conjugate pRluc in the following assay.

We then optimized the bioconjugation process. We first examined the effect of ratio of pRluc and MUA-Au NPs to the recovery of BL, by fixing the amount of the conjugation

reagent EDC. Figure 5.4 b shows that the best molar ratio of pRluc to MUA Au NPs is 10000:1. Then we fixed this ratio to analyze the effect of the ratio of EDC/MUA Au NPs to the rate of recovered BL. We found that high concentration of EDC could cause the aggregation of nanoparticles with decreasing of the recovered BL intensity. The best molar ratio of EDC to Au NPs is found at 10000:1 (Figure 5.4 c). Thus, the optimized molar ratio of MUA-Au NPs, pRluc and EDC is 1:10000:10000.

We further analyzed the time effect on BL recovery by thrombin digestion. As shown in Figure 5.4d, the relative BL ratio reaches to its first peak after 30 min incubation. No significant changes in BL ratio with the incubation time from 1 h to 4 h. The recovered BL ratio is 20% higher by overnight incubation than that from 1 h incubation. However, to reduce the assay time, we determine the incubation time to one hour for our assay.

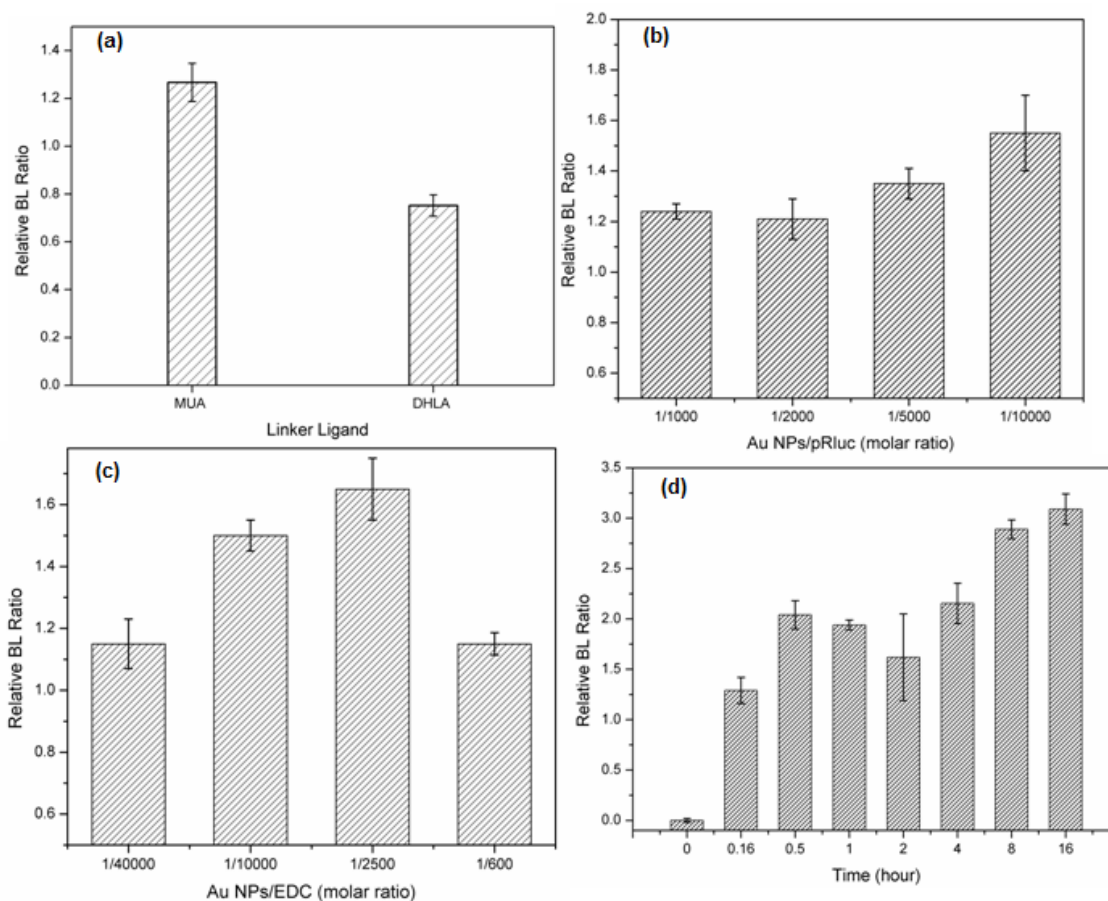


Figure 5.4 The effect of (a) ligand length, (b) the molar ratio of Au NPs and pRluc, (c) the molar ratio of Au NPs and EDC, and (d) digestion time to the relative BL ratio.

### 5.3.3 Determination of thrombin concentration in both buffer and urine samples

We then evaluated the capability of our nanosensor to measure the activity of thrombin under our optimized condition. As shown in Figure 5.5 a, increasing of thrombin concentration results in an increasing of the BL emission. A linear relationship between thrombin concentration and BL relative emission intensity is found in the range of 300 ng/mL to 300  $\mu$ g/mL, which is under the range of thrombin in human blood<sup>23</sup>. The limit of detection (LOD) for this assay is found to be 3 ng/mL.

We then tested nanosensor for detection of thrombin in urine samples in order to test the influence of the biological matrix to our assay performance. By spiking the different concentration of thrombin and pRLuc Au NPs in TBS with 10% urine from healthy subject, we did not find any significant changes for the overall assay performance in term of both detection limit and linear response, as shown in Figure 5.5b. Therefore, the results indicate that our nanosensor could be a potential tool for clinical diagnostic of thrombin related diseases.

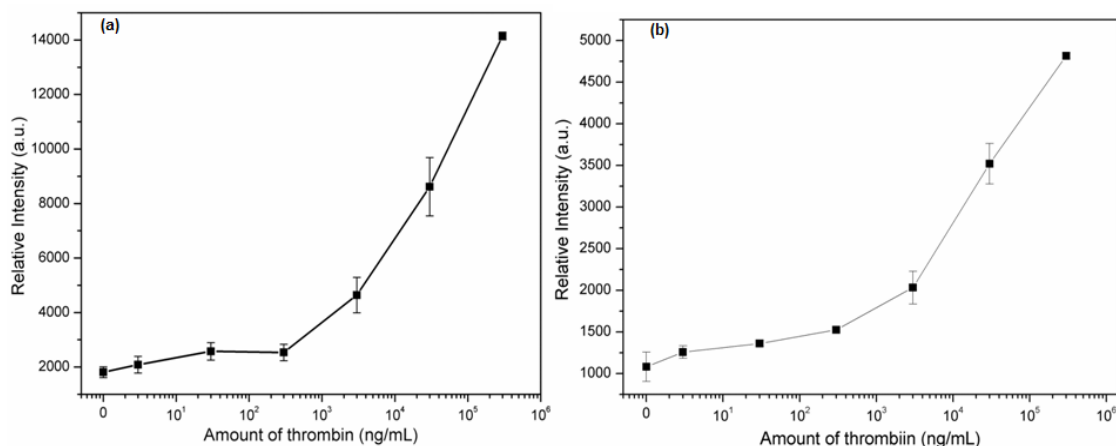


Figure 5.5 Detection of thrombin by using pRLuc-Au NPs nanosensor in (a) TBS buffer and in (b) TBS buffer spiked with human urine.

## 5.4 Conclusions and Prospects

In conclusion, we describe a bioluminescence nanosensor for highly sensitive determination of thrombin. A linear assay response is found between 300 ng/mL to 300 µg/mL with LOD of 3 ng/mL in both buffer and urine samples. The detection of thrombin could be achieved in 15 min. The detection range is among the range of thrombin in Glomerulo-nephritis patients. The nanosensor can thus be a promising tool for clinical diagnostic of thrombin related diseases.

## 5.5 References

1. Roda, A.; Guardigli, M.; Michelini, E.; Mirasoli, M., Nanobioanalytical luminescence: Förster-type energy transfer methods. *Analytical and Bioanalytical Chemistry* **2009**, 393, (1), 109-123.
2. Kwon, J. Y.; Jang, Y. J.; Lee, Y. J.; Kim, K. M.; Seo, M. S.; Nam, W.; Yoon, J., A Highly Selective Fluorescent Chemosensor for Pb<sup>2+</sup>. *Journal of the American Chemical Society* **2005**, 127, (28), 10107-10111.
3. Mello, J. V.; Finney, N. S., Dual-Signaling Fluorescent Chemosensors Based on Conformational Restriction and Induced Charge Transfer. *Angewandte Chemie International Edition* **2001**, 40, (8), 1536-1538.
4. Sapsford, K. E.; Berti, L.; Medintz, I. L., Materials for Fluorescence Resonance Energy Transfer Analysis: Beyond Traditional Donor–Acceptor Combinations. *Angewandte Chemie International Edition* **2006**, 45, (28), 4562-4589.
5. Jain, P. K.; El-Sayed, I. H.; El-Sayed, M. A., Au nanoparticles target cancer. *Nano Today* **2007**, 2, (1), 18-29.
6. Huang, C.-C.; Chang, H.-T., Selective Gold-Nanoparticle-Based "Turn-On" Fluorescent Sensors for Detection of Mercury(II) in Aqueous Solution. *Analytical Chemistry* **2006**, 78, (24), 8332-8338.
7. He, X.; Liu, H.; Li, Y.; Wang, S.; Li, Y.; Wang, N.; Xiao, J.; Xu, X.; Zhu, D., Gold Nanoparticle-Based Fluorometric and Colorimetric Sensing of Copper(II) Ions. *Advanced Materials* **2005**, 17, (23), 2811-2815.
8. Huang, T.; Murray, R. W., Quenching of [Ru(bpy)<sub>3</sub>]<sup>2+</sup> Fluorescence by Binding to Au Nanoparticles. *Langmuir* **2002**, 18, (18), 7077-7081.
9. Zhang, N.; Liu, Y.; Tong, L.; Xu, K.; Zhuo, L.; Tang, B., A novel assembly of Au NPs-β-CDs-FL for the fluorescent probing of cholesterol and its application in blood serum. *Analyst* **2008**, 133, (9), 1176-1181.
10. Chen, S.-J.; Chang, H.-T., Nile Red-Adsorbed Gold Nanoparticles for Selective Determination of Thiols Based on Energy Transfer and Aggregation. *Analytical Chemistry* **2004**, 76, (13), 3727-3734.
11. Dyadyusha, L.; Yin, H.; Jaiswal, S.; Brown, T.; Baumberg, J. J.; Booy, F. P.; Melvin, T., Quenching of CdSe quantum dot emission, a new approach for biosensing. *Chemical Communications* **2005**, (25), 3201-3203.

12. Xia, X.; Yang, M.; Oetjen, L. K.; Zhang, Y.; Li, Q.; Chen, J.; Xia, Y., An enzyme-sensitive probe for photoacoustic imaging and fluorescence detection of protease activity. *Nanoscale* **2011**, 3, (3), 950-953.
13. Lee, S.; Cha, E.-J.; Park, K.; Lee, S.-Y.; Hong, J.-K.; Sun, I.-C.; Kim, S. Y.; Choi, K.; Kwon, I. C.; Kim, K.; Ahn, C.-H., A Near-Infrared-Fluorescence-Quenched Gold-Nanoparticle Imaging Probe for In Vivo Drug Screening and Protease Activity Determination. *Angewandte Chemie International Edition* **2008**, 47, (15), 2804-2807.
14. Leung, D.; Abbenante, G.; Fairlie, D. P., Protease Inhibitors: Current Status and Future Prospects. *Journal of Medicinal Chemistry* **2000**, 43, (3), 305-341.
15. Zhang, B., Design of FRET-based GFP probes for detection of protease inhibitors. *Biochemical and Biophysical Research Communications* **2004**, 323, (2), 674-678.
16. Nelson, D. D. L.; Lehninger, A. L.; Cox, M. M., *Lehninger Principles of Biochemistry*. W.H. Freeman: 2013.
17. Turk, B., Targeting proteases: successes, failures and future prospects. *Nature reviews Drug discovery* **2006**, 5, (9), 785-799.
18. Chang, J.-Y., Thrombin specificity. *European Journal of Biochemistry* **1985**, 151, (2), 217-224.
19. Shuman, M. A., Thrombin-Cellular Interactions. *Annals of the New York Academy of Sciences* **1986**, 485, (1), 228-239.
20. Bar-Shavit, R.; Benezra, M.; Eldor, A.; Hy-Am, E.; Fenton, J. W., 2nd; Wilner, G. D.; Vlodavsky, I., Thrombin immobilized to extracellular matrix is a potent mitogen for vascular smooth muscle cells: nonenzymatic mode of action. *Cell Regulation* **1990**, 1, (6), 453-63.
21. Hernández-Rodríguez, N. A.; Cambrey, A. D.; Chambers, R. C.; Gray, A. J.; McAnulty, R. J.; Laurent, G. J.; Harrison, N. K.; Southcott, A. M.; duBois, R. M.; Black, C. M.; Scully, M. F., Role of thrombin in pulmonary fibrosis. *The Lancet* **1995**, 346, (8982), 1071-1073.
22. Kitamoto, Y.; Immura, T.; Fukui, H.; Tomita, K., Role of thrombin in mesangial proliferative glomerulonephritis. *Kidney International* **1998**, 54, (5), 1767-1768.
23. Shuman, M. A.; Majerus, P. W., The measurement of thrombin in clotting blood by radioimmunoassay. *The Journal of Clinical Investigation* **1976**, 58, (5), 1249-1258.
24. Kitamoto, Y.; Tomita, K.; Imamura, T., Assessment of thrombin in the urine of glomerulonephritic patients by enzyme-linked immunosorbent assay. *Annals of Clinical Biochemistry* **2004**, 41, (2), 133-137.
25. Jaffer, F. A.; Tung, C.-H.; Gerszten, R. E.; Weissleder, R., In Vivo Imaging of Thrombin Activity in Experimental Thrombi With Thrombin-Sensitive Near-Infrared Molecular Probe. *Arterioscler Thromb Vasc Biol* **2002**, 22, (11), 1929-1935.
26. Tung, C.-H.; Gerszten, R. E.; Jaffer, F. A.; Weissleder, R., A Novel Near-Infrared Fluorescence Sensor for Detection of Thrombin Activation in Blood. *ChemBioChem* **2002**, 3, (2-3), 207-211.
27. Olson, E. S.; Whitney, M. A.; Friedman, B.; Aguilera, T. A.; Crisp, J. L.; Baik, F. M.; Jiang, T.; Baird, S. M.; Tsimikas, S.; Tsien, R. Y.; Nguyen, Q. T., In vivo

- fluorescence imaging of atherosclerotic plaques with activatable cell-penetrating peptides targeting thrombin activity. *Integrative Biology* **2012**, 4, (6), 595-605.
28. Lin, K. Y.; Kwong, G. A.; Warren, A. D.; Wood, D. K.; Bhatia, S. N., Nanoparticles That Sense Thrombin Activity As Synthetic Urinary Biomarkers of Thrombosis. *ACS Nano* **2013**, 7, (10), 9001-9009.
  29. Huang, D.-W.; Niu, C.-G.; Qin, P.-Z.; Ruan, M.; Zeng, G.-M., Time-resolved fluorescence aptamer-based sandwich assay for thrombin detection. *Talanta* **2010**, 83, (1), 185-189.
  30. Tennico, Y. H.; Hutanu, D.; Koesdjojo, M. T.; Bartel, C. M.; Remcho, V. T., On-Chip Aptamer-Based Sandwich Assay for Thrombin Detection Employing Magnetic Beads and Quantum Dots. *Analytical Chemistry* **2010**, 82, (13), 5591-5597.
  31. Zhao, Q.; Lu, X.; Yuan, C.-G.; Li, X.-F.; Le, X. C., Aptamer-Linked Assay for Thrombin Using Gold Nanoparticle Amplification and Inductively Coupled Plasma-mass Spectrometry Detection. *Analytical Chemistry* **2009**, 81, (17), 7484-7489.
  32. Dubertret, B.; Calame, M.; Libchaber, A. J., Single-mismatch detection using gold-quenched fluorescent oligonucleotides. *Nature Biotechnology* **2001**, 19, (4), 365-370.
  33. Hazarika, P.; Kukolka, F.; Niemeyer, C. M., Reversible Binding of Fluorescent Proteins at DNA–Gold Nanoparticles. *Angewandte Chemie International Edition* **2006**, 45, (41), 6827-6830.
  34. Kim, Y.-P.; Oh, Y.-H.; Oh, E.; Ko, S.; Han, M.-K.; Kim, H.-S., Energy Transfer-Based Multiplexed Assay of Proteases by Using Gold Nanoparticle and Quantum Dot Conjugates on a Surface. *Analytical Chemistry* **2008**, 80, (12), 4634-4641.
  35. Kim, Y.-P.; Daniel, W. L.; Xia, Z.; Xie, H.; Mirkin, C. A.; Rao, J., Bioluminescent nanosensors for protease detection based upon gold nanoparticle-luciferase conjugates. *Chemical Communications* **2010**, 46, (1), 76-78.
  36. Yonezawa, T.; Yasui, K.; Kimizuka, N., Controlled Formation of Smaller Gold Nanoparticles by the Use of Four-Chained Disulfide Stabilizer. *Langmuir* **2000**, 17, (2), 271-273.
  37. Frens, G., Controlled nucleation for the regulation of the particle size in monodisperse gold suspensions. *Nature* **1973**, 241, (105), 20-22.
  38. LaVallie, E. R.; DiBlasio, E. A.; Kovacic, S.; Grant, K. L.; Schendel, P. F.; McCoy, J. M., A thioredoxin gene fusion expression system that circumvents inclusion body formation in the E. coli cytoplasm. *Nature Biotechnology* **1993**, 11, (2), 187-193.
  39. Schroedter, A.; Weller, H., Ligand Design and Bioconjugation of Colloidal Gold Nanoparticles. *Angewandte Chemie International Edition* **2002**, 41, (17), 3218-3221.
  40. Aslan, K.; Pérez-Luna, V. H., Surface Modification of Colloidal Gold by Chemisorption of Alkanethiols in the Presence of a Nonionic Surfactant. *Langmuir* **2002**, 18, (16), 6059-6065.
  41. Lakowicz, J., Energy Transfer. In *Principles of Fluorescence Spectroscopy*, Springer US: 2006; pp 443-475.

42. Singh, V.; Nair, S. P. N.; Aradhyam, G. K., Chemistry of conjugation to gold nanoparticles affects G-protein activity differently. *Journal of Nanobiotechnology* **2013**, 11, (1), 7.
43. Wangoo, N.; Suri, C. R.; Shekhawat, G., Interaction of gold nanoparticles with protein: A spectroscopic study to monitor protein conformational changes. *Applied Physics Letters* **2008**, 92, 133104-1.

## **CHAPTER 6**

### **SUMMARY AND RECOMMENDATIONS**



## 6.1 Summary and Conclusion

The overall objective of this thesis is to develop advanced nanoparticles (NPs) with well-tailored surface modification and/or bioconjugation for the applications in cell tracking, and target molecule detection. Since 1990's, development of well-defined NPs in terms of particles size and shape has evolved into the formation of more complex nanosystems by combining more than two components together at nanoscale, including layer-by-layer NPs, core-shell NPs, and organic-inorganic hybrid nanostructures. In this thesis, hybrid NPs with special and enhanced luminescent and magnetic properties have been developed through cost-effective chemical processes. To further apply these hybrid NPs with enhanced chemical and physical properties in bio-imaging and bio-sensors, I applied different strategies to engineer the hybrid NPs: (1) modify the surface of the hybrid NPs to enhance their biocompatibility for achieving in vitro bio-imaging; (2) bioconjugate the hybrid NPs with enzyme(s) to develop BRET nanostructured sensors. The results of my study are briefly summarized below.

*Develop biocompatible luminescent hybrid NPs for cell-tracking.* In Chapter 3, the biocompatible luminescence quantum dots (QDs) have been incorporated into gelatin nanoparticles (NPs) through two different methods, i.e. QDs-GNP1 by encapsulating QDs with gelatin polymer and core-shell QDs-GNP2 by layer-by-layer (LBL) coating approach, respectively. Both gelatin/QDs systems exhibit bright luminescence and good biocompatibility. No study has been found in using LBL techniques to prepare QDs loaded gelatin NPs. The main points are summarized below.

1. By comparing to two synthesis processes, LBL technique indicate its advantage to enhance the photostability of QDs over the directly encapsulation method.
2. Using LBL technique, QDs-GNPs show the typical core-shell structure. The shell made of assembled QDs is modified by a negatively charged layer to enhance the interaction with NIH/3T3 mouse fibroblast cells 3T3.
3. Polyelectrolytes (PE) mediated LBL coating can improve the quantum yields of QDs by nearly two folds, and the lifetime of luminescence is found three-fold longer than that of QDs without PE modification.

4. We demonstrated that the luminescence of QDs in multiple-layer QDs/gelatin NPs is of unique proton resistant, which indicates it could be a suitable imaging agents in certain environment such as cancer cells.

*Development of bioconjugated magnetic fluorescent nanomaterials for bacterial capture, detection and antibacterial applications* – Chapter 4 describes preparation of antibiotic gentamicin (Gm) conjugated fluorescent magnetic nanoparticles (FMNPs) for rapid capture, detection and decontamination of bacteria. The NPs consist of a fluorescent silica shell and an iron oxide magnetic core. Initially we prepared the core-shell FMNP1 through a one-pot reaction. The NPs were then conjugated with antibiotic gentamicin. We then demonstrated the gentamicin conjugated fluorescent magnetic nanoparticles (Gm-FMNP1) were able to capture, detect and deactivate bacteria *Escherichia coli*. To improve the stability and capture efficiency, we further developed a two-step thermal decomposition method to produce the fluorescent magnetic core-shell nanoparticles (i.e. FMNP2). We extensively demonstrated the gentamicin conjugated FMNP2 (Gm-FMNP2) were able to capture both Gram-negative bacteria *E. coli* and Gram-positive bacteria *Staphylococcus aureus* in 1 minute.

1. FMNPs consist of  $\text{Fe}_3\text{O}_4$  core and silica shell was produced. The FMNPs exhibit superparamagnetic property.
2. Gentamicin conjugated FMNPs are able to capture both *E. coli* and *S. aureus* in as fast as 1 minute.
3. By utilizing the fluorescent property of Gm-FMNPs, we are able to detect bacterial cells at a concentration as low as of  $1 \times 10^4$  CFU/mL.
4. We demonstrated 20% higher of the antibacterial efficiency of Gm-FMNPs than that of free gentamicin.

*Luciferase conjugated NPs for biosensing applications* – Chapter 5 describes the development of bioluminescence resonance energy transfer (BRET) based nanosensors for biosensing application. A nanosensor containing a recombinant protein (pRLuc) that consists of Renilla luciferase and a short thrombin substrate peptide at its N-terminal

was conjugated to gold nanoparticles (Au NPs) for detecting protease thrombin in both buffer and human urine sample spiked buffer.

1. Quench of bioluminescence was found while conjugating pRluc to Au NPs.
2. Increasing of thrombin concentration results in increasing of bioluminescence intensity due to release of the pRluc from Au NPs.
3. Thrombin concentrations are measured in both buffer and human urine sample spiked buffer over 300 ng/mL to 300  $\mu$ g/mL with proportional relationship to the recovery of bioluminescence.
4. The limit of detection is achieved to be 3 ng/mL. The detection of thrombin could be achieved in 15 min.

## 6.2 Contributions of the Research to the Current State of Knowledge.

Historical perspective – Prerequisite for the use of inorganic colloidal nanoparticle in biomedicine is the proper surface functionalization of such NPs, which determine their target applications. Critical considerations for the design of such proper surface can be summarized below:<sup>1-3</sup>

1. The surface can stabilize the NPs in solution, particularly in water as almost all biochemical processes occur in water. In some instances, hydrophobic surface is required to control the growth of embryonic particles and determine the size and/or shape of NPs. However, a ligand exchange process is necessary to bring particles water solubility.
2. The surface must offer a reduction of toxicity of NPs in some instances, for example for *in vivo* applications. A comprehensive consideration of the toxicity effect includes *in vitro* and *in vivo* cytotoxicity, cell adhesion, circulation, etc.
3. Capping layers can offer additional functional groups at the surface for further derivatization, such as conjugation with biomolecules.

4. A proper surface may alter the physical properties (electronic, optical, spectroscopic and magnetic) or chemical properties of NPs, which provides the potentials to build multifunctional nanotools.
5. The surface layers can improve the mechanical and chemical performance of the NPs, for example protecting core against oxidation.
6. Bioconjugated surface can ultimately determine the targeted applications of such NPs, as well as their efficiency and specificity.

Advances in surface chemistry research offer a great of opportunities in manufacturing NPs for the use in the field of biomedicine. The overall objective of current research projects was the design and development of NPs with proper surface for biomedical applications. NPs were designed to meet as many of the above criteria as possible in order to promote their target applications.

*Development of biocompatible luminescent nanocomposites for bioimaging applications*

– Luminescent quantum dots (QDs) offer unique optical properties and promise significant advantages as a new class of imaging and analytical probes in biomedical field. However, since a large portion of the QDs is obtained in organic solvents, a phase transfer procedure is usually required before using them in biomedical applications [9]. Another key challenge in bio-imaging application of QDs is the inherent biological toxicity of some common used QDs (e.g. CdSe QDs).<sup>4, 5</sup> A biocompatible layer is thus required. Although small molecules (e.g. alkanethiol acids) have been used as a simple and effective ligand to render hydrophobic QDs water solubility,<sup>6-11</sup> colloidal instability and quenching of luminescent have been reported in such QDs due to easy oxidation of core materials and acid etching in certain physiological conditions.<sup>12</sup> Encapsulation of biocompatible polymer layer can offer great opportunities to overcome such drawbacks, as they can protect the core materials from oxidation, avoid the direct interaction of between core and living cells, and render new chemical functionalities for further grafting of biomolecules.

The biocompatible polymer used in my study is gelatin, a nature biocompatible biopolymer derived from collagen. Initially, we have successfully coated QDs with gelatin polymer by direct encapsulation (QDs-GNP1). The nano-system was found with good biocompatibility and bright luminescent. To improve photostability of QDs encapsulated NPs, we further applied the layer-by-layer (LBL) assembly technique to develop a new type of gelatin/QDs core/shell nanocomposites (QDs-GNP2). To our best knowledge, this is the first time using LBL technique to develop a gelatin-QDs nano-system.

One of the significant features of our QDs-GNP2 is the stable luminescence with unique proton resistant property. Multiplayer coating of polyelectrolytes (PE) was found to enhance the QDs quantum yield and lifetime in our study. It could be attributed to that the PE matrix may minimize the nonradiative recombination on the surface of QDs and increase confinement of charge carrier.<sup>13, 14</sup> In addition, we show the QDs-GNP2 with good dispersibility and extremely stable luminescence in a wide range of pH value (pH 1.0 to 9.0). It should be noted that acid etching can cause photo bleaching of CdSe QDs,<sup>8, 15</sup> which limit the use of QDs in some important physiological environments, such as endosomes and lysosomes inside cells and tumor cells, where the pH are in moderate acidic range.<sup>16, 17</sup> Therefore the pH independent photostability of our QDs-GNP2 nano-system may offer extra advantages for use in such conditions as imaging agents.

Furthermore, gelatin nanoparticles (GNPs) have been demonstrated as an excellent carrier in drug and gene delivery,<sup>18-20</sup> it is thus possible that our system that combining QDs and gelatin materials can be an all-in-one tool for simultaneously using in drug delivery and bio-imaging applications. In addition, the negative charge of PE coating in our QDs-GNP2 nano-system can potentially promote the adhesion of nanocomposites to cells surface, which may lead to longer circulation time in vivo and hence enhance the efficiency for delivery of drug.<sup>21</sup>

*Multifunctional NPs for ubiquitous capture of bacteria.* MNPs have been employed for rapid capture and detection of pathogens. The effectively and selectively targeting requires stable and mono-dispersive NPs, as well as proper functionality.

Silica coating offers great advantages, including enhanced water solubility, low non-specific interaction and additional functionality.<sup>22</sup> In our study, we have tried two approaches in preparation of fluorescent silica coated magnetic nanoparticles (FMNPs). One-pot synthesis approach directly renders the NPs with hydrophilic property. However, particles are easily to form aggregations and particle size distribution is found relative boarder. The two-step approach undergoes a high temperature synthesis process, which provides a magnetic core with good crystalline structure. The stability of the core-shell NPs is more stable. The small hydro-diameter of the NPs prepared by two-step method is potential to improve the capture efficiency.

Surface functionality of NPs ultimately determines the interaction of NPs with biological species. Antibody-modified particles have found success in cell/biomolecules labelling and targeting. However, antibodies are only specific to certain species of pathogen.<sup>23-25</sup> In our study, we conjugated a small antibiotic molecule gentamicin to FMNPs. The protein nature of antibodies makes them be denatured under certain conditions, such as high temperature, high salt concentration, extreme solution pH, solvent, etc.<sup>26</sup> The strong interaction of gentamicin to cell membrane from gram-negative bacteria and some sensitive gram-positive bacteria enables ubiquitous capture of bacteria by our gentamicin FMNPs. In addition, as gentamicin is one of the few heat-stable antibiotics that remain active even after autoclaving, our Gm-FMNPs are potentially reusable. Furthermore, the intrinsic antibacterial activity of gentamicin makes our Gm-FMNPs as an excellent disinfection agent. Due to the large ratio of surface to volume property of NPs, higher antibacterial efficiency is expected, which is in agreement with our results.

*Luciferase conjugated NPs for biosensing applications.* NPs are required to conjugate with biomolecules (e.g. proteins) of interest for further biomedical applications. Proteins can be conjugated to the surface of NPs by adsorption, covalent conjugation and binding through bio-affinity interaction.<sup>27</sup> However, successful conjugation of protein to NPs should be evaluated by several factors, such as protein activity, protein amount, orientation, and the interaction between nanoparticle and proteins. One of the most common used approaches is covalent conjugation mediated by carbodiimide chemistry. In our study, we have used EDC as conjugation reagent. However, we demonstrated that

a systematic optimization is required for EDC mediated conjugation for better assay performance, including the molar ratio of proteins, NPs and EDC, in agreement with others' report.<sup>28</sup>

### 6.3 Limitations of the Research and Suggestions for Future Studies

#### *Development of biocompatible luminescent nanocomposites for bioimaging applications*

Despite of the versatility of LBL coating technique for enhancing the MUA-QDs luminescent property, the QDs used in our study exhibited low quantum yield and relative short lifetime comparing to the commercial products. The colloid stability of MUA coated QDs is relative poor, which could be attributed the desorption of MUA from the surface of QDs.<sup>12, 29</sup> It is suggested that PEG derived polymer or copolymer may be used to improve the stability.<sup>30</sup> In addition, coating of CdSe QDs with ZnS shell was also reported to increase the quantum yield.<sup>6</sup> Thus, much effort is required to make QDs with good stability and bright luminescence.

Targeting imaging requires specific interaction of luminescent NPs with certain cells. In our study, the adhesion of nanocomposites to cell membrane is based on electrostatic interaction and it is non-specific. It is expected that in the future work, conjugation of biomolecules (e.g. antibody) to nanocomposites can promote the target imaging. Additionally, as gelatin could be an excellent carrier for drug and gene deliver, it is promising to load drugs in the nanocomposites and realize simultaneous use in imaging and drug delivery.

#### *Development of bioconjugated magnetic luminescent nanomaterials for bacterial*

*capture, detection and antibacterial applications.* Initial objective of this study is to provide an all-in-one nanotool for simultaneous capture, detection and decontamination of bacteria. However, the detection of bacteria in our study is based on the observation of capture bacterial cells from fluorescent microscopy. Therefore, it is difficult to get quantitative results. In the future work, proper readout strategies may be required. Some of the common used techniques are fluorescent labelling of bacterial cell,<sup>31, 32</sup> MALDI-MS,<sup>33</sup> etc. In addition, the detection sensitivity can be improved through optimizing the

conjugation conditions (For example, use of EDC mediated conjugation rather than glutaraldehyde cross-linking to improve conjugation efficiency).

Another critical step is to test the versatility of our Gm-FMNPs in real world applications, such as the use in clinical diagnostic and wastewater treatment. Many challenges may occur, including matrix interference, antibiotic resistant bacterial strains, bacterial spores, etc. It seems that a combination of other technologies such as filtration in wastewater treatment may be required. Furthermore, magnetically capture of the pathogen from large sample volumes into much smaller ones allows their incorporation onto a microfluidic device platform for development of portable analytical tools.

*Luciferase conjugated NPs for biosensing applications.* In chapter 5, we conjugated a recombinant luciferase to Au NPs through EDC mediated reaction. The assay sensitivity is largely dependent on the efficiency of luciferase released from Au NPs by thrombin cleavage. However, some of the luciferase molecules may remain conjugated on the NPs, if the position of the amino groups involved in the conjugation located at the C-terminal of the substrate peptide. Therefore, a proper conjugation orientation is important for increasing the assay sensitivity. As discussed in Chapter 2, it is promising to use expressed protein ligation strategy to produce site-specific conjugation of protein to NPs. One example is to use intein mediated conjugation approach to enhance such assay sensitivity.<sup>34</sup>

## 6.4 References

1. de Dios, A. S.; Díaz-García, M. E., Multifunctional nanoparticles: Analytical prospects. *Analytica Chimica Acta* **2010**, 666, (1-2), 1-22.
2. Sanvicens, N.; Marco, M. P., Multifunctional nanoparticles-properties and prospects for their use in human medicine. *Trends in Biotechnology* **2008**, 26, (8), 425-433.
3. Thanh, N. T. K.; Green, L. A. W., Functionalisation of nanoparticles for biomedical applications. *Nano Today* **2010**, 5, (3), 213-230.
4. Chang, E.; Thekkekk, N.; Yu, W. W.; Colvin, V. L.; Drezek, R., Evaluation of Quantum Dot Cytotoxicity Based on Intracellular Uptake. *Small* **2006**, 2, (12), 1412-1417.
5. Derfus, A. M.; Chan, W. C. W.; Bhatia, S. N., Probing the Cytotoxicity of Semiconductor Quantum Dots. *Nano Letters* **2003**, 4, (1), 11-18.
6. Chan, W. C. W.; Nie, S., Quantum Dot Bioconjugates for Ultrasensitive Nonisotopic Detection. *Science* **1998**, 281, (5385), 2016-2018.



7. Pinaud, F.; King, D.; Moore, H.-P.; Weiss, S., Bioactivation and Cell Targeting of Semiconductor CdSe/ZnS Nanocrystals with Phytochelatin-Related Peptides. *Journal of the American Chemical Society* **2004**, 126, (19), 6115-6123.
8. Guo, W.; Li, J. J.; Wang, Y. A.; Peng, X., Conjugation Chemistry and Bioapplications of Semiconductor Box Nanocrystals Prepared via Dendrimer Bridging. *Chemistry of Materials* **2003**, 15, (16), 3125-3133.
9. Pathak, S.; Choi, S.-K.; Arnheim, N.; Thompson, M. E., Hydroxylated Quantum Dots as Luminescent Probes for in Situ Hybridization. *Journal of the American Chemical Society* **2001**, 123, (17), 4103-4104.
10. Kim, S.; Bawendi, M. G., Oligomeric Ligands for Luminescent and Stable Nanocrystal Quantum Dots. *Journal of the American Chemical Society* **2003**, 125, (48), 14652-14653.
11. Osaki, F.; Kanamori, T.; Sando, S.; Sera, T.; Aoyama, Y., A Quantum Dot Conjugated Sugar Ball and Its Cellular Uptake. On the Size Effects of Endocytosis in the Subviral Region. *Journal of the American Chemical Society* **2004**, 126, (21), 6520-6521.
12. Aldana, J.; Wang, Y. A.; Peng, X., Photochemical Instability of CdSe Nanocrystals Coated by Hydrophilic Thiols. *Journal of the American Chemical Society* **2001**, 123, (36), 8844-8850.
13. Komarala, V. K.; Rakovich, Y. P.; Bradley, A. L.; Byrne, S. J.; Corr, S. A.; Gun'ko, Y. K., Emission properties of colloidal quantum dots on polyelectrolyte multilayers. *Nanotechnology* **2006**, 17, (16), 4117-22.
14. Maule, C.; Gonçalves, H.; Mendonça, C.; Sampaio, P.; Esteves da Silva, J. C. G.; Jorge, P., Wavelength encoded analytical imaging and fiber optic sensing with pH sensitive CdTe quantum dots. *Talanta* **2010**, 80, (5), 1932-1938.
15. Jiang, W.; Mardyani, S.; Fischer, H.; Chan, W. C. W., Design and Characterization of Lysine Cross-Linked Mercapto-Acid Biocompatible Quantum Dots. *Chemistry of Materials* **2006**, 18, (4), 872-878.
16. Ganta, S.; Devalapally, H.; Shahiwala, A.; Amiji, M., A review of stimuli-responsive nanocarriers for drug and gene delivery. *Journal of Controlled Release* **2008**, 126, (3), 187-204.
17. Wan, X.; Wang, D.; Liu, S., Fluorescent pH-Sensing Organic/Inorganic Hybrid Mesoporous Silica Nanoparticles with Tunable Redox-Responsive Release Capability. *Langmuir* **2010**, 26, (19), 15574-15579.
18. Kumari, A.; Yadav, S. K.; Yadav, S. C., Biodegradable polymeric nanoparticles based drug delivery systems. *Colloids and Surfaces B: Biointerfaces* **2010**, 75, (1), 1-18.
19. Coester, C. J.; Langer, K.; Briesen, H. V.; Kreuter, J., Gelatin nanoparticles by two step desolvation a new preparation method, surface modifications and cell uptake. *Journal of Microencapsulation* **2000**, 17, (2), 187-193.
20. Balthasar, S.; Michaelis, K.; Dinauer, N.; von Briesen, H.; Kreuter, J. r.; Langer, K., Preparation and characterisation of antibody modified gelatin nanoparticles as drug carrier system for uptake in lymphocytes. *Biomaterials* **2005**, 26, (15), 2723-2732.

21. Moghimi, S. M.; Hunter, A. C.; Murray, J. C., Long-Circulating and Target-Specific Nanoparticles: Theory to Practice. *Pharmacological reviews* **2001**, 53, (2), 283-318.
22. Giaume, D.; Poggi, M. I.; Casanova, D.; Mialon, G. v.; Lahlil, K.; Alexandrou, A.; Gacoin, T.; Boilot, J.-P., Organic Functionalization of Luminescent Oxide Nanoparticles toward Their Application As Biological Probes. *Langmuir* **2008**, 24, (19), 11018-11026.
23. Grossman, H. L.; Myers, W. R.; Vreeland, V. J.; Bruehl, R.; Alper, M. D.; Bertozzi, C. R.; Clarke, J., Detection of bacteria in suspension by using a superconducting quantum interference device. *Proceedings of the National Academy of Sciences of the United States of America* **2004**, 101, (1), 129-134.
24. Tu, S.-I.; Uknalis, J. O. E.; Gore, M.; Irwin, P., The Capture Of Escherichia Coli O157:H7 For Light Addressable Potentiometric Sensor (Laps) Using Two Different Types Of Magnetic Beads1. *Journal of Rapid Methods & Automation in Microbiology* **2002**, 10, (3), 185-195.
25. Kaittanis, C.; Naser, S. A.; Perez, J. M., One-Step, Nanoparticle-Mediated Bacterial Detection with Magnetic Relaxation. *Nano Letters* **2006**, 7, (2), 380-383.
26. Dill, K. A.; Shortle, D., Denatured States of Proteins. *Annual Review of Biochemistry* **1991**, 60, (1), 795-825.
27. Di Marco, M.; Shamsuddin, S.; Razak, K. A.; Aziz, A. A.; Devaux, C.; Borghi, E.; Levy, L.; Sadun, C., Overview of the main methods used to combine proteins with nanosystems: absorption, bioconjugation, and encapsulation. *International journal of nanomedicine* **2010**, 5, 37.
28. Fayi Song and Warren, C. W. C., Principles of conjugating quantum dots to proteins via carbodiimide chemistry. *Nanotechnology* **2011**, 22, (49), 494006.
29. Kloefer, J. A.; Bradforth, S. E.; Nadeau, J. L., Photophysical Properties of Biologically Compatible CdSe Quantum Dot Structures. *The Journal of Physical Chemistry B* **2005**, 109, (20), 9996-10003.
30. Zhang, F.; Lees, E.; Amin, F.; Rivera\_Gil, P.; Yang, F.; Mulvaney, P.; Parak, W. J., Polymer-Coated Nanoparticles: A Universal Tool for Biolabelling Experiments. *Small* **2007**, 3, (22), 3113-3127.
31. El-Boubbou, K.; Gruden, C.; Huang, X., Magnetic Glyco-nanoparticles: A Unique Tool for Rapid Pathogen Detection, Decontamination, and Strain Differentiation. *Journal of the American Chemical Society* **2007**, 129, (44), 13392-13393.
32. Gao, J.; Li, L.; Ho, P. L.; Mak, G. C.; Gu, H.; Xu, B., Combining Fluorescent Probes and Biofunctional Magnetic Nanoparticles for Rapid Detection of Bacteria in Human Blood. *Advanced Materials* **2006**, 18, (23), 3145-3148.
33. Lin, Y.-S.; Tsai, P.-J.; Weng, M.-F.; Chen, Y.-C., Affinity Capture Using Vancomycin-Bound Magnetic Nanoparticles for the MALDI-MS Analysis of Bacteria. *Analytical Chemistry* **2005**, 77, (6), 1753-1760.
34. Kim, Y.-P.; Daniel, W. L.; Xia, Z.; Xie, H.; Mirkin, C. A.; Rao, J., Bioluminescent nanosensors for protease detection based upon gold nanoparticle-luciferase conjugates. *Chemical Communications* **2010**, 46, (1), 76-78.

## **Appendices**

## Appendix 1. Quantification of QD coated onto GNs

The amount of QDs in the core-shell QDs-GNs with LBL coating was determined by measuring the emission intensity of QDs as a function of the concentration in triplicate at the 470 nm of excitation. The standard curve of the emission intensity of QDs as a function of the concentration was obtained as follows.

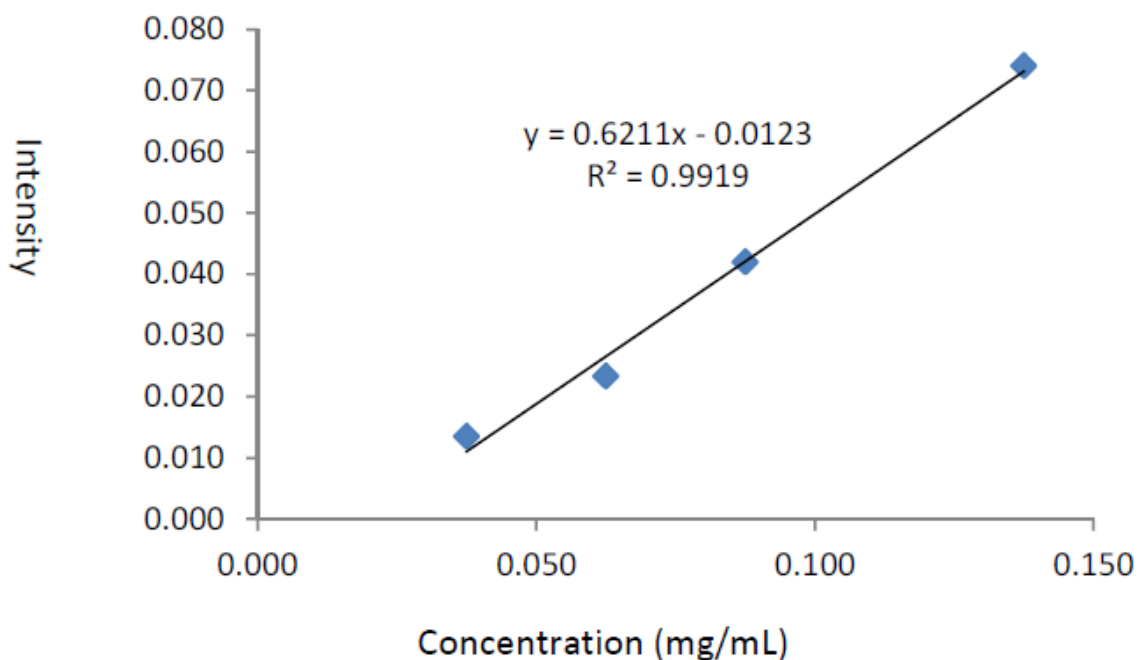
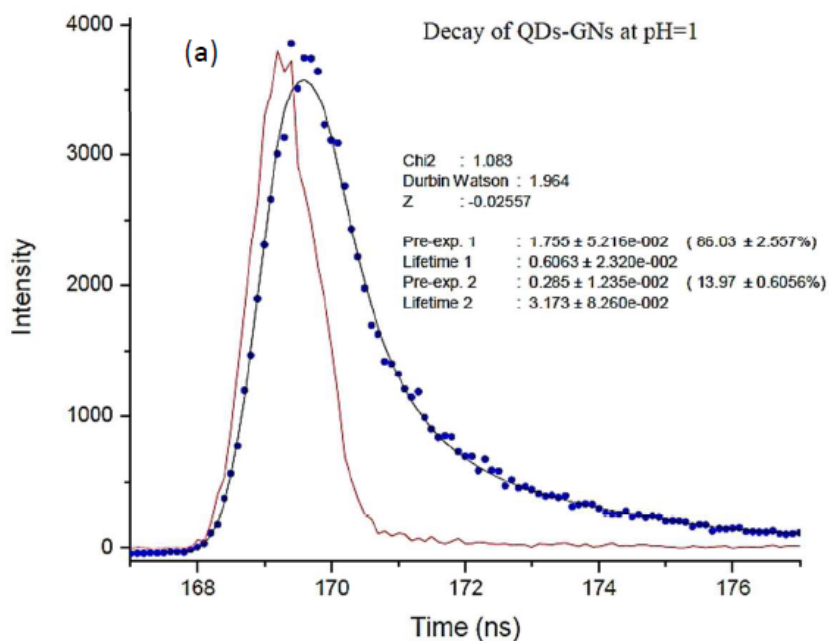


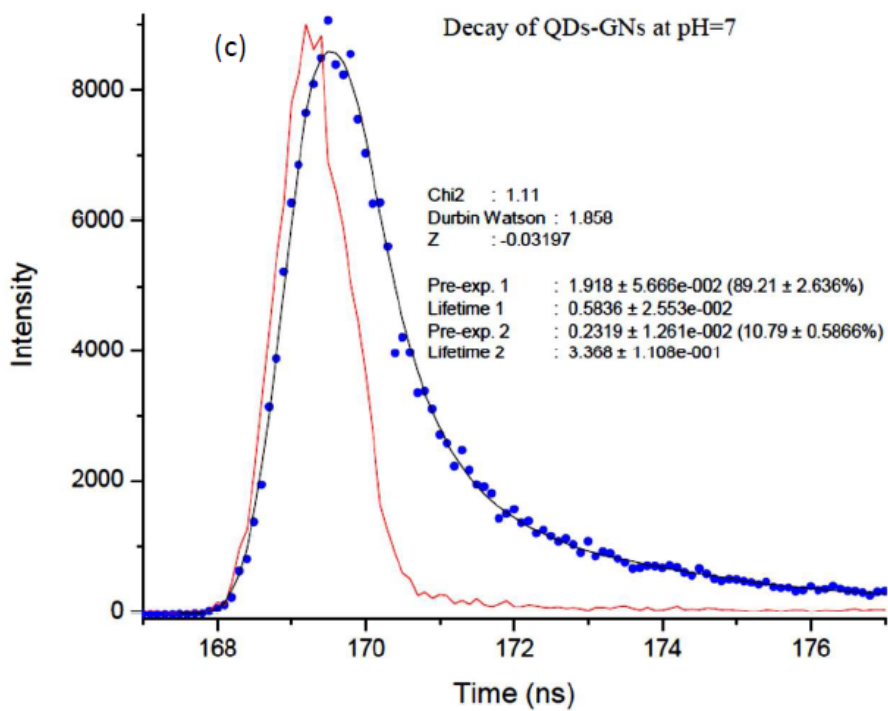
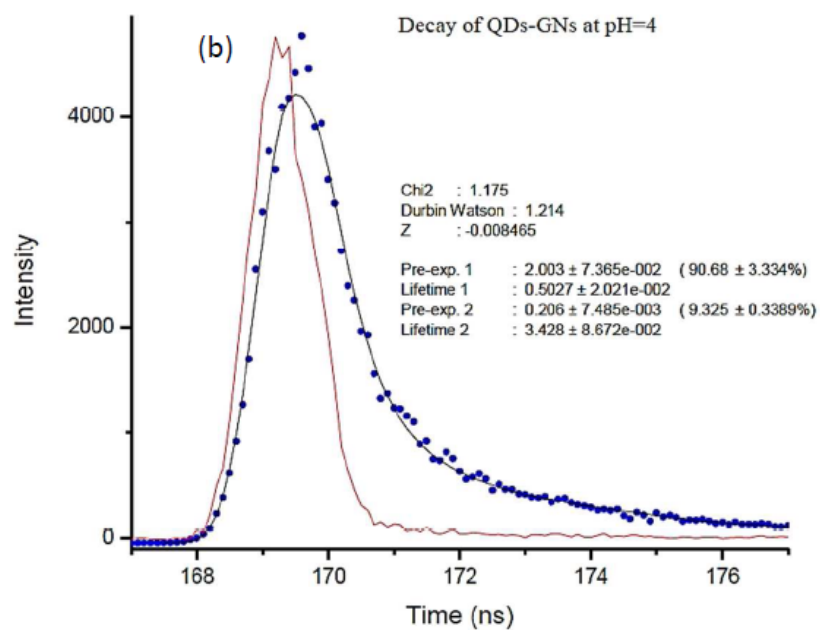
Figure A1. Standard curve of the emission intensity of the QDs as a function of their concentration.

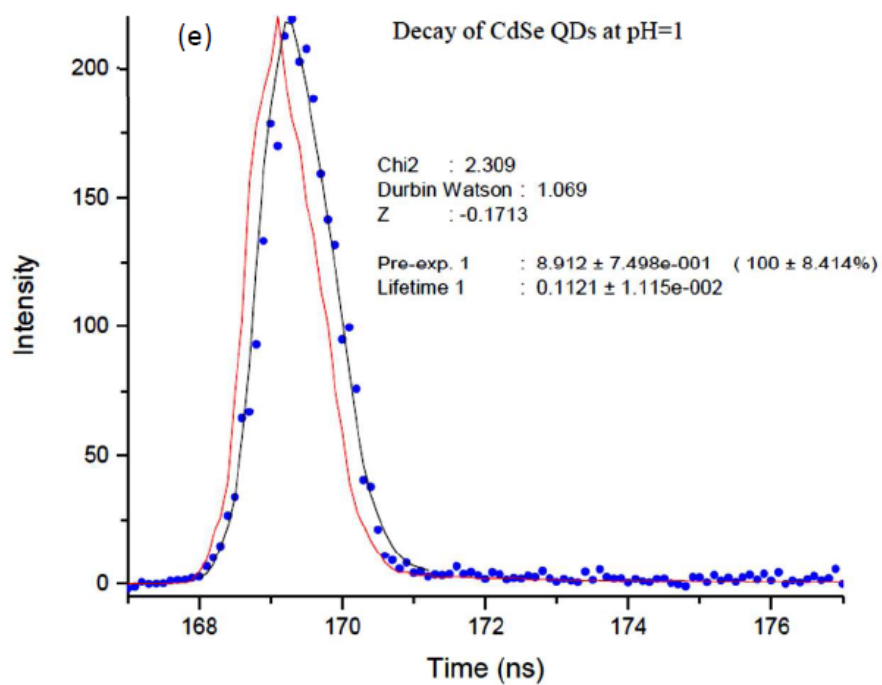
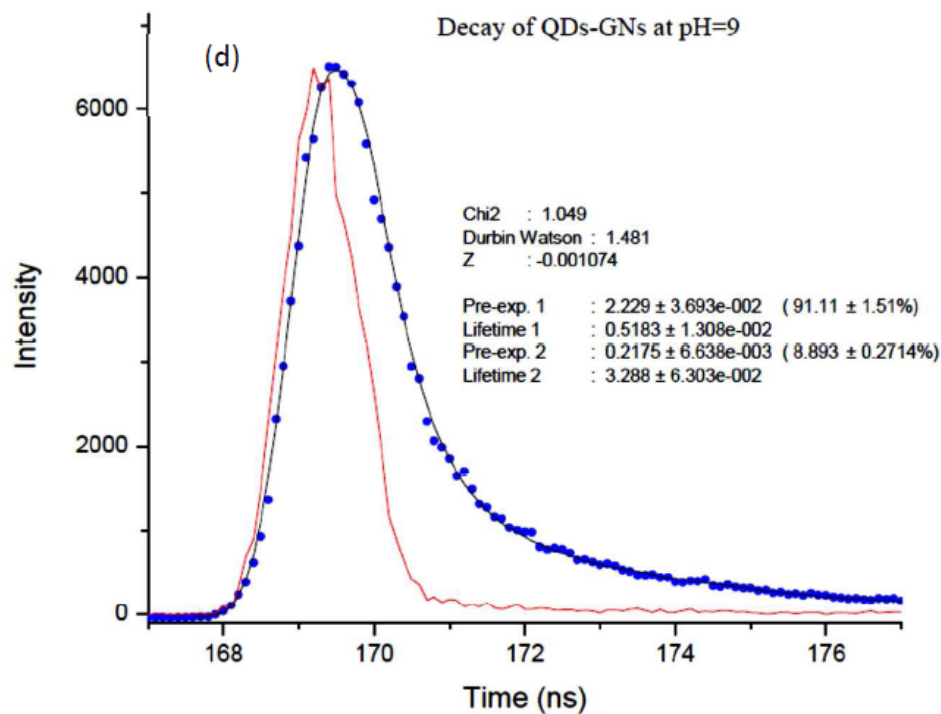
## Appendix 2. pH value effects on fluorescence decay of QDs and core-shell QDs-GNP2

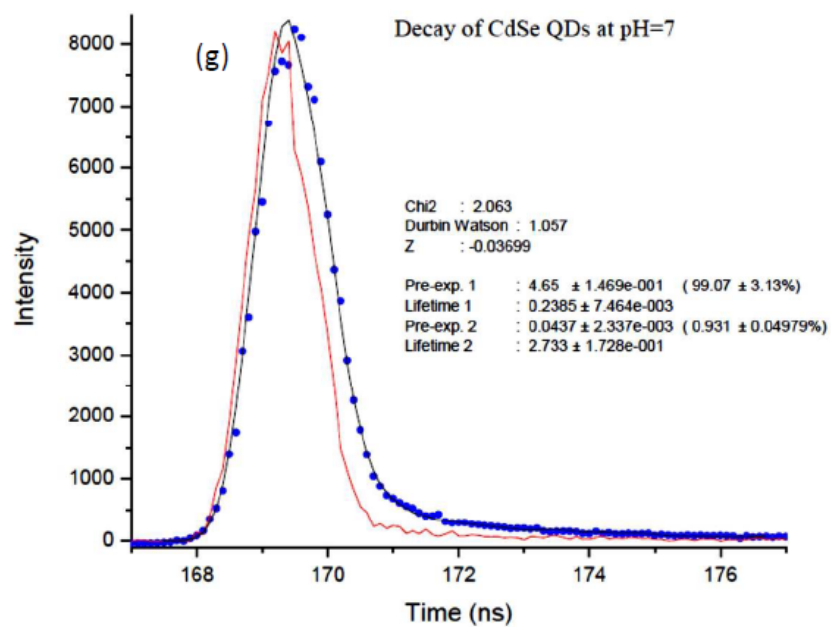
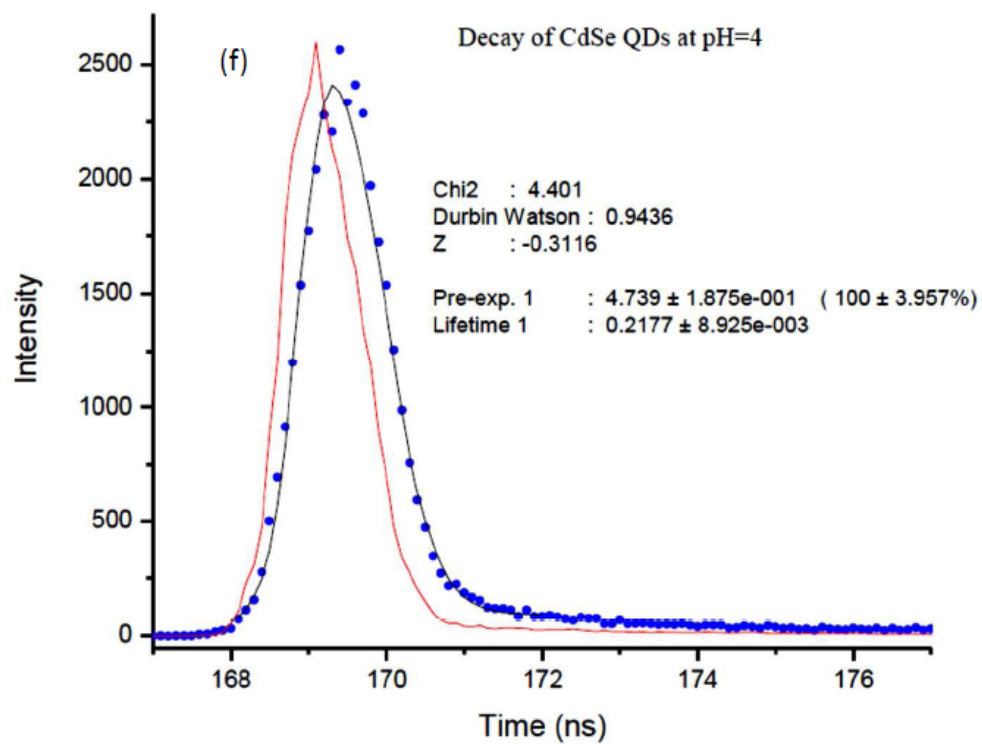
Time-resolved fluorescence measurements were measured by the TM-30 Laser Strobe timeresolved fluorometer (Photon Technology International. PTI, London, Ontario, Canada). The average lifetime of QDs-GNP2 (a-d) and MUA-QDs (e-h) in pH at 1, 4, 7, and 9 are shown as follows, in which the experimental data are shown as dots, and numerical fits as lines.

Figure A2 Fluorescence decay of QDs-GNP2 (a-d) and CdSe QDs (e-h) when the pH value of aqueous media is 1, 4, 7, and 9, respectively; the experimental data are shown as dots, and numerical fits as lines.

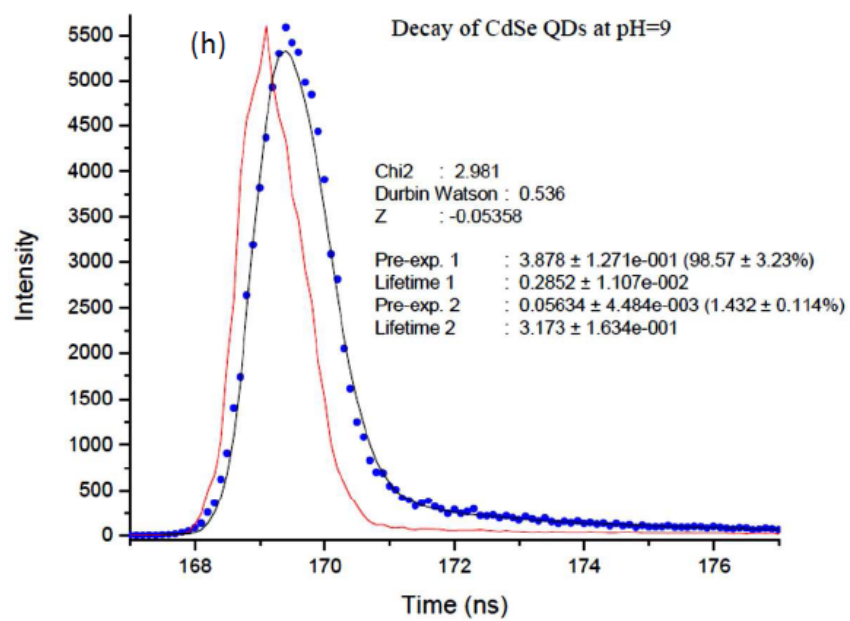












### Appendix 3. XANES spectra of FMNPs

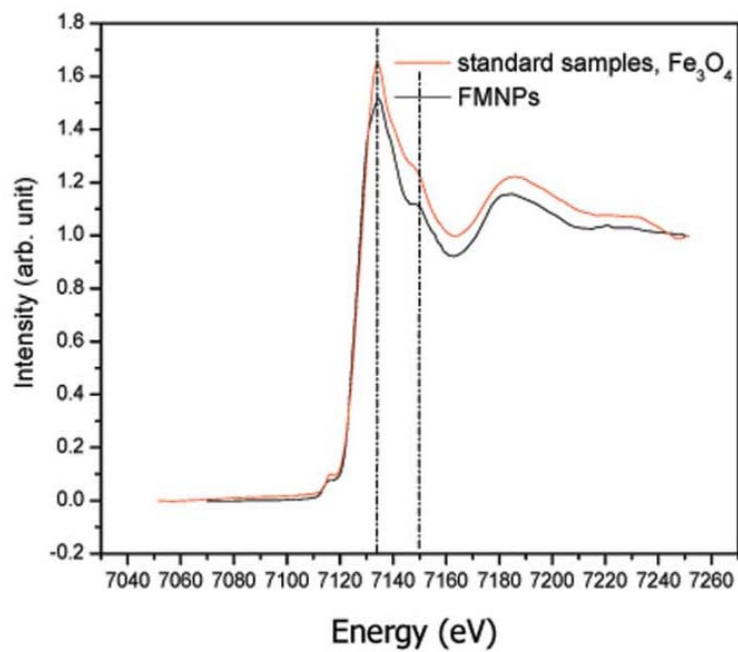


Figure A3 Fe K-edge XANES spectra of FMNPs (black line) and model compound,  $\text{Fe}_3\text{O}_4$  (red line)

#### Appendix 4. Determine the concentration of gentamicin on Gm-FMNP1.

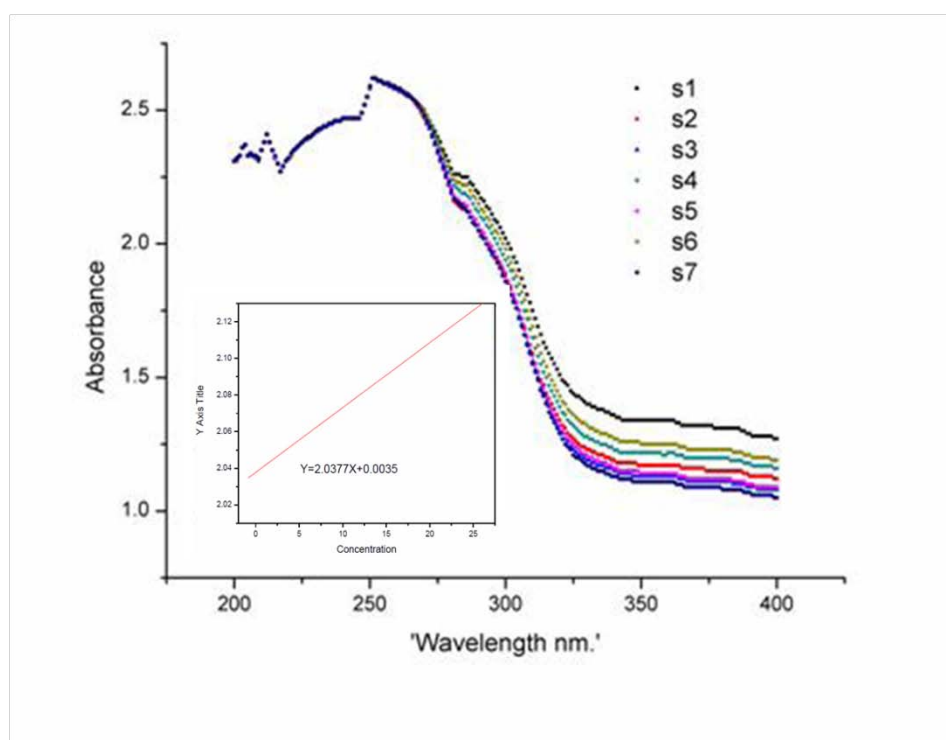


Figure A4. UV-vis spectra of the *o*-phthalaldehyde derived gentamicin products from standard gentamicin solutions.

Table A1. Absorption values at 292 nm of *o*-phthalaldehyde -derived Gm-FMNPs

UV Absorption	Sample of Gm-FMNP1 (fresh sample, 0.5 mg/mL)	Sample of Gm-FMNP1 (sored for two months, 0.5 mg/mL)
<b>Absorbance</b>	2.44	2.15

## Appendix 5. Plasmid map of recombinant protein pRluc

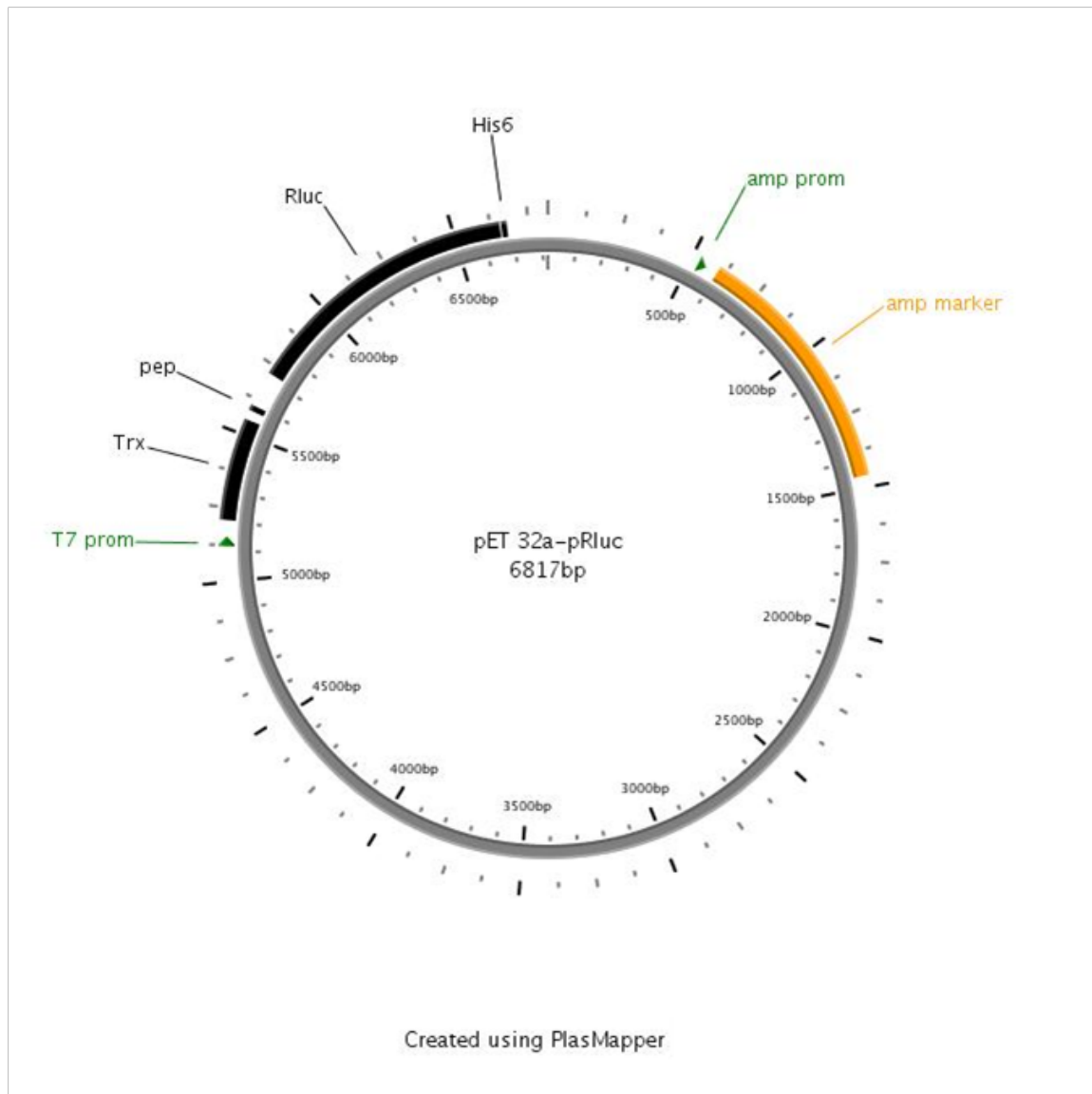


Figure A5. Map of plasmid containing recombinant protein pRluc (Obtained by PlasMapper web server, <http://wishart.biology.ualberta.ca/PlasMapper/>)

## Appendix 6. TEM image of Au NPs and SDS-PAGE of pRluc

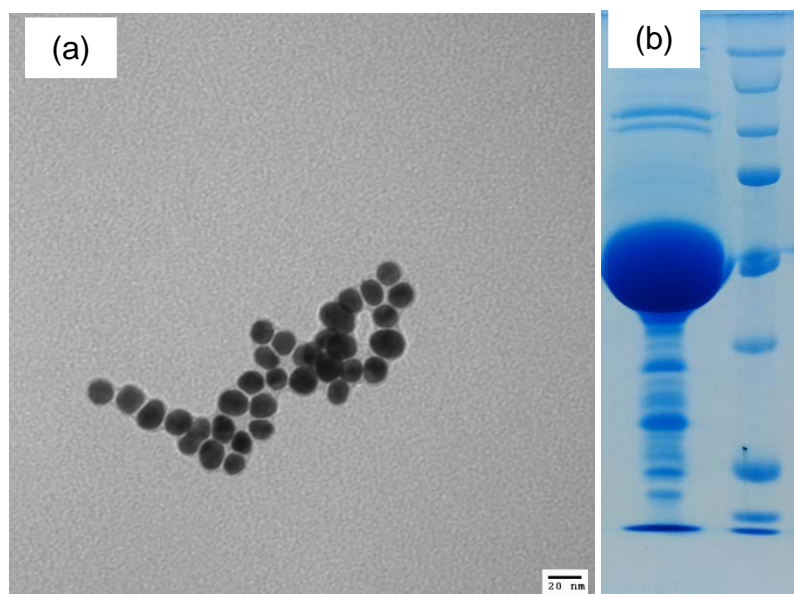





Figure A6 (a) TEM image of Au NPs and (b) SDS-PAGE of pRluc

## Appendix 7. Copyright permission

Rightslink® by Copyright Clearance Center

<https://sl00.copyright.com/AppDispatchServlet>

		<a href="#">Home</a> <a href="#">Create Account</a> <a href="#">Help</a>
	<b>ACS Publications Title:</b> The Optical Properties of Metal Nanoparticles: The Influence of Size, Shape, and Dielectric Environment	<div>User ID</div> <div>Password</div> <div><input type="checkbox"/> Enable Auto Login</div> <div><a href="#">LOGIN</a></div> <div><a href="#">Forgot Password/User ID?</a></div> <div>If you're a <a href="#">copyright.com</a> user, you can login to RightsLink using your <a href="#">copyright.com</a> credentials. Already a <a href="#">RightsLink</a> user or want to <a href="#">learn more?</a></div>
<b>Author:</b>	K. Lance Kelly, Eduardo Coronado, Lin Lin Zhao, and, and George C. Schatz*	
<b>Publication:</b>	The Journal of Physical Chemistry B	
<b>Publisher:</b>	American Chemical Society	
<b>Date:</b>	Jan 1, 2003	
Copyright © 2003, American Chemical Society		

### PERMISSION/LICENSE IS GRANTED FOR YOUR ORDER AT NO CHARGE

This type of permission/license, instead of the standard Terms & Conditions, is sent to you because no fee is being charged for your order. Please note the following:

- Permission is granted for your request in both print and electronic formats, and translations.
- If figures and/or tables were requested, they may be adapted or used in part.
- Please print this page for your records and send a copy of it to your publisher/graduate school.
- Appropriate credit for the requested material should be given as follows: "Reprinted (adapted) with permission from (COMPLETE REFERENCE CITATION). Copyright (YEAR) American Chemical Society." Insert appropriate information in place of the capitalized words.
- One-time permission is granted only for the use specified in your request. No additional uses are granted (such as derivative works or other editions). For any other uses, please submit a new request.

If credit is given to another source for the material you requested, permission must be obtained from that source.

[BACK](#)[CLOSE WINDOW](#)

Copyright © 2013 Copyright Clearance Center, Inc. All Rights Reserved. [Privacy statement](#).  
Comments? We would like to hear from you. E-mail us at

**JOHN WILEY AND SONS LICENSE  
TERMS AND CONDITIONS**

Nov 08, 2013

---

This is a License Agreement between Longyan Chen ("You") and John Wiley and Sons ("John Wiley and Sons") provided by Copyright Clearance Center ("CCC"). The license consists of your order details, the terms and conditions provided by John Wiley and Sons, and the payment terms and conditions.

**All payments must be made in full to CCC. For payment instructions, please see information listed at the bottom of this form.**

License Number	3264321475887
License date	Nov 08, 2013
Licensed content publisher	John Wiley and Sons
Licensed content publication	Luminescence
Licensed content title	Luminescent gelatin nanospheres by encapsulating CdSe quantum dots
Licensed copyright line	Copyright © 2013 John Wiley & Sons, Ltd.
Licensed content author	Longyan Chen,Adrienne Willoughby,Jin Zhang
Licensed content date	Mar 27, 2013
Start page	n/a
End page	n/a
Type of use	Dissertation/Thesis
Requestor type	Author of this Wiley article
Format	Electronic
Portion	Full article
Will you be translating?	No
Total	0.00 USD
Terms and Conditions	

**TERMS AND CONDITIONS**

This copyrighted material is owned by or exclusively licensed to John Wiley & Sons, Inc. or one of its group companies (each a "Wiley Company") or a society for whom a Wiley Company has exclusive publishing rights in relation to a particular journal (collectively "WILEY"). By clicking "accept" in connection with completing this licensing transaction, you agree that the following terms and conditions apply to this transaction (along with the billing and payment terms and conditions established by the Copyright Clearance Center Inc., ("CCC's Billing and Payment terms and conditions"), at the time that you opened your RightsLink account (these are available at any time at <http://myaccount.copyright.com>).

### Terms and Conditions

1. The materials you have requested permission to reproduce (the "Materials") are protected by copyright.
2. You are hereby granted a personal, non-exclusive, non-sublicensable, non-transferable, worldwide, limited license to reproduce the Materials for the purpose specified in the licensing process. This license is for a one-time use only with a maximum distribution equal to the number that you identified in the licensing process. Any form of republication granted by this license must be completed within two years of the date of the grant of this license (although copies prepared before may be distributed thereafter). The Materials shall not be used in any other manner or for any other purpose. Permission is granted subject to an appropriate acknowledgement given to the author, title of the material/book/journal and the publisher. You shall also duplicate the copyright notice that appears in the Wiley publication in your use of the Material. Permission is also granted on the understanding that nowhere in the text is a previously published source acknowledged for all or part of this Material. Any third party material is expressly excluded from this permission.
3. With respect to the Materials, all rights are reserved. Except as expressly granted by the terms of the license, no part of the Materials may be copied, modified, adapted (except for minor reformatting required by the new Publication), translated, reproduced, transferred or distributed, in any form or by any means, and no derivative works may be made based on the Materials without the prior permission of the respective copyright owner. You may not alter, remove or suppress in any manner any copyright, trademark or other notices displayed by the Materials. You may not license, rent, sell, loan, lease, pledge, offer as security, transfer or assign the Materials, or any of the rights granted to you hereunder to any other person.
4. The Materials and all of the intellectual property rights therein shall at all times remain the exclusive property of John Wiley & Sons Inc or one of its related companies (WILEY) or their respective licensors, and your interest therein is only that of having possession of and the right to reproduce the Materials pursuant to Section 2 herein during the continuance of this Agreement. You agree that you own no right, title or interest in or to the Materials or any of the intellectual property rights therein. You shall have no rights hereunder other than the license as provided for above in Section 2. No right, license or interest to any trademark, trade name, service mark or other branding ("Marks") of WILEY or its licensors is granted hereunder, and you agree that you shall not assert any such right, license or interest with respect thereto.
5. NEITHER WILEY NOR ITS LICENSORS MAKES ANY WARRANTY OR REPRESENTATION OF ANY KIND TO YOU OR ANY THIRD PARTY, EXPRESS, IMPLIED OR STATUTORY, WITH RESPECT TO THE MATERIALS OR THE ACCURACY OF ANY INFORMATION CONTAINED IN THE MATERIALS, INCLUDING, WITHOUT LIMITATION, ANY IMPLIED WARRANTY OF MERCHANTABILITY, ACCURACY, SATISFACTORY QUALITY, FITNESS FOR A PARTICULAR PURPOSE, USABILITY, INTEGRATION OR NON-INFRINGEMENT AND ALL SUCH WARRANTIES ARE HEREBY EXCLUDED BY WILEY AND ITS LICENSORS AND WAIVED BY YOU.



6. WILEY shall have the right to terminate this Agreement immediately upon breach of this Agreement by you.

7. You shall indemnify, defend and hold harmless WILEY, its Licensors and their respective directors, officers, agents and employees, from and against any actual or threatened claims, demands, causes of action or proceedings arising from any breach of this Agreement by you.

8. IN NO EVENT SHALL WILEY OR ITS LICENSORS BE LIABLE TO YOU OR ANY OTHER PARTY OR ANY OTHER PERSON OR ENTITY FOR ANY SPECIAL, CONSEQUENTIAL, INCIDENTAL, INDIRECT, EXEMPLARY OR PUNITIVE DAMAGES, HOWEVER CAUSED, ARISING OUT OF OR IN CONNECTION WITH THE DOWNLOADING, PROVISIONING, VIEWING OR USE OF THE MATERIALS REGARDLESS OF THE FORM OF ACTION, WHETHER FOR BREACH OF CONTRACT, BREACH OF WARRANTY, TORT, NEGLIGENCE, INFRINGEMENT OR OTHERWISE (INCLUDING, WITHOUT LIMITATION, DAMAGES BASED ON LOSS OF PROFITS, DATA, FILES, USE, BUSINESS OPPORTUNITY OR CLAIMS OF THIRD PARTIES), AND WHETHER OR NOT THE PARTY HAS BEEN ADVISED OF THE POSSIBILITY OF SUCH DAMAGES. THIS LIMITATION SHALL APPLY NOTWITHSTANDING ANY FAILURE OF ESSENTIAL PURPOSE OF ANY LIMITED REMEDY PROVIDED HEREIN.

9. Should any provision of this Agreement be held by a court of competent jurisdiction to be illegal, invalid, or unenforceable, that provision shall be deemed amended to achieve as nearly as possible the same economic effect as the original provision, and the legality, validity and enforceability of the remaining provisions of this Agreement shall not be affected or impaired thereby.

10. The failure of either party to enforce any term or condition of this Agreement shall not constitute a waiver of either party's right to enforce each and every term and condition of this Agreement. No breach under this agreement shall be deemed waived or excused by either party unless such waiver or consent is in writing signed by the party granting such waiver or consent. The waiver by or consent of a party to a breach of any provision of this Agreement shall not operate or be construed as a waiver of or consent to any other or subsequent breach by such other party.

11. This Agreement may not be assigned (including by operation of law or otherwise) by you without WILEY's prior written consent.

12. Any fee required for this permission shall be non-refundable after thirty (30) days from receipt

13. These terms and conditions together with CCC's Billing and Payment terms and conditions (which are incorporated herein) form the entire agreement between you and WILEY concerning this licensing transaction and (in the absence of fraud) supersedes all prior agreements and representations of the parties, oral or written. This Agreement may not be amended except in writing signed by both parties. This Agreement shall be binding upon and inure to the benefit of the parties' successors, legal representatives, and authorized assigns.

14. In the event of any conflict between your obligations established by these terms and conditions and those established by CCC's Billing and Payment terms and conditions, these terms and conditions shall prevail.

15. WILEY expressly reserves all rights not specifically granted in the combination of (i) the license details provided by you and accepted in the course of this licensing transaction, (ii) these terms and conditions and (iii) CCC's Billing and Payment terms and conditions.

16. This Agreement will be void if the Type of Use, Format, Circulation, or Requestor Type was misrepresented during the licensing process.

17. This Agreement shall be governed by and construed in accordance with the laws of the State of New York, USA, without regards to such state's conflict of law rules. Any legal action, suit or proceeding arising out of or relating to these Terms and Conditions or the breach thereof shall be instituted in a court of competent jurisdiction in New York County in the State of New York in the United States of America and each party hereby consents and submits to the personal jurisdiction of such court, waives any objection to venue in such court and consents to service of process by registered or certified mail, return receipt requested, at the last known address of such party.

#### **Wiley Open Access Terms and Conditions**

Wiley publishes Open Access articles in both its Wiley Open Access Journals program [<http://www.wileyopenaccess.com/view/index.html>] and as Online Open articles in its subscription journals. The majority of Wiley Open Access Journals have adopted the [Creative Commons Attribution License](#) (CC BY) which permits the unrestricted use, distribution, reproduction, adaptation and commercial exploitation of the article in any medium. No permission is required to use the article in this way provided that the article is properly cited and other license terms are observed. A small number of Wiley Open Access journals have retained the [Creative Commons Attribution Non Commercial License](#) (CC BY-NC), which permits use, distribution and reproduction in any medium, provided the original work is properly cited and is not used for commercial purposes.

Online Open articles - Authors selecting Online Open are, unless particular exceptions apply, offered a choice of Creative Commons licenses. They may therefore select from the CC BY, the CC BY-NC and the [Attribution-NoDerivatives](#) (CC BY-NC-ND). The CC BY-NC-ND is more restrictive than the CC BY-NC as it does not permit adaptations or modifications without rights holder consent.

Wiley Open Access articles are protected by copyright and are posted to repositories and websites in accordance with the terms of the applicable Creative Commons license referenced on the article. At the time of deposit, Wiley Open Access articles include all changes made during peer review, copyediting, and publishing. Repositories and websites that host the article are responsible for incorporating any publisher-supplied amendments or retractions issued subsequently.

Wiley Open Access articles are also available without charge on Wiley's publishing platform, **Wiley Online Library** or any successor sites.

Conditions applicable to all Wiley Open Access articles:

- The authors' moral rights must not be compromised. These rights include the right of "paternity" (also known as "attribution" - the right for the author to be identified as such) and "integrity" (the right for the author not to have the work altered in such a way that the author's reputation or integrity may be damaged).
- Where content in the article is identified as belonging to a third party, it is the obligation of the user to ensure that any reuse complies with the copyright policies of the owner of that content.
- If article content is copied, downloaded or otherwise reused for research and other purposes as permitted, a link to the appropriate bibliographic citation (authors, journal, article title, volume, issue, page numbers, DOI and the link to the definitive published version on Wiley Online Library) should be maintained. Copyright notices and disclaimers must not be deleted.
  - Creative Commons licenses are copyright licenses and do not confer any other rights, including but not limited to trademark or patent rights.
- Any translations, for which a prior translation agreement with Wiley has not been agreed, must prominently display the statement: "This is an unofficial translation of an article that appeared in a Wiley publication. The publisher has not endorsed this translation."

**Conditions applicable to non-commercial licenses (CC BY-NC and CC BY-NC-ND)**

For non-commercial and non-promotional purposes individual non-commercial users may access, download, copy, display and redistribute to colleagues Wiley Open Access articles. In addition, articles adopting the CC BY-NC may be adapted, translated, and text- and data-mined subject to the conditions above.

**Use by commercial "for-profit" organizations**

Use of non-commercial Wiley Open Access articles for commercial, promotional, or marketing purposes requires further explicit permission from Wiley and will be subject to a fee. Commercial purposes include:

- Copying or downloading of articles, or linking to such articles for further redistribution, sale or licensing;
- Copying, downloading or posting by a site or service that incorporates advertising with such content;
- The inclusion or incorporation of article content in other works or services (other than normal quotations with an appropriate citation) that is then available

for sale or licensing, for a fee (for example, a compilation produced for marketing purposes, inclusion in a sales pack)

- Use of article content (other than normal quotations with appropriate citation) by for-profit organizations for promotional purposes
- Linking to article content in e-mails redistributed for promotional, marketing or educational purposes;
- Use for the purposes of monetary reward by means of sale, resale, license, loan, transfer or other form of commercial exploitation such as marketing products
- Print reprints of Wiley Open Access articles can be purchased from:

The modification or adaptation for any purpose of an article referencing the CC BY-NC-ND License requires consent which can be requested from

Other Terms and Conditions:

BY CLICKING ON THE "I AGREE..." BOX, YOU ACKNOWLEDGE THAT YOU HAVE READ AND FULLY UNDERSTAND EACH OF THE SECTIONS OF AND PROVISIONS SET FORTH IN THIS AGREEMENT AND THAT YOU ARE IN AGREEMENT WITH AND ARE WILLING TO ACCEPT ALL OF YOUR OBLIGATIONS AS SET FORTH IN THIS AGREEMENT.

v1.8

**If you would like to pay for this license now, please remit this license along with your payment made payable to "COPYRIGHT CLEARANCE CENTER" otherwise you will be invoiced within 48 hours of the license date. Payment should be in the form of a check or money order referencing your account number and this invoice number RLNK501154860.**

**Once you receive your invoice for this order, you may pay your invoice by credit card. Please follow instructions provided at that time.**

**Make Payment To:**

**For suggestions or comments regarding this order, contact RightsLink Customer Support: (toll free in the US) or**

**Gratis licenses (referencing \$0 in the Total field) are free. Please retain this printable license for your reference. No payment is required.**

---

---



RightsLink®

[Home](#)[Account  
Info](#)[Help](#)ACS Publications  
High quality. High impact.

Title:

Development of Biocompatible  
and Proton-Resistant Quantum  
Dots Assembled on Gelatin  
Nanospheres

Logged in as:

Author:

Longyan Chen, Alex  
Siemiarczuk, Hong Hai, Yi Chen,  
Guobang Huang, and Jin Zhang[LOGOUT](#)

Publication: Langmuir

Publisher: American Chemical Society

Date: Feb 1, 2014

Copyright © 2014, American Chemical Society

**PERMISSION/LICENSE IS GRANTED FOR YOUR ORDER AT NO CHARGE**

This type of permission/license, instead of the standard Terms & Conditions, is sent to you because no fee is being charged for your order. Please note the following:

- Permission is granted for your request in both print and electronic formats, and translations.
- If figures and/or tables were requested, they may be adapted or used in part.
- Please print this page for your records and send a copy of it to your publisher/graduate school.
- Appropriate credit for the requested material should be given as follows: "Reprinted (adapted) with permission from (COMPLETE REFERENCE CITATION). Copyright (YEAR) American Chemical Society." Insert appropriate information in place of the capitalized words.
- One-time permission is granted only for the use specified in your request. No additional uses are granted (such as derivative works or other editions). For any other uses, please submit a new request.

[BACK](#)[CLOSE WINDOW](#)

Copyright © 2014 [Copyright Clearance Center, Inc.](#) All Rights Reserved. [Privacy statement.](#)  
Comments? We would like to hear from you. E-mail us at

# Multifunctional nanoparticles for rapid bacterial capture, detection, and decontamination

L. Chen, F. S. Razavi, A. Mumin, X. Guo, T. Sham and J. Zhang, *RSC Adv.*, 2013, **3**, 2390

DOI: 10.1039/C2RA22286H

If you are not the author of this article and you wish to reproduce material from it in a third party non-RSC publication you must [formally request permission](#) using RightsLink. Go to our [Instructions for using RightsLink page](#) for details.

Authors contributing to RSC publications (journal articles, books or book chapters) do not need to formally request permission to reproduce material contained in this article provided that the correct acknowledgement is given with the reproduced material.

Reproduced material should be attributed as follows:

- For reproduction of material from NJC:  
Reproduced from Ref. XX with permission from the Centre National de la Recherche Scientifique (CNRS) and The Royal Society of Chemistry.
- For reproduction of material from PCCP:  
Reproduced from Ref. XX with permission from the PCCP Owner Societies.
- For reproduction of material from PPS:  
Reproduced from Ref. XX with permission from the European Society for Photobiology, the European Photochemistry Association, and The Royal Society of Chemistry.
- For reproduction of material from all other RSC journals and books:  
Reproduced from Ref. XX with permission from The Royal Society of Chemistry.

If the material has been adapted instead of reproduced from the original RSC publication "Reproduced from" can be substituted with "Adapted from".

In all cases the Ref. XX is the XXth reference in the list of references.

If you are the author of this article you do not need to formally request permission to reproduce figures, diagrams etc. contained in this article in third party publications or in a thesis or dissertation provided that the correct acknowledgement is given with the reproduced material.

Reproduced material should be attributed as follows:

- For reproduction of material from NJC:  
[Original citation] - Reproduced by permission of The Royal Society of Chemistry (RSC) on behalf of the Centre National de la Recherche Scientifique (CNRS) and the RSC
- For reproduction of material from PCCP:  
[Original citation] - Reproduced by permission of the PCCP Owner Societies
- For reproduction of material from PPS:  
[Original citation] - Reproduced by permission of The Royal Society of Chemistry (RSC) on behalf of the European Society for Photobiology, the European Photochemistry Association, and RSC
- For reproduction of material from all other RSC journals:  
[Original citation] - Reproduced by permission of The Royal Society of Chemistry

## Acknowledgements to be used by RSC authors

Authors of RSC books and journal articles can reproduce material (for example a figure) from the RSC publication in a non-RSC publication, including theses, without formally requesting permission providing that the correct acknowledgement is given to the RSC publication. This permission extends to reproduction of large portions of text or the whole article or book chapter when being reproduced in a thesis.

The acknowledgement to be used depends on the RSC publication in which the material was published and the form of the acknowledgements is as follows:

- For material being reproduced from an article in *New Journal of Chemistry* the acknowledgement should be in the form:
  - [Original citation] - Reproduced by permission of The Royal Society of Chemistry (RSC) on behalf of the Centre National de la Recherche Scientifique (CNRS) and the RSC
- For material being reproduced from an article *Photochemical & Photobiological Sciences* the acknowledgement should be in the form:
  - [Original citation] - Reproduced by permission of The Royal Society of Chemistry (RSC) on behalf of the European Society for Photobiology, the European Photochemistry Association, and RSC
- For material being reproduced from an article in *Physical Chemistry Chemical Physics* the acknowledgement should be in the form:
  - [Original citation] - Reproduced by permission of the PCCP Owner Societies
- For material reproduced from books and any other journal the acknowledgement should be in the form:
  - [Original citation] - Reproduced by permission of The Royal Society of Chemistry


The acknowledgement should also include a hyperlink to the article on the RSC website.

The form of the acknowledgement is also specified in the RSC agreement/licence signed by the corresponding author.

Except in cases of republication in a thesis, this express permission does not cover the reproduction of large portions of text from the RSC publication or reproduction of the whole article or book chapter.

A publisher of a non-RSC publication can use this document as proof that permission is granted to use the material in the non-RSC publication.





# OMICS Group

An Open Access Publisher and Scientific Events Organizer  
for the Advancement of Science & Technology

[Home](#) | [Join](#) | [Contact](#) | [Sitemap](#) | [FAQs](#)

[Publications A-Z](#)  
[Browse by Subjects](#)  
[Conferences](#)

[Journals](#)
[Conferences](#)

[Advanced Search](#)

[Support Us »](#)

[About us](#)
[Open Access](#)
[Journals](#)
[Conferences](#)
[Scientific Credits](#)
[Membership](#)
[Submit Manuscript](#)
[Editors-in-Chief](#)

## Open Access License

### No Permission Required

The OMICS Publishing Group applies the Creative Commons Attribution License (CCAL) to all works we publish (read the human-readable summary or the full license legal code). Under the CCAL, authors retain ownership of the copyright for their article, but authors allow anyone to download, reuse, reprint, modify, distribute, and/or copy articles in OMICS journals, so long as the original authors and source are cited. **No permission is required from the authors or the publishers.**

The broad license was developed to facilitate open access to, and free use of, original works of all types. Applying this standard license to your own work will ensure your right to make your work freely and openly available. Learn more about [open access](#). For queries about the license, please [contact us](#).

All Published content, except where otherwise noted, is licensed under a [Creative Commons Attribution License](#).

**Science for Society – Technology for Tactics**

## Open Access Scientific Reports

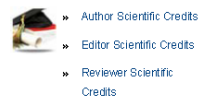
### OMICS Journals in News



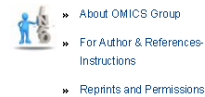
## Explore OMICS



## Scientific Credits



## Information



## Testimonials

**Warning:** include(test.html)  
[function.include]: failed to open stream: No such file or directory in /home/www/omics/public\_html/right-content.html on line 164

**Warning:** include(test.html)  
[function.include]: failed to open stream: No such file or

directory in /home/wwwomics  
/public\_html/right-  
content.html on line 164

Warning: include()  
[function.include]: Failed  
opening 'test.html' for inclusion  
(include\_path='./:/usr/lib/php:  
/usr/local/lib/php') in  
/home/wwwomics/public\_html  
/right-content.html on line 164

Follow Us

 Advertise With Us

OMICS Publishing Group is the member of/publishing partner of/source content provider to



[About Us](#) | [Open Access](#) | [Journals](#) | [OMICS Group Conferences](#) | [Scientific Credits](#) | [Membership](#) | [Submit Manuscript](#) | [OMICS Publishing Group](#)  
[Manuscript Submission & Tracking System](#) | [Open Access Publishing](#) | [Open Access Publication](#)

Best viewed in Mozilla Firefox | Google Chrome | Above IE 7.0 version

Copyright © 2014 OMICS Group, All Rights Reserved.



## Open Access

An [Open Access publication](#) is one that meets the following conditions:

- » The author(s) and copyright holder(s) grant to all users a free, irrevocable, worldwide, perpetual right of access and a license to copy, use, distribute, transmit and display the work publicly and to make and distribute derivative works in any digital medium for any responsible purpose, subject to proper attribution of authorship, as well as the right to make small number of printed copies for their personal use.
- » A complete version of the work and all supplemental materials, including a copy of the permission as stated above, in a suitable standard electronic format is deposited immediately upon initial publication in at least one online repository that is supported by an academic institution, scholarly society, government agency, or other well-established organization that seeks to enable [Open Access](#), unrestricted distribution, interoperability, and long-term archiving (for the biomedical sciences, PubMed Central is such a repository).
- » Open Access is a property of individual works.
- » Community standards, rather than copyright law, will continue to provide the mechanism for enforcement of proper attribution and responsible use of the published work.

### The Open Access movement - A comprehensive outlook

- » In recent times, there has been a lot of debate on the implementation of Open Access for research publications. Keeping this in mind, a comprehensive outlook on Open Access and its impact on scientific community is being provided in this article.
- » Open Access should be seen as a means of accelerating scientific discovery by providing free and unrestricted access of scientific knowledge via the Internet. An essential role of Open Access is the long-term preservation of peer-reviewed scholarly journal articles and research data. Open Access is not only used for journal articles but is also being implemented to theses, scholarly monographs, and book chapters. Promotion of Open Access is very crucial to encourage innovation, socio-economic development, and flow of knowledge around the world. As such, Open Access can be defined as an instrument ultimately used for public welfare to stimulate the growth of global science, as well as maintain the quality of scientific achievements at the same time.
- » Restricted access to research findings and scientific discovery through subscription and pay-per-view journals will only impede communication through the scientific community. In addition, restricted access can also hamper the education and dissemination of scientific knowledge to the aspiring younger generations who are keen to pursue a career in science. Increased productivity and development of science can only be achieved by diffusing knowledge and providing the facilities for creating permanent repositories such as Open Access.
- » Through Open Access publications, scientists can avoid subscription fees and copyright and licensing restrictions to access free scholarly literature. Since Open Access publishing allows the permanent restoration of scientific data through digital copies, other than the constraint of Internet access, scientists around the world can freely share information and collaborate to enhance the progress of science. [Open Access journals](#) not only give royalty to free literature, but also reduce costs for paper-copy production, physical storage, and distribution through digitalized copies.
- » The benefits of implementing Open Access are reaped by many end users, such as, students, researchers, clinicians, patients, policy makers, and journalists. As long as there is Internet access, people from all over the world, be it an underdeveloped country in Africa, a developing country like India or developed countries such as USA or UK, will have immediate access to latest research findings. Thus, [Open Access initiative](#) helps in unlocking the traditional methods of subscription articles and releasing information to tertiary level readers, who normally would not have access to first hand research studies.
- » Realizing the potential of Open Access in terms of greater visibility within and beyond the scientific community, in recent years, there has been a tremendous boost to Open Access movement through various Open Access publishers. OMICS is one such publishing group that believes in this movement and is most ardently working towards the welfare and progress of scientific community. [OMICS Group](#) is built upon the principles of Open Access and is determined to provide free and unrestricted access of research articles to scientists around the world for the advancement of science and technology.

[OMICS Publishing Group](#) is the member of/publishing partner of/source content provider to


[READ MORE](#)


[About Us](#) | [Open Access](#) | [Journals](#) | [OMICS Group Conferences](#) | [Scientific Credits](#) | [Membership](#) | [Submit Manuscript](#) | [OMICS Publishing Group](#)

[Manuscript Submission & Tracking System](#) | [Open Access Publishing](#) | [Open Access Publication](#)

Best viewed in [Mozilla Firefox](#) | [Google Chrome](#) | [Above IE 7.0 version](#)

Copyright © 2014 [OMICS Group](#). All Rights Reserved.



## Curriculum Vitae

**Name:** Longyan Chen

**Post-secondary Education and Degrees:** Nanchang University  
Nanchang, Jiangxi province, China  
2001-2005 B.E.

Graduate University of Chinese Academy of Sciences  
Wuhan, Hubei province, China  
2005-2008 M.Sc.

**Related Work Experience** Research Assistant & Lab Manager  
Department of Haematology,  
the 1<sup>st</sup> affiliated hospital of Zhejiang University  
2008-2009

### **Publications:**

L. Chen, Y. Bao and J. Zhang “Luciferase Conjugated Gold Nanoparticles for Thrombin Detection” (2014) In preparation.

L. Chen, A. Siemiarzuk, H. Hai, Y. Chen, G. Huang and J. Zhang, Development of Biocompatible and Proton-Resistant Quantum Dots Assembled on Gelatin Nanospheres, Langmuir (2014) 30:1893.

L. Chen, A. Willoughby and J. Zhang, Luminescent Gelatin Nanospheres by Encapsulating CdSe Quantum Dots, Luminescence (2013) 29:74.

L. Chen, F. Razavi, A. Mumin, X. Guo, T-K. Sham, and J. Zhang, Multifunctional Nanoparticles for Rapid Bacterial Capture, Detection, and Decontamination, RSC advance (2013) 3:2390.

L. Chen and J. Zhang, Bioconjugated Magnetic Nanoparticles for Rapid Capture of Gram-positive Bacteria, Journal of Biosensor and Bioelectronics (2012) S11:005.

J. Zhang, X. Wang, L. Chen, J. Li, and K. Luzak, Harnessing Nanostructured FRET Sensor for Quick Detection of Extremely Small Amount of Glucose, Journal of Diabetes Science and Technology (2012) 7:45.

L. Chen and J. Zhang, Development of Hydrophilic Iron Oxide Nanocubes, Science of Advanced Materials (2012) 4:859.

J. Zhang and L. Chen, Nico Films with Perpendicular Magnetization Anisotropy Deposited on Dielectric Substrate by Using Polyol Process, Materials Letters (2011) 65: 2944.

L. Chen, H. Wei, Y. Guo, Z. Cui, Z. Zhang, X. Zhang. Gold Nanoparticle Enhanced Immuno-PCR for Ultrasensitive Detection of Hantaan Virus Nucleocapsid Protein, Journal of Immunological Methods (2009) 346:64.

### **Conferences presentations**

Jun. 2012. Synthesis and Controlling Assembly Of Iron Oxide Nanocubes, The 24th Canadian Materials Science Conference, London, Ontario, Canada (Oral).

Oct. 2011. Development of Multifunctional Magnetic Nanoparticles for Biomedical Applications, The 61st Canadian Chemical Engineering Conference, London, Ontario, Canada (Oral).

May 2008. Developing A Fluorescence Immunoassay Based on Gold Nanoparticle Amplification for Ultrasensitive Detection of Botulinum Toxin A. The 10th World Congress on Biosensor, Shanghai, P. R. China (Poster).

.